CBPF-NF-010/95

The Pomeron: Yesterday, Today and Tomorrow[†]

Eugene Levin[*]

Centro Brasileiro de Pesquisas Físicas - CBPF-LAFEX
Rua Dr. Xavier Sigaud 150,
22290 - 180 Rio de Janeiro, RJ, Brasil

and

Theory Department, Petersburg Nuclear Physics Institute
188350, Gatchina, St. Petersburg, RUSSIA

Abstract

These lectures are the review of the main ideas and approaches to the structure of the Pomeron. They are divided in three natural parts:

(i) the brief review of the Reggeon Calculus, which was the first attempt to build the effective theory of the strong interaction at high energy. In spite of the fact that this approach turns out to be inconsistent and in lectures we show why, the Reggeon approach was and is the main source of the terminology and phenomenology for high energy "soft" interactions.

(ii) the detail description of the QCD approach to high energy interaction. We try to combine the rigorous approach in perturbative QCD with more simple, intuitive guess based on general properties of QCD to clarify our expectations and predictions.

(iii) the outline of my personal opinion what problems will be important in the future.

The main reason for the lectures was just the last part to agitate you to think about this difficult but because of that interesting problem. The motto of my lectures is *" there is nothing more exciting than to solve a difficult problem. Pomeron is the one."*

Key-words: Pomeron; Reggeons; Perturbative QCD; Evolution equation; High density QCD.

[†]Lectures given at the III Gleb Watagin School, Campinas, July 1994 and at the LAFEX,CBPF, Rio de Janeiro, September 1994

[*]Email: levin@lafex.cbpf.br; levin@fnalv.fnal.gov; levin@ccsg.tau.ac.il

Introduction

In these lectures I want to give the brief review of the main ideas and approaches to the structure of the Pomeron. For young generation even the word "Pomeron" sounds not familiar. It makes very difficult to explain in the introduction what we are going to discuss. In some sense it is the reason why we think that we shall start from the short review of the situation with the strong interaction in the past because the terminology that we still use came from so called Regge approach which was in the past the common language for the phenomenology of high energy strong interaction.

This is why instead of the usual introduction in which I have to explain the subject of the talk I am going to provide you some general outline of the main ideas of the talk.

I'll start from the review of the Regge approach and I'll try to give you the basics of this approach, namely the theoretical background and the main phenomenological ideas that had been used in this approach. Just from the beginning I would like to stress that inspite of the pure phenomenological input the Reggeon approach was and is the main source of the ideas even now for the "soft" high energy interaction. The main reason for this is the rich input from the understanding of the general properties of the scattering amplitude based on the analyticity and symmetry of strong interaction. The analysis of the theoretical problems made at that time (more than 30 years ago) is still fresh and the principle problems which have been pointed out are still with us.

After the introduction in the past and present problems with the "soft" interaction I am going to present what is known about high energy interaction in perturbative QCD which is the microscopic theory now. We will go back to old problems and I'll show you what kind of understanding we have reached in framework of perturbative QCD (pQCD). This understanding consists of two things: the sructure of the Pomeron in perturbative QCD (so called the BFKL Pomeron) and the theory of shadowing correction in the deeply inelastic processes. The main idea of this part of my lectures is to show you that we are on the right road but only in the beginning. The principle problems are non perturbative ones and we have made only the first try to attack them.

The last, third part will be devoted to outline of my personal opinion what problems will be important in the future. You can easily guess that the main reason for these lectures was just to agitate you to think about these difficult but really interesting problems.

As far as concerned the style of these lectures, we tried to follow the Landau ten commandments of theoretical physics, at least, the first three of them:

• Only prediction is a theory, only calculation is a result. Don't believe in a qualitative "theory".

• Try to solve a problem exactly, if not try to find a small parameter, if not try again.

• A model is the theory which we apply to the kinematic region where we cannot prove that the theory is wrong. Don't be afraid to build a model, this is the only way to be original.

We would like to make several comments on the quotations. In the first part of the lectures we avoid the references except the most important ones. The reason is twofold: first is the fact that everybody can find detail description of the Reggeon approach in any textbook written in 70's. The second is the idea to give you a full information in the body of the lectures about all result that we are going to take with us in the future. In the second part we give sufficiently full list of references.

Concluding this introductory section we want to remind you the motto of these lectures:

There is nothing more exciting than to solve a difficult problem. Pomeron is the one.

YESTERDAY:

REGGEON APPROACH

1 The basic ideas.

1.1 Our strategy.

To understand our theoretical background in the past let me remind you that before the year 1974 the study of the high energy asymptotic was the high priority job, because we believed that:

$$Analyticity + Asymptotic = Theory \ \ of \ \ Everything.$$

Roughly speaking we needed asymptotic at high energy to specify how many substructions we have to make in the dispersion relations to calculate the scattering amplitude using them.

Now situation is quite different, we have good microscopic theory (QCD) and certainly we have a lot of problems in QCD which have to be solved. High energy asymptotic is only one of many. I think it is time to ask yourselves why we spend our time and brain trying nevertheless to find the high energy asymptotic in QCD. My lectures will be an answer to this question, but I would like to start recalling you the main theorems for the high energy behaviour of the scattering amplitude which follow directly from the general property of analyticity and crossing symmetry and should be fulfilled in any microscopic theory including QCD.

1.2 The great theorems.

1. *Optical Theorem*

Our amplitude is normalized so that

$$\frac{d\sigma}{dt} = \pi |f(s,t)|^2 \tag{1}$$

Within this normalization the optical theorem says:

$$\sigma_{tot} = 4\pi Im f(s,0) \tag{2}$$

Therefore the optical theorem gives us the relationship between the behaviour of the imaginary part of the scattering amplitude at zero scattering angle and the total cross section that can be measured experimentally.

2. *The Froissart boundary.*

We call the Froissart boundary the following limit of the energy growth of the total cross section:

$$\sigma_{tot} \;\leq\; C\; ln^2 s \tag{3}$$

where s is the total energy of our elastic reaction: $a(p_a) + b(p_b) \rightarrow a + b$, namely $s = (p_a + p_b)^2$. Coefficient C has been calculated but we do not need to know its exact value. What is really important is the fact that $C \;\propto \frac{1}{k_t^2}$, where k_t is the minimal transverse momentum which can be in our reaction. Since the minimal mass is the mass of pion in the hadron spectrum the Froissart theorem says that $C \;\propto \frac{1}{m_\pi^2}$. The exact calculation gives $C = 60mbn$.

3. *The Pomeranchuk Theorem.*

The Pomeranchuk theorem is the manifestation of the **crossing symmetry**, which can be formulated as a following statement: one analytic function of two variables s and t describes the scattering amplitude of two different reactions $a + b \rightarrow a + b$ at $s > 0$ and $t < 0$ as well as $\bar{a} + b \rightarrow \bar{a} + b$ at $s < 0 (u = (p_{\bar{a}} + p_b)^2 > 0$ and $t < 0$.

The Pomeranchuk theorem says that the total cross sections of the above two reactions should be equal to each other at high energy if the real part of the amplitude is smaller than the imaginary its part.

•

Problem 1: Prove the Pomeranchuk theorem, using the dispersion relation for the scattering amplitude at $t = 0$.

1.3 Unitarity constraint in impact parameters (b_t).

The scattering amplitude in b_t-space is defined as

$$a(s,b_t) = \frac{1}{2\pi}\int d^2q \;\; e^{-i\mathbf{q}\cdot\mathbf{b_t}} f(s,t) \tag{4}$$

where $t = -q^2$. In this representation

$$\sigma_{tot} = 2 \int d^2 b_t \;\; Ima(s, b_t) \tag{5}$$

$$\sigma_{el} = \int d^2 b_t \;\; |a(s, b_t)|^2 \tag{6}$$

Using the above notations we can write the s- channel unitarity in the general form:

$$2\, Im\; a(s, b_t) \;\; = \;\; |a(s, b_t)|^2 \;\; + \;\; G_{in}(s, b_t) \tag{7}$$

where $a(s, b_t)$ is elastic amplitude while G_{in} is the contribution of the all inelastic processes.

It should be stressed that the above constraint has a general solution if we assume that the scattering amplitude is pure imaginary at high energy, namely

$$a(s, b_t) = i(1 - e^{-\Omega(s, b_t)}) \tag{8}$$

where the opacity $\Omega(s, b)$ is a real function and has a very simple physical meaning. Indeed,

$$G_{in}(s, b_t) \;\; = \;\; 1 \;\; - \;\; e^{-\,2\,\Omega(s, b_t)} \;\; .$$

Therefore $e^{-2\Omega}$ is the probability that the incoming particle has no inelastic interaction.

•

Problem 2: Prove the Froissart theorem, using the general solution of the s - channel unitarity taking into account that at large values of b_t the scattering amplitude is small and behaves as $s^N e^{-\mu b_t}$, where μ is the mass of the lightest hadron.

1.4 The first puzzle.

The first puzzle can be formulated as a question: *What happens with resonances with the values of their spin bigger than 1 in exchange?"* On one hand such resonances have been observed experimentally, on the other hand the exchange of the resonances with spin j lead to the scattering amplitudes which are proportional to s^j where s is the energy of two colliding hadrons. Such a behaviour contradicts the Froissart boundary. It means that we have to find the theoretical solution of this problem.

Let me illustrate the problem considering the exchange of vector particle ($j = 1$) (see Fig.1).

Introducing Sudakov variable we can expand each vector in the following form:

$$q \;=\; \alpha_q\, p_1' \;+\; \beta_q\, p_2' \;+\; q_t \tag{9}$$

where

$$p_1'^2 \;=\; p_2'^2 \;=\; 0$$

and

$$p_1 \;=\; p_1' \;+\; \beta\, p_2' \;\;;\;\; p_2 \;=\; \alpha_2\, p_1' \;+\; p_2' \;\;;$$

It is easy to find that

$$\beta_1 \;=\; \frac{m_1^2}{s} \;\;;\;\; \alpha_1 \;=\; \frac{m_2^2}{s}$$

since

$$p_1^2 \;=\; m_1^2 \;=\; 2\,\beta_1 p_1' \cdot p_2' \;=\; \beta_1\, s$$

¿From equations

$$p_1'^2 \;=\; M_1^2 \;\;;\;\; p_2'^2 \;=\; M_2^2$$

we can find the values of α_q and β_q. Indeed,

$$p_1'^2 \;=\; (p_q - q)^2 \;=\; (\,(1-\alpha_q)p_1' \;+\; (\beta_1 - \beta_q)p_2'\,)^2 \;=\; (1-\alpha_q)(\beta_1 - \beta_q)s \;-\; q_t^2 \;=\; M_1^2$$

and

$$p_2'^2 \;=\; (1+\beta_q)(\alpha_2 + \alpha_q)s \;-\; q_t^2 \;=\; M_2^2$$

Therefore

$$\alpha_q \;=\; \frac{M_2^2 - m_2^2}{s} \;\;;\;\; \beta_q \;=\; \frac{m_1^2 - M_1^2}{s} \tag{10}$$

It is easy to get from the above equations that

$$|q^2| \;\;=\;\; |\alpha_q \beta_q s - q_t^2| \;=\; \frac{(M_2^2 - m_2^2)(M_1^2 - m_1^2)}{s} \;+\; q_t^2 \;\;\rightarrow |_{s\to\infty}\; q_t^2 \tag{11}$$

Now we are prepared to write to expression for the diagram of Fig.1:

$$A(s,t) \;\;=\;\; g_1\, g_2 \frac{(p_1 + p_1')_\mu (p_2 + p_2')_\mu}{q_t^2 + m_V^2} \;=\; g_1\, g_2\, \frac{4s}{q_t^2 + m_V^2} \tag{12}$$

where m_V is the mass of the vector meson.

•

Problem 3: Using the above example show that the exchange of the resonance with spin j gives the scattering amplitude equals

$$A(s, t = -q_t^2) \; = \; g_1 \, g_2 \, \frac{(4s)^j}{q_t^2 + m_R^2}$$

•

Problem 4: Show that the exchange of the resonance with spin j leads to the amplitude in b_t which behaves as $s^j \; exp(-m_R b_t)$ at large values of b_t and s.

1.5 Reggeons - solutions to the first puzzle.

The solution to the first puzzle has been found. It turns out that the exchange of all resonances can be described as an exchange of the new object - Reggeon and its contribution to the scattering amplitude is given by the simple function (see Fig.2):

$$A_R(s,t) \; = \; g_1(m_1, M_1, t) \, g_2(m_2, M_2, t) \cdot \frac{s^{\alpha(t)} \; \pm \; (-s)^{\alpha(t)}}{sin\pi\alpha(t)} \tag{13}$$

$\alpha(t)$ is a function of the momentum transfer which we call the Reggeon trajectory. The name of the new object as well as the form of the amplitude came from the analysis of the properties of the scattering amplitude in t channel using angular momentum representation. However, today it is not important the whole history of the approach. What we need to understand and take for the future studies are the main properties of the above function which plays the crucial role in the theory and phenomenology of the high energy interaction.

2 The main properties of the Reggeon exchange.

2.1 Analyticity.

It is obvious that the Reggeon exchange is the analytic function in s, which has the imaginary part equals to

$$\pm \, g_1 \, g_2 \, s^{\alpha(t)}$$

in the s - channel and the imaginary part

$$g_1\, g_2\, s^{\alpha(t)}$$

in the u - channel (for $\bar{a}+b \to \bar{a}+b$ reaction). For different signes in eq.(13) the function has different properties with respect to crossing symmetry. For plus (positive signature) the function is symmetric while for minus (negative signature) it is antisymmetric.

2.2 s - channel unitarity

To satisfy the s - channel unitarity we have to assume that trajectory $\alpha(t) \leq 1$ in the scattering kinematic region ($t < 0$). This is why the exchange of the Reggeons can solve our first puzzle.

2.3 Resonances.

Let us consider the same function but in the resonance kinematic region at $t > 4m_\pi^2$. Here $\alpha(t)$ is a complex function. If $t \to t_0$ $\alpha(t_0) = j = 2k$ where $k = 1, 2, 3, ..$ the Reggeon exchange has a form for the positive signature:

$$A_R(s,t) \;\to_{t\to t_0}\; g_1\, g_2 \cdot \frac{s^{2k}}{\alpha'(t_0)\,(t-t_0) \,+\, iIm\alpha(t_0)} \tag{14}$$

Since in this kinematic region the amplitude A_R describes the reaction $\bar{a} + a \to \bar{b} + b$

$$s \;=\; p^2 sin\theta$$

where $p = \frac{\sqrt{t_0}}{2}$, the amplitude has a form

$$A_R \;=\; g_1\, g_2 \cdot \frac{s^j}{\alpha'(t_0)(t-t_0) \,+\, iIm\alpha(t_0)} \;=\; \frac{g_1 g_2}{\alpha'(t_0)} \cdot \frac{p^{2j} sin^j\theta}{t - t_0 + i\Gamma} \tag{15}$$

where the resonance width $\Gamma = \frac{Im\alpha(t_0)}{\alpha'(t_0)}$.

Therefore the Reggeon gives the Breit - Wigner amplitude of the resonance contribution at $t > 4m_\pi^2$. It is easy to show that the Reggeon exchange with the negative signature describes the contribution of a resonances with odd spin $j = 2k + 1$.

2.4 Trajectories.

We can rephrase the previous observation in different words saying that the Reggeon describes the family of resonances that lies on the same trajectory $\alpha(t)$. It gives us a new approach to the classification of the resonances, which is quite different from usual SU_3 classification. Fig.3 shows the bosonic resonances classified according the Reggeon trajectories. The surprising experimental fact is that all trajectories are the straight lines

$$\alpha(t) \; = \; \alpha(0) \; + \; \alpha' \, t \tag{16}$$

with the same value of the slope $\alpha' \simeq 1 GeV^{-2}$.

We would like to draw your attention to the fact that this simple linear form comes from two experimental facts: 1) the width of resonances are much smaller than their mass ($\Gamma_i \; \ll \; M_{R_i}$) and 2) the slope of the trajectories which is responsible for the shrinkage of the diffraction peak turns out to be the same from the experiments in the scattering kinematic region.

The SU_3 means in terms of trajectories that

$$\alpha_\rho(0) \; = \; \alpha_\omega(0) \; = \; \alpha_\phi(0)$$

in addition to the same value of the slope. The simple estimates show that the value of the intercept $\alpha(0) \; \simeq \; 0.5$ and therefore the exchange of the Reggeons give the cross section falling down as function of the energy without any violation of the Froissart theorem.

2.5 Definite phase.

The Reggeon amplitude of eq. (13) can be rewritten in the form:

$$A_R \; = \; g_1 g_2 \eta_\pm s^{\alpha(t)} \tag{17}$$

where η is the signature factor

$$\eta_+ \; = \; ctg \frac{\pi \alpha(t)}{2} \; + \; i$$

$$\eta_- \; = \; tg \frac{\pi \alpha(t)}{2} \; - \; i$$

It means that the exchange of the Reggeon brings very definite phase of the scattering amplitude. This fact is very important especially for the description of the interaction with a polarized target.

2.6 Factorization.

The amplitude of eq. (13) has a simple factorized form in which all dependences on the particular properties of colliding hadrons are concentrated in the vertex functions g_1 and g_2. To make it clear let us rewrite this factorization property in an explicit way:

$$A_R \;=\; g_1(m_1, M_1, q_t^2)\, g_2(m_2, M_2, q_t^2) \cdot \eta_\pm \cdot s^{\alpha(q_t^2)} \tag{18}$$

For example this form of the Reggeon exchange means that if we try to describe the electron deep inelastic scattering with the target through the Reggeon exchange, only the vertex function should depend on the value of the virtuality of photon (Q^2) while the energy dependance does not depends on Q^2.

•

Problem 5: Show that the Reggeon exchange has the following form in b_t:

$$A_R(s, b_t) \;=\; g_1(0)\, g_2(0) s^{\alpha(0)} \cdot \frac{1}{4\pi(R_1^2 + R_2^2 n + \alpha' \ln s} \cdot e^{-\frac{b_t^2}{4(R_1^2+R_2^2+\alpha' \ln s)}}$$

if we assume the simple exponential parameterization for the vertices:

$$g_1(q_t^2) = g_1(0)\, e^{-R_1^2\, q_t^2}$$

$$g_2(q_t^2) = g_2(0)\, e^{-R_2^2\, q_t^2}$$

2.7 Shrinkage of the diffraction peak.

Using the linear trajectory for the Reggeons it is easy to see that the elastic cross section due to the exchange of the Reggeon can be written in the form:

$$\frac{d\sigma_{el}}{dt} \;=\; g_1^2(q_t^2) \cdot q_2^2(q_t^2) \cdot s^{2(\alpha(0)-1)} \cdot e^{-2\alpha'(0)\, \ln s\, q_t^2} \tag{19}$$

The last exponent reflects the phenomena that is called as the shrinkage of the diffraction peak. Indeed, at very high energy the elastic cross section is concentrated at values of $q_t^2 < \frac{1}{\alpha' \ln s}$. It means that the diffraction peak becomes narrower at higher energies.

3 Analyticity + Reggeons.

Now we can come back to the main idea of the approach and try to construct the amplitude from the analytic properties and the Reggeon asymptotic at high energy. Veneziano [1] suggested the amplitude that satisfies the following constraint: it is the sum of all resonances in s - channel with zero width and simultaneously the same amplitude is the sum of the exchanges of all possible Reggeons. Taking the simplest case of the scattering of scalar particle, the Veneziano amplitude looks as follows:

$$A \;=\; g\,[\,V(s,t) \,+\, V(u,t) \,+\, V(s,u)\,] \tag{20}$$

where

$$V(s,t) \;=\; \frac{\Gamma(1-\alpha(t))\Gamma(1-\alpha(s))}{\Gamma(1-\alpha(t)-\alpha(s))} \tag{21}$$

One can see that the Veneziano amplitude has resonances at $\alpha(s) = n+1$ where $n = 1,2,3...$, since $\Gamma(z) \to \frac{1}{z+n}$ at $z \to -n$. At the same time

$$A \;\to_{s\to\infty}\; \Gamma(1-\alpha(t))[(-\alpha(s))^{\alpha(t)} \;+\; (-\alpha(u))^{\alpha(t)}]$$

and therefore reproduces the Reggeon exchange at high energies.

This simple model was the triumph of the whole approach showing us how we can construct the theory using analyticity and asymptotic. The idea was to use the Veneziano model as the first approximation or in other word as a new Born term in the theory and to try to build the new theory starting with the new Born Approximation. The coupling constant g turns out to be dimensionless and smaller than unity. This fact certainly also encouraged the theoreticians in 70's to try this new approach.

4 The second and the third puzzles: the Pomeron?!

The experiment shows that:

1. *There is no particles (resonances) on the Reggeon trajectory with the value of the intercept which is close to unity ($\alpha(0) \to 1$).* As it has been mentioned the typical highest value of the intercept is $\alpha(0) \sim 0.5$ which generates the cross section of the order of $\sigma_{tot} \propto s^{\alpha(0)-1} \propto s^{-\frac{1}{2}}$.

2. *The total cross section is approximately constant at high energy.* It means that we have to assume in the framework of the Reggeon approach that there is the Reggeon with the intercept close to 1.

The above two statement we call the second and the third puzzles that have to be solved in theory. The strategy of the approach was to assume that the Reggeon with the intercept close to 1 exists and tried to understand how and why it would be different from other Reggeons, in particular, why there is no particle on this trajectory. Now, let me introduce for the first time the word Pomeron. The first definition of the Pomeron:

The Pomeron is the Reggeon with $\alpha(0) - 1 \equiv \Delta \ll 1$

The name of Pomeron was introduced after russian physicist Pomeranchuk who did a lot to understand this miracle object. By the way, the general name of the Reggeon was given after the italian physicist Regge, who gave a beautiful theoretical arguments why such objects can exist in the quantum mechanics and the field theory [2].

Let me summarize what we know about the Pomeron from the experiment (see for example ref. [3]):

1. $\Delta \simeq 0.08$

2.$\alpha'(0) \simeq 0.25 GeV^{-2}$

Donnachie and Landshoff gave an elegant description of almost all existing experimental data using the hypothesis of the Pomeron with the above parameters of its trajectory. However, we have to find the theoretical approach how to describe the Pomeron and why it is so different from other Reggeons.

5 The Pomeron structure in the parton model.

5.1 The Pomeron in the Veneziano model.

As has been mentioned the Pomeron does not appear in the new Born term of our approach. Therefore the first natural idea was to make an attempt to calculate the next to Born approximation in the Veneziano model to see can the Pomeron appear in it. The basic equation that we want to use is graphically pictured in Fig.5, which is nothing more than the optical theorem. However we have to know the Born approximation for the amplitude of production of n particle.

However to understand the main properties and problems which can arise in this approach let us calculate the contribution in equation of Fig. 5 of the first two particle state. This contribution is equal to:

$$\sigma_{tot} \;=\; s^{2(\alpha_R(0)-1)} \int d^2q'_t \Gamma^2(1-\alpha(q'^2_t)) \cdot e^{-2\alpha' q'^2_t \ln s} \tag{22}$$

since

$$\Gamma(1-\alpha(q_t'^2)) \propto (\frac{\alpha(q_t'^2)}{e})^{2\alpha(q_t'^2)}$$

one can see that the essential values of q' in the integral is rather big, of the order of $q_t'^2 \sim s$. It means that we have to believe in the Veneziano amplitude at the large value of momentum transfer. Thus the lesson that we have learned from this exercise is the following:

To understand the Pomeron structure we have to understand better the structure of the scattering amplitude at large values of the momentum transfer or in other words we should know the interaction at small distances.

5.2 The parton model.

Feynman [4] and Gribov [5] suggested the simple model for the scattering amplitude at small distances that manifests itself in the deep inelastic scattering [6],so called the parton model. Let us assume that in the production amplitude the mean transverse momentum of the secondary particles does not depend on the energy ($k_{it} = Const(s)$ (see Fig.6). If it is so, the main contribution to the equation of Fig.5 comes from very specific region of integration. Indeed, the total cross section can be written as follows:

$$\sigma_{tot} \;=\; \Sigma_n \int |M_n^2(x_i p, k_{ti})| \Pi_i \frac{dx_i}{x_i}\; d^2k_{ti} \tag{23}$$

where x_i is the fraction of energy that carried by the i-th particle. Let's call all secondary particle partons.

It is clear that the biggest contribution in the above equation comes from the region of integration with strong ordering in x_i for all produced partons,namely

$$x_1 \gg x_2 \gg ..... \gg x_i \gg x_{i+1} \gg ..... \gg x_n = \frac{m^2}{s} \tag{24}$$

Integrating in this kinematic region we can put all $x_i = 0$ in the amplitude M_n. Finally,

$$\sigma_{tot} \;=\; \Sigma_n \int \Pi_i d^2k_{ti} |M_n^2(k_{ti})| \int_{\frac{m^2}{s}}^1 \frac{dx_1}{x_i} ..... \int_{\frac{m^2}{s}}^{x_{i-1}} \frac{dx_i}{x_i} ... \int_{\frac{m^2}{s}}^{x_{n-1}} \frac{dx_n}{x_n} \tag{25}$$

$$= \Sigma_n \int \Pi_i d^2k_{ti} |M_n^2(k_{ti})| \cdot \frac{1}{n!} \ln^n s$$

This equation shows one very general property of the high energy interactions, namely the longitudinal coordinates (x_i) and the transverse ones (k_{ti}) turns out to be separated and should be treated differently. In some sense the above equation reduced the problem of high energy behaviour of the total cross section to the calculation of the amplitude M_n which depend only on transverse coordinates. Assuming, for example, that $\int \Pi d^2k_{ti}|M_n^2(k_{ti})|^2 \propto \frac{1}{m^2}g^n$ we can derive from the eq.(25)

$$\sigma_{tot} \;=\; \frac{1}{m^2}\,\Sigma_n\,\frac{g^n}{n!}\,\ln^n s \;=\; \frac{1}{m^2}\cdot s^g \tag{26}$$

which looks just as Pomeron - like behaviour.

•

Problem 6: Show that in $g\phi^3$ - theory where ϕ is the scalar particle with mass m the total cross section is equal to

$$\sigma_{tot} \;=\; \frac{g^4}{m^2 4\pi s}\;s^{\frac{g^2}{4\pi m^2}}$$

5.3 Random walk in b_t.

The simple parton picture reproduces also the shrinkage of the diffraction peak. Indeed, due to the uncertainty principle

$$\Delta b_{ti}\;k_{ti}\;\sim\;1 \tag{27}$$

or in different form

$$\Delta b_{ti}\;\sim\frac{1}{<k_t>}$$

Therefore after each emission the position of the parton will be shifted on the value of Δb_t which is the same in average. After n emission we have the picture given in Fig.7, namely the total shift in b_t is equal to

$$b_{tn}^2 \;=\; \frac{1}{<k_t>^2}\cdot n \tag{28}$$

which is typical answer for the random walk in two dimensions (see Fig.7). The value of the average number of emission n can be estimated from the expression for the total cross section, because

$$\sigma_{tot} \;=\; \frac{1}{m^2}\,\Sigma_n\,\frac{g^n}{n!}\,\ln^n s \;=\; \frac{1}{m^2}\cdot s^g\;\sigma_0\,\Sigma_n\frac{<n>^n}{n!}$$

and the value of $<n>\simeq g\ln s$. If we substitute this value of $<n>$ in the eq.(0) We get the radius of interaction

$$R^2 \;=<b_{tn}^2>\;\frac{g}{<k_t>^2}\cdot\ln s \;=\; \alpha'\,\ln s$$

6 Reggeon Calculus.

6.1 The main idea of the approach.

The Reggeon Calculus was the first attempt to build the effective theory at high energy with the goal to define the asymptotic behaviour of the scattering amplitude. The brick from which we wanted to do this was the Pomeron. However, it turns out that the simple hypothesis that the Pomeron gives you the asymptotic behaviour of the amplitude is not correct. We have to take into account the interaction of the Pomerons. To illustrate this fact let us consider so called the triple Pomeron interaction which related to the process of the diffraction dissociation (see Fig.8).

The cross section of the diffraction dissociation (single diffraction SD) can be written in the form:

$$\frac{M^2 d\sigma_{SD}}{dM^2} \;=\; \frac{\sigma_0}{2\pi R_1^2(\frac{s}{M^2})}\cdot(\frac{s}{M^2})^{2\Delta}\cdot\gamma\cdot(\frac{M^2}{s_0})^{\Delta} \tag{29}$$

where σ_0 is the total cross section at $s = s_0$ due to exchange of one Pomeron and $R_1^2 = 2B_{SD}$, where B_{SD} denotes the slope of the SD cross section. It should be stressed that at very high energy when $\alpha'_P \gg R_0^2$, $R_1^2 \to 4\alpha'_P \ln(s/M^2)$

Integrating over M^2 the SD cross section one can see that the total cross section of SD

$$\sigma_{SD} \;\propto\; (\frac{s}{s_0})^{2\Delta} \;\gg\; \sigma_{tot} \propto (\frac{s}{s_0})^{\Delta}\;.$$

It means that we have to consider the interaction of the Pomerons to get the correct asymptotic at high energy.

•

Problem 7: Show that energy s' in Fig.8 is proportional to $\frac{s}{M^2}$.

•

Problem 8: Show that the total cross section of SD is larger that one Pomeron exchange even at $\Delta = 0$.

6.2 Reggeon Diagram Technique.

It turns out that the simplest way to deal with the Pomeron interaction is to use the Mellin transform of the amplitude [7]

$$A(\omega, t) \;=\; \int_0^\infty \; s^{-1-\omega} d\, s \; Im A(s,t) \tag{30}$$

•

Problem 9: Show that the Mellin transform of the single Pomeron exchange gives

$$A_P \;=\; \frac{1}{\omega \;-\; \Delta \;-\; \alpha'_P\, q_t^2}$$

where $t = -q_t^2$.

•

Using the above Pomeron propagator it is easy to write any diagram for Pomeron interaction. For example, for the triple Pomeron interaction the diagram of Fig.9 can be written in the form:

$$A_{3P} \;=\; g\, \frac{1}{\omega - \Delta - \alpha'_P q_t^2}\, \gamma\, \frac{1}{\omega - 2\Delta - \alpha'_P\, [\, (q-k)_t^2 \;+\; k_t^2\,]}\, N \tag{31}$$

6.3 The effective Lagrangian.

The above examples show that the new effective theory can be build as the theory of the interaction of the effective degrees of freedom (Pomerons) in $(1 + 2)$ dimensions. However, it is obvious that we cannot built the closed theory without specification what kind of interaction we want to take into account. On this pure phenomenological stage we have no selection rules and at first sight have to include any possible interactions. The idea was to start from triple Pomeron interaction, to solve the problem and to check back whether the more complicated interactions would be essential.

For triple Pomeron interaction the effective Lagrangian looks very attractive:

$$L \;=\; -\,\frac{1}{2}\,[\,\phi^+ \frac{\partial \phi}{\partial t} \;+\; \frac{\partial \phi^+}{\partial t}\phi\,] \;+\; \Delta \phi^+\, \phi \;-\; \frac{1}{2}\,\gamma\,[\,\phi^+ \;+\; \phi\,]\phi^+\phi \tag{32}$$

where $t = lns$ and the propagator of the Pomeron is defined as the Green function of the Lagrangian without interaction ($\gamma = 0$). We will discuss a bit later the sign minus in front of the last term.

The attempts to solve the effective theory were very interesting and we learned a lot, but we will not discuss them because we will show later that the whole approach is deadly sick.

6.4 The AGK cutting rules.

The AGK cutting rules [8] establish the generalization of the optical theorem on the case of the multi Pomeron interaction and in the simplest example of two Pomeron exchange they are pictured in Fig.11. The meaning of the AGK cutting rules is very simple. Each Pomeron interaction contribution to the total cross section really corresponds to the cross section of the different processes. In the case of the two Pomeron exchange these processes are (i) the diffraction dissociation ($\sigma^{(0)}$) , (ii) the production of the secondary hadrons with the same multiplicity as for one Pomeron exchange ($\sigma^{(1)}$) and (iii) the production of the secondary hadrons with multiplicity in two times larger than for one Pomeron exchange ($\sigma^{(2)}$).

The AGK cutting rules claim:

$$\sigma^{(0)} \div \sigma^{(1)} \div \sigma^{(2)} = 1 \div -4 \div 2 \tag{33}$$

Two important consequences follow from the AGK cutting rules:

1. The total cross section of the diffraction dissociation (DD) is equal to the contribution of two Pomeron exchange to the total cross section ($\sigma_{tot}^{(2P)}$) with opposite sign:

$$\sigma^{(DD)} = -\sigma^{(2P)}$$

2. The two Pomeron exchange does not contribute to the total inclusive cross section in central kinematical region. Indeed only two processes $\sigma^{(1)}$ and $\sigma^{(2)}$ are the sources of the produced particle in the central region. It means that the total inclusive cross section due to two Pomeron exchange is equal to

$$\sigma_{inc} = \sigma^{(1)} + 2\,\sigma^{(2)} = 0$$

Factor 2 comes from the fact that the particle can be produced from two different parton showers (see Fig.11).

Now let me give you a brief proof of the AGK cutting rules for the case of hadron - deuteron interaction. For simplicity let us assume that $G_{in}(b_t) = \kappa = Const(b_t)$ for $b_t < R_N$ and $G_{in} = 0$ for $b_t > R_N$, so the inelastic cross section for hadron - nucleon interaction is equal to

$$\sigma_N^{inel} = \kappa S$$

where S is the area of the nucleon ($S = \pi R_N^2$). To calculate the elastic cross section we need to use the unitarity constraint in b_t (see eq.(7)) and the answer is

$$\sigma_N^{el} = (\frac{\kappa}{2})^2 S$$

Note that the flux of incoming particles after the first interaction becomes $(1-\kappa)$ we can calculate the total inelastic interaction with the deutron, namely

$$\sigma_D^{inel} = \kappa S + \kappa(1-\kappa)S = 2\,\sigma_N^{inel} - \kappa^2 S$$

Using unitarity we have to calculate the elastic cross section for the interaction with deuteron which is equal to

$$\sigma_D^{el} = (\frac{2\kappa}{2})^2 S$$

Therefore the total cross section for hadron - deutron interaction can be presented in the form:

$$\sigma_D^{tot} = 2\,\sigma_N^{tot} - \Delta\sigma$$

where

$$\Delta\sigma = \Delta\sigma^{inel} + \Delta\sigma^{el} = -\frac{\kappa^2}{2} S = -\frac{(\sigma_N^{inel})^2}{2\pi R^2}$$

Everybody can recognize the usual Glauber formula for hadron - deutron interaction.

As has been mentioned we have two sources of the inelastic cross section which are pictured in Fig. 13 for the case of the deutron. The cross section of the inelastic process with double multiplicity is easy to calculate, because it is equal to the probability of two inelastic interaction:

$$\Delta\sigma_D^{(2)} = \kappa^2 \cdot S$$

To calculate;ate $\sigma_D^{(1)}$ we have to remember that

$$\Delta\sigma^{inel} = \sigma^{(2)} + \sigma^{(1)} = -\kappa S$$

Therefore $\sigma^{(1)} = -2\kappa S$. Remembering that $\Delta\sigma^{(0)} = \sigma_D^{el} - 2\sigma_N^{el}$ we get

n	0	$< n >_N$	$2< n >_N$
$\Delta\sigma_{tot}$	$\frac{\kappa^2}{2}S$	$-2\kappa^2 S$	$\kappa^2 S$

Therefore we get the AGK cutting rules for the hadron - deuteron interaction, since $\sigma_D^{tot} = 2\sigma_N^{tot}$ corresponds to one Pomeron exchange and the correction to this simple formula just originated from the two Pomeron exchange in our Reggeon approach. However the above discussion, I hope, shows you that the AGK cutting rules have more general background than the Reggeon approach. For example, they hold in QCD providing the so called factorization theorem.

Let me give here the general formula for the AGK cutting rules [8]. If we have the contribution to the total cross section with the exchange of ν Pomerons (σ_{tot}^{ν}), the cross sections of the process with the multiplicity of produced particles equal $\mu < n >$ which are generated by the same diagram (see Fig.13) are equal*:

$$\frac{\sigma^{(\mu)}}{\sigma_{tot}^{\nu}}\,|_{\mu\neq 0} \;=\; (-1)^{\nu-\mu}\cdot\frac{\nu!}{\mu!\,(\nu-\mu)!}\cdot 2^{\nu} \tag{34}$$

while for $\mu = 0$ the ratio is equal

$$\frac{\sigma^{(0)}}{\sigma_{tot}^{\nu}} \;=\; (-1)^{\nu}\cdot[\,2^{\nu-1}\,-\,1\,] \tag{35}$$

For the first 5 exchange you can find these factors in the following table.

$\nu \setminus \mu$	0	1	2	3	4	5
1	0	1	0	0	0	0
2	1	- 4	2	0	0	0
3	- 3	12	- 12	4	0	0
4	7	- 32	48	- 32	8	0
5	- 15	80	- 160	160	- 80	16

6.5 Different processes in the Reggeon Approach.

The AGK cutting rules together with Mueller theorem [9] establish the relationship between the contribution of many Pomeron exchanges and different exclusive and inclusive processes in the Reggeon Approach. Here we want to write down several examples of different processes that can be treated on the same footing in the reggeon approach.

*$< n >$ is the average multiplicity in one Pomeron exchange

6.5.1 Total cross section.

As has been mentioned in one Pomeron exchange approximation the total cross section is given by the following expression (see Fig. 15 †):

$$\sigma_{tot} \;=\; 4\pi g_1(0)\, g_2(0)(\frac{s}{s_0})^{\Delta}\; \sigma_0(\frac{s}{s_0})^{\Delta} \tag{36}$$

We would like to remind you that multi Pomeron exchange is very essential in the total cross section but we postpone the discussion of their contribution to the second part of our lectures.

6.5.2 Elastic cross section.

•

Problem 10: Show that for one Pomeron exchange the total elastic cross section is equal to

$$\sigma_{el} \;=\; \frac{\sigma_{tot}}{16\pi B_{el}}$$

where

$$B_{el} \;=\; 2R_{01}^2 \;+\; 2R_{02}^2 \;+\; 2\alpha'_P \ln s/s_0$$

in the exponential parameterization for the vertices $g(t)$ (see Problem 5).

6.5.3 Single diffraction dissociation

The cross section of the single diffraction (see Fig.15) has the following form:

$$\frac{M^2 d\sigma_{SD}}{dM^2} \;=\; \frac{\sigma_0}{2\pi R_1^2(\frac{s}{M^2})}\;\cdot\;(\frac{s}{M^2})^{2\Delta}\;\cdot\;[\,G_{3P}(0)\;\cdot\;(\frac{M^2}{s_0})^{\Delta}\;+\;G_{PPR}(0)(\frac{M^2}{s_0})^{\alpha_R(0)-1}\,] \tag{37}$$

•

Problem 11: Show that in exponential parameterization for vertices (see Problem 5)

$$R^2(\frac{s}{M^2}) \;=\; 2R_{01}^2 \;+\; r_0^2 \;+\; 4\alpha'_P \ln(s/M^2)$$

†In Fig. 15 we use a little bit different notation, namely $\beta(t)$ instead of g (t) and g (t) for $G_{3P}(t)$. We did this because we had nice prepared pictures in such notations. Hope that this fact will not lead to misunderstanding.

where r_0^2 is the radius of the triple Pomeron vertex which experimentally is very small ($r_0^2 \leq 1GeV^{-2}$).

•

One can see that we include in the expression for the cross section of the single diffraction also the contribution of the secondary Reggeon trajectory which describes the behaviour of the cross section at rather small values of produced mass (M^2).

6.5.4 Double diffraction dissociation.

•

Problem 12: Show that the cross section of the double diffraction dissociation (DD) process (see Fig.15) is equal to:

$$\frac{M_1^2 M_2^2 d^2\sigma_{DD}}{dM_1^2 dM_2^2} \;=\; \frac{\sigma_0}{2\pi R_0^2(\frac{ss_0}{M_1^2M_2^2})} \cdot G_{3P}^2(0) \cdot (\frac{ss_0}{M_1^2M_2^2})^{2\Delta} \cdot (\frac{M_1^2}{s_0})^{\Delta} \cdot (\frac{M_2^2}{s_0})^{\Delta} \qquad (38)$$

in the region of large values of produced masses (M_1 and M_2).

•

Problem 13: Show that R_0^2 in the above equation is equal

$$R_0^2 \;=\; \frac{1}{2}r_0^2 \;+\; 4\alpha'_P \ln(ss_0/M_1^2M_2^2)$$

in exponential parameterization of the vertices (see Problem 5).

•

Comparing the cross section for double and single diffraction as well as for elastic cross section one can get the following factorization relation:

$$\frac{M_1^2 M_2^2 d^2\sigma_{DD}}{dM_1^2 dM_2^2} \;=\; \frac{\frac{M_1^2 d\sigma_{SD}}{dM_1^2}\frac{M_2^2 d\sigma_{SD}}{dM_2^2}}{\sigma_{el}} \cdot \frac{R_1^2(\frac{s}{M_1^2})R_2^2(\frac{s}{M_2^2})}{R_0^2(\frac{ss_0}{M_1^2M_2^2})R_{el}^2(s)} \qquad (39)$$

where

$$R_{el}^2 = 2R_{01}^2 + 2R_{02}^2 + 4\alpha'_p \ln(s/s_0)$$

The structure of the event which corresponds to double diffraction is pictured in Fig.15 in lego - plot. In the region of rapidity Δy we have no produced particles.

6.5.5 Central Diffraction.

In this process we produced the bunch of secondary particle in the central rapidity region, while there are no secondary particles in other regions in rapidity.

The first diagram that describes this process gives the answer:

$$M^2\frac{d\sigma}{dM^2} = \frac{1}{2\alpha'}\sigma_{PP}(M^2)g_0^4(\frac{s}{M^2})^{2\Delta}e^{\frac{1}{2}(R_0^2+\alpha' ln\frac{s}{M^2})q^2}\frac{1}{R_0^2+\alpha' ln\frac{s}{M^2}} \cdot ln[\frac{R_0^2+2\alpha' ln\frac{s}{M^2}}{R_0^2}] \quad (40)$$

The above examples demonstrate how we can calculate the exclusive processes using several phenomenological inputs in the Reggeon Approach, however all these processes are crucially affected by multi Pomeron contributions and this subject we are going to discuss later.

6.5.6 Inclusive cross section.

As has been discussed the inclusive production does not depend on multi Pomeron exchanges. Using Mueller technique (see Fig.16) which is a generalization of the optical theorem for more complicated than total cross sections cases the inclusive cross section can be written in a very simple form:

$$\frac{d\sigma}{dy_c} \;=\; a\cdot\sigma_{tot} \quad (41)$$

where a is the new vertex for the emission of the particle c. The inclusive reaction that is under consideration is

$$a \;+\; b \;\rightarrow\; c(y) \;+\; anything$$

6.5.7 Two particle rapidity correlation.

The Reggeon approach we can use for the estimates of the two particle rapidity correlation function, which is defined as:

$$R \;=\; \frac{\frac{d^2\sigma(y_1,y_2)}{\sigma_{tot}dy_1dy_2}}{\frac{d\sigma(y_1)}{dy_1}\frac{d\sigma(y_2)}{dy_2}} \;-1 \quad (42)$$

where $\frac{d^2\sigma}{dy_1 dy_2}$ is the double inclusive cross section of the reaction:

$$a \ + \ b \ \rightarrow \ 1(y_1) \ + \ 2(y_2) \ + \ anything$$

•

Problem 14: Show using the AGK cutting rules that the correlation function R is equal:

$$R(\Delta y = |y_1 - y_2|) \ = \ \frac{a^2_{PR}}{a^2_{PP}} \cdot e^{(1-\alpha_R(0))\,\Delta y} \ + \ 2\,\frac{\sigma^{(2P)}_{tot}}{\sigma^{(P)}_{tot}} \tag{43}$$

All notations are clear from Fig.16.

•

It should be stressed that the Reggeon approach gives the estimates for the correlation length (*Lcor*) and the the strength of the long range correlations (note, that the second term does not depends on rapitidies of produced hadrons). Namely, we can rewrite the above formula in the form:

$$R \ = \ SR \cdot e^{-\frac{\Delta y}{L_{cor}}} \ + \ LR$$

and from our Reggeon formula we have $L_{cor} \simeq 2$. To evaluate the second term we have to develop some model for including the multi Pomeron exchanges in the calculation of the total cross section. We will do this in the second part of the lectures.

6.6 Hopes.

The main idea of the Reggeon Calculus was to build the effective theory for the strong interaction at high energy starting from the effective Lagrangian and the AGK cutting rules. The last one played a very crucial role giving us the possibility to look insight of the inelastic interaction using only general ideas on the structure of the Pomeron.

Of course one defect of the approach has been seen from the beginning, namely the absence of a theoretical idea how to select the interaction between Pomerons. However we could hope that the future theory will provide us such selection rules and we will be able to adjust the developed formalism.

7 The death of the Reggeon Approach.

In 1974 - 1975 in ref. [10] was shown that all our hopes were in vain. T.T. Wu and McCoy and S.Matinian and A. Sedrokian proved that in the general class of the theories (all theoretical model that existed at that time) our hope that the Pomeron and Pomeron interaction can describe the high energy asymptotic is not correct.

Let me illustrate this point using the parton model. In this model the Pomeron is the sum of "ladder" diagrams while the two Pomeron exchange corresponds to the diagram of Fig.17 where the partons are produced and absorbed by the same "ladders". These diagrams have the probabilistic interpretation and look very natural in the parton model. However it turns out that the diagrams where the secondary partons are produced by one "ladder" and are absorbed by the second one give bigger contribution. These diagrams have not been included neither in one Pomeron exchange nor in two Pomeron exchange.

It means that our hope to reduce the whole theory to Pomeron interaction can not be right or at least we have to build more complicated picture for the Pomeron structure, which is impossible to do without detailed microscopic theory.

It means also that the AGK cutting rules we cannot apply for the process of the Pomeron interaction. For example, if we want to calculate the inclusive production of the hadron in the single diffraction process we cannot restrict ourselves by calculation of only two diagrams of Fig.18, but we should add also the third diagram.

8 Lessons for future.

Inspite of the fact that we failed to construct the effective theory for high energy interaction starting from the new effective degree of freedom -Pomeron we certainly learned a lot about properties of high energy interaction. In this section I want to summarize those lessons that we have learned and which could be useful for future.

1. The longitudinal and transverse degrees of freedoms look differently at high energy and can be treated separately and in different ways.

2.The effective theory at high energy can be reduced to two dimensional theory and we need to find the energy spectrum of this two dimensional theory to specify the high energy asymptotic.

3.The major problem of any affective theory at high energy is to find correct degree of freedom or in other words the correct effective particle which is responsible for high

energy asymptotic. The concrete realization, namely Reggeon Calculus failed, because the Pomeron, effective particle of that time, turns out to be not the correct one to construct theory at high energy (see the previous section).

4. The only way to invent correct effective particle is to develop the consistent approach starting from microscopic theory but not from phenomenology.

At that time we had no microscopic theory and in the best tradition of high energy physics the experts left the field. Now situation is quite different, we have good microscopic theory (QCD) and certainly we have a lot of problems in QCD which have to be solved. High energy asymptotic is only one of many. I think it is time to ask yourselves why we spend our time and brain trying nevertheless to find the high energy asymptotic in DIS. Let me give the first answer to this question, namely it seems extremely interesting to go back to old problems to see how far away was our guess from the systematic approach. It is rather private but strong motivation for many experts including me. Later we will discuss this problem in more details.

We want to finish our review of the past in high energy physics with a statement, that inspite of all theoretical inconsistency, all intristic contradictions of the Reggeon Calculus, this old fashioned approach is still the main source of our terminology in high energy theory and still the only phenomenological approach that we have in hand even now when we discuss so called "soft" processes. It is why the knowledge of this approach is still the alpha and omega of high energy strong interaction theory. We hope that we gave you just right amount of information to move to more theoretical approach based on QCD.

TODAY:

POMERON WITHOUT MAGIC IN PERTURBATIVE QCD

9 Basics of perturbative QCD (pQCD)

9.1 The basics of pQCD for high energy scattering.

In this subsection we are going to discuss the main ideas of perturbative QCD, which is our microscopic theory of the strong interaction. The goal of our approach is to understand what is the Pomeron in QCD, but we start from the several things that everybody knows about QCD.

1. If the typical distances (r) in our process are small we have a natural small parameter in QCD, namely the strong coupling constant

$$\alpha_S(r) \;=\; \frac{4\pi}{b \ln \frac{1}{r^2\Lambda^2}} \;=\; \frac{\alpha_S(\mu^2)}{1 + \frac{\alpha_S(\mu^2) b}{4\pi} \ln \frac{1}{r^2\mu^2}} \ll 1$$

where $b = 11 - \frac{2}{3} n_f$, n_f is the number of quarks, Λ is the QCD confinement scale and μ is the renormalisation scale.

It means that we can start to calculate the amplitude of our process using the expansion with respect to small α_S.

2. The Born approximation of pQCD gives the cross section which is constant at high energy

$$\sigma_t \;\to |_{s\to\infty}\; Const$$

We will discuss this property in details in the next section.

3. The more complicated diagrams lead to increase of the total cross section with energy as we will discuss later

$$\sigma_t \;\to |_{s\to\infty}\; s^{\Delta}$$

where $\Delta = C\alpha_S$.

All the above properties show us that we have a good chance to get in QCD the high energy asymptotic which looks like the one Pomeron exchange (the word Pomeron I use here in the traditional sense as the Reggeon with intercept close to 1) and we are able to examine how good or bad is our traditional Reggeon - like approach. However, we are going to start with the brief review what we have learned about pQCD to give you an impression what kind of theory we have to attack the Pomeron structure.

9.2 The map of QCD.

Describing the basic features of QCD, we will start to answer in this subsection the following questions: (i) What we have learned about QCD; (ii) What problems are still unsolved in QCD?; (iii) Can we relate the kinematical region in which we have to face these unsolved problems to collision processes?

Fig.19 displays the 'map of QCD'. Shown are three separate regions, distinguished by the size of the variables Q^2 and x, which will be defined momentarily. Each region corresponds to quite different physics and enjoys a different level of understanding. Before we discuss these three regions in more detail let us introduce the necessary notational conventions and definitions.

Deeply Inelastic Scattering (DIS).

In Fig.19 r is the distance that can be resolved by the scattering process under consideration. From the uncertainty principle this distance is of the order of $\frac{1}{Q}$ where Q is the typical large transverse momentum in our experiment. E.g. in deeply inelastic electron scattering Q is the transverse momentum of the recoiled electron. We recall that deeply inelastic scattering is the reaction:

$$e \ + \ p \ \rightarrow \ e' \ + \ anything.$$

Thus, this reaction acts as a powerful microscope which is able to resolve the constituents of a hadron (quarks, antiquarks and gluons, collectively called partons) with a transverse size of the order of $\frac{1}{Q}$. The second kinematical variable that we can introduce for such constituents is the fraction of energy (x) that a parton carries with respect to the parent hadron.

It should be stressed that the energy in DIS is equal to $s = \frac{Q^2}{x}$. It means that we are interested in low x DIS if we are going to discuss the high energy asymptotic. If $N(x, Q^2)dx$ is the number of gluons in a small x-interval centered around the value x at scale Q^2. We will show later that the number of gluons increases in the region of small x.

All physics in this kinematical region is strongly connected to this fact. It is the reason we concentrate on the discussion of the gluon density here.

The gluon structure function $xG(x,Q^2)$ tells us what the gluon density at a definite value of $\ln\frac{1}{x}$ is,

$$xG(x,Q^2) \;=\; |\frac{dN(x,Q^2)}{d\ln\frac{1}{x}}| \;.$$

Let us for convenience introduce the transverse density of gluons ρ,

$$\rho(x,Q^2) \;=\; \frac{xG(x,Q^2)}{\pi\,R^2} \tag{44}$$

where R is the radius of the hadron.

We plot this on the vertical axis in Fig.19. In this figure we can see three different regions:

1. *The region of small parton density at small distances (low density (pQCD) region).*

This is the region where we can apply the powerful methods of perturbative QCD since the value of running coupling constant $\alpha_s(1/r^2)$ is small ($\alpha_s(1/r^2) \;\ll\; 1$). During two decades remarkable theoretical progress has been achieved here (GLAP evolution equation [11], gluon bremshtrahlung for jet decay [12] , factorization theorem (J.Collins,D.Soper and G.Sterman (1983) [13]) and the main property of "hard" processes has been experimentally confirmed at LEP and at the Tevatron.

2. *The region of large distances (npQCD region).*

Here we have to deal with the confinement problems of QCD, since $\alpha_s(1/r^2) \gg 1$. In this kinematical region we need to use nonperturbative methods such as lattice calculation [14] or QCG Sum Rules [15]. The progress here is remarkable but all developed methods cannot yet be applied to scattering processes.

3 *The region of small distances but high parton density (hdQCD region).*

Here we have a unique situation in which the coupling constant α_s is still small but the density is so large that we cannot use the usual methods of perturbation theory.

In essence the theoretical problem here is also a nonperturbative one but the origin of the nonperturbative effects here is quite different from that in the previous region. Here we face the situation where we have to develop new methods that let deal with a dense relativistic system of gluons in a nonequilibrium state. Unfortunately we are only at the beginning of this road.

Fortunately, we can control theoretically this dense system of partons in some transition region on the border of the pQCD and hdQCD regions and here we can study this remarkable system of partons in great detail. Thus the right strategy is to approach this interesting kinematic region from the low density pQCD region.

In my opinion the interest to high energy scattering was revived only because moving from pQCD region to hdQCD region we can open new window to study a nonperturbative nature of QCD.

9.3 What fundamental problems could be solved?

This is why we want to list here the fundamental problems that we hope to solve penetrating high density QCD region. We hope:

1. to specify the kinematical region in which we can trust pQCD (GLAP evolution equation, gluon bremstrahlung, factorization theorem ...);

2. to find new collective phenomena for nonabelian theories such as QCD ;

3. to find the analytic solution of hd QCD which is nonperturbative but looks simpler than np QCD since $\alpha_s \ll 1$ here;

4. to develop methods with which build an effective theory for hd QCD.

We need the effective theory because we can use the Lagrangian of such a theory for exact calculation on lattice, for example, or even we can try to solve problem analytically.

9.4 How to penetrate the high density QCD region.

Access to this interesting kinematical region is actually easily achieved in our scattering processes. We know at least three ways to prepare a large density system of partons.

1. The first is given by nature, which supplies us with large and heavy nuclei. In ion-ion collisions we can already reach a very high density of partons at not so high energies, because the partons from different nucleons in a nucleus are freed.

2. The second relates to hard processes in hadron-hadron collisions or in deep inelastic scattering. These also give us access to a high density of partons because we expect a substantial increase in the parton density in the region of small Bjorken x. The experimental data from HERA show the significant increase of the deep inelastic structure function:

$$F_2(Q^2, x_B) \propto (\frac{1}{x_B})^{0.33} \; at \; Q^2 \sim 10\, GeV^2.$$

3. The third is to measure the event with sufficiently large multiplicity of produced particles, larger than the multiplicity in the typical inelastic (bias) event.

Thus we can formulate the ideal experiment for search of high density partonic system:

" The deeply inelastic scattering with nucleus at low x with special selection of events with large multiplicity of produced particles. "

9.5 Method of pQCD(two diabols that we are fighting with).

Accordingly to our strategy we start with perturbative QCD in that region of Fig.19 where the density and coupling QCD constant (α_s) are small. Each observable (i.e gluon structure function) could be written in pQCD as following series:

$$xG(x,Q^2) \;=\; \Sigma_{n=0}\, C_n(\alpha_s)^n \cdot (L^n + a_{n-1}L^{n-1}...a_0)\ ,\ . \tag{45}$$

We have two big problems with this perturbative series which are two our biggest enemies:

1. The natural small parameter α_s is compensated by large log (L). The value of L depends on the process and kinematic region. For example in deeply inelastic scattering (DIS):

$$\Lambda \;=\; \log Q^2 \quad at \;\; Q^2 \gg Q_0^2 \; but \; x \;\sim\; 1$$
$$\Lambda \;=\; \log(1/x) \quad at \;\; Q^2 \;\sim\; Q_0^2 \; and \, x \;\to\; 0$$
$$\Lambda \;=\; \log Q^2 \cdot \log(1/x) \; at \;\; Q^2 \;\gg Q_0^2 \; and \, x \;\to\; 0$$
$$\Lambda \;=\; \log(1-x) \;\; at \;\; Q^2 \;\sim\; Q_0^2 \; and \; x \;\to\; 1$$

Of course it is not the full list of scales. The only that I would like to emphasize that L depends on the kinematic region. Thus to calculate $xG(x,Q^2)$ one cannot calculate only the Born Approximation but has to calculate the huge number of Feynman diagrams.

2.

$$C_N \;\to\; n! \quad at \quad n \;\gg\; 1$$

It means that we are dealing with asymptotic series and we do not know the general rules what to do with such series. There is only one rule, namely to find the analytic function which has the same perturbative series. Sometimes but very rarely we can find such analytic function. In this case this is the exact solution of our problem. Mainly we develop some general approach based on Leading Log Approximation (LLA). The idea is simple. Let us find the analytic function that sums the series:

$$xG(x,Q^2)_{LLA} \;=\; \Sigma_{n=0} C_n\,(\alpha_s \cdot L)^n\ . \tag{46}$$

Ussualy we can write the equation for function $xG(x,Q^2)_{LLA}$. The most famous one, the GLAP evolution equation [11], sums eq.(2) if L= $\log Q^2$. The BFKL [16] equation gives the answer for eq.(2) in the case when Λ=log$(1/x)$. Using the solution of the LLA equation we built the ratio:

$$R(x,Q^2)\ \frac{xG(x,Q^2)}{xG(x,Q^2)_{LLA}}\ =\ \Sigma_{n=0}r^n\ =\Sigma_{n=0}c_n\cdot(L^{n-1}+a_{n-1}L^{n-2}+...a_0)\ . \qquad (47)$$

This ratio is also asymptotic series but what we are doing we calculate this series term by term. Our hope is that the value of the next term will be smaller then the previous one ($\frac{r_n}{r_{n-1}}\ll 1$) for sufficiently large n. However we know that at some value of $n=N$ $\frac{r_N}{r_{N-1}}\sim 1$. The only that we can say about such situation in general that our calculation has intristic theoretical accuracy and the result of calculation should be presented in the form

$$R(x,Q^2)\ =\ \Sigma_{n=0}^{n=N-1}r_n\ \pm r_N\ . \qquad (48)$$

How big is the value of N depends mostly on how well we chose the LLA and how well we established the value of scale L in the process of interest.

9.6 Present Theoretical Status = Regeneration of Reggeon Calculus.

What we are doing now approaching the high density QCD domain is really the regeneration of the old idea of Reggeon Calculus, namely we reduce the complicated problem of quark and gluon interaction in the dense parton system to the interaction of our "building bricks", so called Pomerons (see Fig. 20, where the structure of our approach is shown). It looks like in old, good time of Reggeon Dominance but we have two new and very important ingredients:

1. The QCD Pomeron is not an invention but naturally appears in perturbative QCD in the leading $log(1/x)$ approximation (LL (x)A) to the scattering amplitude at high energy (the Balitski - Fadin -Kuraev - Lipatov (BFKL) equation [16]). It means that in a restricted kinematical region the BFKL Pomeron describes the high energy interaction within a certain guaranteed theoretical accuracy. This fact makes it unavoidable that one should build an effective theory starting with the BFKL Pomeron.

2. The vertices of the Pomeron interactions are not phenomenological parameters but can be calculated in perturbative QCD. It turns out that only two of them are essential in the vicinity of the border between pQCD and hdQCD regions in Fig.19, namely triple Pomeron vertex (γ) and rescattering of two Pomerons (λ) (see Fig.20).

We are going to discuss in detail the structure of the BFKL Pomeron as well as the theory of the shadowing corrections. The process which we consider is the deeply inelastic scattering in which all high energy phenomena occur at small distances where we can trust the pQCD calculation.

10 Pomeron in pQCD (the BFKL Pomeron)

The BFKL equation was derived in so called Leading Log (1/x) Approximation, in which we would like to keep the contribution of the order of $(\alpha_S log(1/x))^n$ and neglect all other contributions, even of the order of $\alpha_S\ log(Q^2/Q_0^2)$. So the set of parameters in LL(1/x)A is obvious:

$$\begin{aligned} \alpha_S\ log\frac{1}{x}\ &\sim\ 1\ ; \\ \alpha_S\ log\frac{Q^2}{Q_0^2}\ &<\ 1\ ; \\ \alpha_S\ &\ll\ 1\ ; \end{aligned} \tag{49}$$

Let us consider the simplest process: the quark - quark scattering at high energy at zero momentum transfer . All problems of infrared divergency in such a process is irrelevant since they are canceled in the scattering of two colorless hadrons . We will show this fact using the example of the first diagram (the Born Approximation (BA)).

10.1 The Born Approximation

In the Born Approximation the only diagram of Fig. 21(a) contributes to the imaginary part of the scattering amplitude (A). It is easy to understand that the result of calculation of this diagram gives [‡]:

$$2\,\mathrm{Im}\{A^{BA}(s,t=0)\}\ =\ \int\frac{d^2k_t}{(2\pi)^2}|\ M(2\to 2;\,\alpha_S\mid s,t=-k_t^2)\ |^2\ =\ s\frac{C_2^2\alpha_S^2}{N^2-1}\int\frac{d^2k_t}{k_t^4}\ , \tag{50}$$

where $M(2\to 2;\,\alpha_S\,|\,s,t=-k_t^2)$ denotes the amplitude in the lowest order of α_S for quark - quark scattering at transfer momentum $t=-k_t^2$ through one gluon exchange (see Fig.21(a)), N is the number of colours and $C_2\ =\ \frac{N^2-1}{2N}$. One can recognize the Low - Nussinov mechanism [17] of high energy interaction in this simple example.

[‡]Let me recall you that we are keeping the coupling constant fixed.

Let us consider the BA in more detail for the scattering of two mesons (a and b), assuming that each of them consists of two heavy quarks. Such a system has sufficiently small size, namely

$$r \ \propto \ \frac{1}{M_Q \alpha_{\rm S}}$$

and can be treated in pQCD.

Let me remind you why the size is small. The total energy of two quarks in Coulomb potential is equal:

$$E \ = \ \frac{p^2}{M_Q} \ - \ \frac{\alpha_{\rm S}}{r}$$

If we remember the uncertainty principle

$$\Delta p \Delta r \ \simeq 1 \ \ or \ \ p \ \simeq \ \frac{1}{r}$$

we get for the system with $E \to 0$ that size which we have mentioned before.

Repeating the calculations we get the same answer as for quark - quark scattering, namely

$$\sigma^{BA} \ = \ \alpha_{\rm S}^2 \, \frac{2}{9} \cdot 4 \cdot n_a n_b \int \frac{d^2 k_t}{(k - \frac{q}{2})_t^2 \, (k + \frac{q}{2})_t^2} \ \cdot \ \Phi_a(k,q) \, \Phi_b(k,q) \qquad (51)$$

where $n_a (n_b)$ is the number of quarks in the meson $a(b)$, the factor $\frac{2}{9}$ is the result of averaging over colours of the initial quarks and $\Phi(k,q)$ is the amplitude of the emission of two gluons by a meson.

•

Problem 15: Show that the emission amplitude Φ can be expressed in terms of meson formfactors if we can treat the heavy quarks as nonrelativistic particles (see Fig.22(c)) :

$$G(q^2)_a \ = \ \int dp \Psi_a(p) \, \Psi_a^*(p-q);$$

$$\Phi_a(k,q) \ = \ \int dp \Psi_a(p) \, \Psi_a^*(p-q) \ - \ \int dp \Psi_a(p+\frac{q}{2}+k) \, \Psi_a^*(p+\frac{q}{2}-k) \ = \ G_a(q^2) - G_a(4k^2).$$

•

Finally, we have

$$\sigma^{BA} \ = \ \alpha_{\rm S}^2 \, \frac{2}{9} \cdot 4 \cdot n_a n_b \int \frac{d^2 k_t}{k_t^4} \ \cdot \ [\, G_a(0) - G_a(4k^2) \,] \, [\, G_b(0) - G_b(4k^2) \,] \qquad (52)$$

Now let us ask the question what kinematic region of integration over k_t gives the biggest contribution to the total cross section if two mesons have different sizes, let say $r_a \gg r_b$. We can study three regions of integration:

1. $\lambda > r_a$, where λ is the wave length of the gluon ($\lambda = \frac{1}{k_t}$).

In this case $k_t r_a < 1$ as well as $k_t\, r_b < 1$ and

$$G_a(0) - G_a(4k^2) \,\rightarrow\, \frac{4}{6} r_a^2 k_t^2$$

$$G_b(0) - G_b(4k^2) \,\rightarrow\, \frac{4}{6} r_b^2 k_t^2$$

The integral over k_t gives you the answer

$$\sigma^{BA} \,\simeq\, r_b^2$$

2.$r_a > \lambda > r_b$

In this case $k_t r_a > 1$ as well as $k_t\, r_b < 1$ and

$$G_a(0) - G_a(4k^2) \,\rightarrow\, 1$$

$$G_b(0) - G_b(4k^2) \,\rightarrow\, \frac{4}{6} r_b^2 k_t^2$$

The integral over k_t gives you the answer

$$\sigma^{BA} \;=\; \alpha_{\rm S}^2 \frac{2\pi}{9} \cdot 4 \cdot n_a n_b \cdot \frac{2}{3} \cdot r_b^2 \ln \frac{r_a^2}{r_b^2} \tag{53}$$

3. $r_b > \lambda$

It means that $k_t r_a > 1$ as well as $k_t\, r_b > 1$ and

$$G_a(0) - G_a(4k^2) \,\rightarrow\, 1$$

$$G_b(0) - G_b(4k^2) \,\rightarrow\, 1$$

The integral over k_t gives you the same answer as in the first kinematic region, namely:

$$\sigma^{BA} \,\simeq\, r_b^2$$

This example is very instructive, because our standard process - DIS which we can treat using pQCD and in DIS the typical size of our probe - virtual photon is the smallest one in the process and is of the order of $\frac{1}{Q}$. It means that the BA gives for the DIS the total cross section which is proportional $\frac{1}{Q^2} \ln(Q^2 R^2)$ where R is the size of the target. It should be stressed as has been mentioned that the total cross section does not depend on energy in BA.

10.2 The next order of α_S approximation.

In the next order we have to consider a larger number of the diagrams, but we can write down the answer in the following general form:

$$2\,\mathrm{Im}\{A^{NBA}(s,t=0)\} \;= \tag{54}$$

$$\int (2\pi)^4\delta^{(4)}(\mathbf{p_1}+\mathbf{p_2}-\mathbf{p'_1}-\mathbf{p'_2}-\mathbf{q})|\; M(2\to 3;g^3)\;|^2\;\Pi_{i=1}^{i=3}\frac{d^3p'_i}{(2\pi)^3 2E'_i}\;+$$

$$\int (2\pi)^4\delta^{(4)}(\mathbf{p_1}+\mathbf{p_1}-\mathbf{p'_1}-\mathbf{p'_2})\cdot 2\;\mathrm{Re}\{M(2\to 2;\alpha_S^2)\cdot M^*(2\to 2;\alpha_S)\}\Pi_{i=1}^{i=2}\;\frac{d^3p'_i}{(2\pi)^3 2E'_i}\;,$$

where g is coupling constant of QCD ($\alpha_S = \frac{g^2}{4\pi}$); $M(2\to 3;g^3)$ is the amplitude for the production of the extra gluon in the Born Approximation, and is given by the set of Feynman diagram in Fig.22 while $M(2\to 2,\alpha_S^2)$ is the amplitude of the elastic scattering in the next to leading Born Approximation (see Fig. 23) at the momentum transfer k_t.

Two terms in eq. (54) have different physical meaning: the first one describes the emission of the additional gluon in the final state of our reaction, while the second term is the virtual correction to the Born Approximation due to the emission of the additional gluon. It corresponds to the same two particle final state, and describes the fact that due to emission the probability to detect this final state becomes smaller (we will see later that the sign of the second term is negative).

In the both terms of eq. (54) we can integrate over $\vec{\mathbf{p_3}}'$ as well as over the longitudinal component of $\vec{\mathbf{p}}'_\mathbf{1}$ (p'_{1L}). Finally, we rewrite the phase space in the following way:

$$\int (2\pi)^4\delta^{(4)}(\mathbf{p_1}+\mathbf{p_2}-\mathbf{p'_1}-\mathbf{p'_2}-\mathbf{q}\;\Pi_{i=1}^{i=3}\frac{d^3p'_i}{(2\pi)^3 2E'_i}\;=\;\frac{1}{4\pi}\cdot\frac{1}{s}\cdot\int_{x_{min}=\frac{m^2}{s}}^1\frac{dx'_3}{x'_3}\int\frac{d^2p'_{1t}d^2p'_{3t}}{(2\pi)^4}\;;$$

$$\int (2\pi)^4\delta^{(4)}(\mathbf{p_1}+\mathbf{p_1}-\mathbf{p'_1}-\mathbf{p'_2})\cdot\Pi_{i=1}^{i=2}\;\frac{d^3p'_i}{(2\pi)^3 2E'_i}\;=\;\frac{1}{s}\cdot\int\frac{d^2p'_{1t}}{(2\pi)^2}\;; \tag{55}$$

where x is the fraction of the longitudinal momentum carried by particle. the value of x_{min} depends on the reaction. For example in the deeply inelastic scattering $x_{min} = x_B = \frac{|Q^2|}{s}$. In the case of the quark scattering $x_{min} = \frac{m_t^2}{s}$ where m_t is the transverse mass of produced quark.

From eq. (55) one can see the origin of the $log(1/x_{min})$ contribution: it stems from the phase space integration, if $M(2\to 3)$ does not go to zero at $x_3\to 0$. To sum the diagrams of Fig. 22 in this limit we can use two tricks. The first one is for each t-

channel gluon one can rewrite the numerator of the gluon propagator at high energy in the following way:

$$g_{\mu\nu} \;=\; \frac{p_{1\mu}p_{2\nu} \;+\; p_{2\mu}p_{1\nu}}{p_1 \cdot p_2} \;+\; O(\;\frac{m^2}{s}\;) \tag{56}$$

The second trick is based on the gauge invariance of the QCD. We look on the subset of the diagrams of Fig. 22 pictured in Fig. 24 as the amplitude of the interaction of gluon k with the quark p_2 (see Fig.24). Since all particles in amplitude M_ν except gluon k are on the mass shell, the gauge invariance leads to the relationship:

$$k_\nu M_\nu \;=\; 0\;. \tag{57}$$

Using Sudakov variables [18] we can expand vector k as

$$k_\nu \;=\; \alpha_k\, p_{1\nu} \;+\; \beta_k\, p_{2\mu} \;+\; k_{t\mu}$$

and rewrite eq. (57) in the form:

$$(\;\alpha_k\, p_{1\nu} \;+\; \beta_k\, p_{2\mu} \;+\; k_{t\mu}\;)\;M_\nu \;=\; 0\;. \tag{58}$$

We note that all particle inside M_ν have a large component of their momentum on p_2. It means that we can neglect the projection of vector M_ν on p_1, or in other words

$$M_\nu \;=\; M^{(1)}p_{1\nu} \;+\; M^{(2)}p_{2\nu} \;+\; M^{(t)}_\nu$$

and $M^{(1)} \ll M^{(2)}$. Thus we can conclude from eq. (58) that

$$p_{1\nu}M_\nu \;=\; -\,\frac{k_{t\nu}M_\nu}{\alpha_k}\;. \tag{59}$$

Using both tricks of eq. (56) and eq. (59) one can easily see that only diagram of Fig. 24(1) contributes in LL(log(1/x)A. Indeed, let us consider for example the diagram of Fig. 24(2), the dominator of the quark propagator $(p_2+k)^2$ is equal to

$$(p_2 \;+\; k)^2 \;=\; \alpha_k s \;+\; k_t^2 \;=\; -\,\frac{p_{3t}'^2}{x_3} \;+\; k_t^2 \;\sim\; -\,\frac{p_{3t}'^2}{x_3}\;.$$

Since due to eq. (59) the polarization of gluon k is transverse we cannot compensate the smallness this diagram at $x_3 \to 0$. Using the same tricks with the upper parts of the diagrams of Fig. 22 we arrive at the conclusion that that the set of the diagrams of Fig. 22 degenerates into one diagram of Fig. 25 with specific vertex for gluon emission:

$$\Gamma_\sigma \;=\; i\,g\,f_{abc}\cdot\frac{2\,k_{t\mu}\,k'_{t\nu}}{\alpha_k\beta_{k'}s}\,\gamma_{\mu\sigma\nu}\;, \tag{60}$$

where $\gamma_{\mu\sigma\nu}$ is given by the usual Feynman rules for QCD.

Substituting eq. (60) into the first term of eq. (54) we get the contribution of the emission of one additional gluon to the next to Born Approximation in the form:

$$\mathrm{Im}\{A^{NBA}_{emission}\} \;=\; s\,\frac{\alpha_S^2\,C_2^2}{N^2\,-\,1}\int_0^y dy'\int\frac{d^2k_t}{\pi\,k^4}\cdot\frac{N\alpha_S}{\pi}\cdot K_{emission}(k_t,k_t')\cdot\frac{d^2k_t'}{\pi\,k'^4}\;, \qquad (61)$$

where $y' = log(1/x_3)$, $y = log(1/x_{min}$ and the kernel $K(k_t, k_t')$ is equal to

$$K_{emission}(k_t,k_t') \;=\; \frac{k_t^2\,k_t'^2}{(\,k_t\;-\;k_t'\,)^2} \qquad (62)$$

.

To calculate the virtual correction in the next to Born Approximation ($M(\,2\,\rightarrow\,2\,;\alpha_S^2\,)$) we have to estimate the contribution of the set of diagrams of Fig. 23. The log (1/x) contribution is hidden in the real part of the amplitude $M(\,2\,\rightarrow\,2\,;\alpha_S^2\,)$, and easiest way to extract this log is to use the dispersion relation:

$$M(\,2\,\rightarrow\,2\,;\,\alpha_S^2\,) \;=\; \frac{1}{\pi}\cdot\{\int\frac{\mathrm{Im}\{M(\,2\,\rightarrow\,2\,;\,\alpha_S^2\,)\}_s}{s'\;-\;s}\,d\,s'\;+\;\frac{\mathrm{Im}\{M(\,2\,\rightarrow\,2\,;\,\alpha_S^2\,)\}_u}{u'\;-\;u}\,d\,u'\,\}\;. \qquad (63)$$

We calculate $\mathrm{Im}\{M(\,2\;\rightarrow\;2\,;\,\alpha_S^2\,)\}_s$ and $\mathrm{Im}\{M(\,2\;\rightarrow\;2\,;\,\alpha_S^2\,)\}_u$ using unitarity (see eq. (50)):

$$\mathrm{Im}\{M(\,2\,\rightarrow\,2\,;\,\alpha_S^2\,|\,t\,=\,-k_t^2\,)\}_s \;= \qquad (64)$$

$$\int\frac{d^2k_t'}{(2\pi)^2}|\;\mathrm{Re}\{M(2\rightarrow 2;\,\alpha_S\mid s,t=-k_t'^2)\;M(2\rightarrow 2;\,\alpha_S\mid s,t=-(k_t-k_t')^2\,)\}\;.$$

The difference between eq. (100) and eq. (50) is that the Born amplitude for one gluon exchange enters these two equations at different values of momentum transferred t. The explicit calculations give:

$$\mathrm{Im}\{M(\,2\,\rightarrow\,2\,;\,\alpha_S^2\,|\,t\,=\,-k_t^2\,)\}_s \;=\; s\,\cdot\,C_s\,\pi\,\Sigma(k_t^2); \qquad (65)$$

$$\mathrm{Im}\{M(\,2\,\rightarrow\,2\,;\,\alpha_S^2\,|\,t\,=\,-k_t^2\,)\}_u \;=\; s\,\cdot\,C_u\,\pi\,\Sigma(k_t^2);$$

$$\Sigma(k_t^2) \;=\; \frac{4\alpha_S}{\pi^2}\int\frac{d^2k_t'}{(\,k_t-k_t'\,)^2\,k_t'^2}\;;$$

Using the dispersion relation of eq. (63) one can reconstruct the real part of the amplitude and the answer is

$$\mathrm{Re}\{M(\,2\,\rightarrow\,2\,;\,\alpha_S^2\,|\,t\,=\,-k_t^2\,)\} \;=\; s\,(\,C_u\;-\;C_s\,)\cdot\Sigma(k_t^2)\cdot logs \qquad (66)$$

The colour coefficients have a very famous relation between them (see Fig. 26) which gives, for the difference of the colour coefficients in eq. (66) the same colour structure as for the diagram of Fig. 23 (3). Thus $\mathrm{Re}\{M(\,2\,\rightarrow\,2\,;\,\alpha_{\mathrm{S}}^2\,|\,t\,=\,-k_t^2\,)\}$ has the same colour structure as one gluon exchange in the Born Approximation. This fact makes it possible to rewrite the second term in eq. (54) as the correction to the gluon trajectory, e.g. instead of gluon with propagator $\frac{1}{k^2}\cdot s$ we can introduce the new propagator

$$\frac{1}{k^2}\cdot s^{\alpha^G(k^2)} \tag{67}$$

$$\alpha^G(k^2)\;=\;1\;-\;\frac{\alpha_{\mathrm{S}}N}{\pi^2}\cdot\int\frac{k_t^2d^2k_t'}{(\,k_t\,-\,k_t'\,)^2\,k_t'^2}\;=\;1\;-\;\frac{\alpha_{\mathrm{S}}N}{2\pi^2}\cdot\int\frac{k_t^2d^2k_t'}{[\,(\,k_t\,-\,k_t'\,)^2\,+\,k_t'^2\,]k_t'^2}$$

The answer for the second term in eq. (54) can be written in the form

$$\mathrm{Im}\{A_{virtual}^{NBA}\}\;=\;s\,\frac{\alpha_{\mathrm{S}}^2C_2^2}{N^2\,-\,1}\int\left(\,\alpha^G(k^2)\;-\;1\,\right)\cdot 2\cdot\frac{d^2k_t}{k_t^4}\;. \tag{68}$$

We can get the full answer for the amplitude in the next to the Born Approximation (α_{S}^3 by summing eq. (61) and eq. (68) and it can be written in the form:

$$\mathrm{Im}\{A^{NBA}(s,t=0)\}\;=\;s\,\frac{\alpha_{\mathrm{S}}^2\,C_2^2}{N^2\,-\,1}\;\int_0^y dy'\int\frac{d^2k_t}{k_t^2}\cdot\frac{\alpha_{\mathrm{S}}N}{\pi^2}\cdot K(k_t,k_t')\cdot\frac{d^2k_t'}{k_t'^2} \tag{69}$$

where $y\,=\,log(1/x_{min}$ and

$$K(k_t,k_t')\cdot\frac{1}{k_t'^2}\;=\;\frac{1}{(\,k_t\,-\,k_t'\,)^2}\cdot\frac{1}{k_t'^2}\;-\;\frac{k_t^2}{(\,k_t\,-\,k_t'\,)^2\,[\,(\,k_t\,-\,k_t'\,)^2\,+\,k_t'^2\,]}\cdot\frac{1}{k_t^2}\;. \tag{70}$$

Using eqs. (69)–(70) we can introduce function $\phi(k_t^2)$ and rewrite the total cross section for quark - quark scattering in the form:

$$\sigma_{qq}\;=\;\frac{\alpha_{\mathrm{S}}C_2}{N^2\,-\,1}\cdot\int\phi(y,k_t^2)\cdot\frac{dk_t^2}{k_t^2}\;. \tag{71}$$

For ϕ eq. (69) gives the equation:

$$\phi^{(2)}(y,k_t^2)\;=\;\frac{\alpha_{\mathrm{S}}N}{\pi^2}\cdot\int_0^y dy'\int d^2k_t'K(k_t,k_t')\;\phi^{(1)}(y',k_t'^2)\;. \tag{72}$$

where

$$K(k_t,k_t')\phi(k_t^2)\;=\;\frac{1}{(\,k_t\,-\,k_t'\,)^2}\cdot\phi(k_t'^2)\;-\;\frac{k_t^2}{(\,k_t\,-\,k_t'\,)^2\,[\,(\,k_t\,-\,k_t'\,)^2\,+\,k_t'^2\,]}\cdot\phi(k_t^2)\;. \tag{73}$$

and

$$\phi^{(1)}\;=\;\frac{\alpha_{\mathrm{S}}C_2}{k_t^2}\;. \tag{74}$$

10.3 The main property of the BFKL equation.

From the simplest calculation in α_S^3 order one can guess the BFKL equation [16] which looks as follows:

$$\frac{d\phi(\, y\, =\, log(1/x), k_t^2\,)}{dy}\;\; =\;\; \frac{\alpha_S N}{\pi^2}\cdot \int K(\, k_t, k_t'\,)\,\phi(\, y, k_t'^2\,)\, d^2k_t'\;, \tag{75}$$

where kernel $K(k_t, k_t')$ is defined by eq. (73). This equation sums the $(\alpha_S log(1/x))^n$ contributions and has "ladder" - like structure (see Fig. 27). However, such "ladder" diagrams are only an effective representation of the whole huge set of the Feynman diagrams, as explained in the simplest example of the previous subsection. The first part of the kernel $K(k_t, k_t')$ describes the emission of new gluon, but with the vertex which differs from the vertex in the Feynman diagram, while the second one is related to the reggeization of all t-channel gluons in the "ladder".

The solution of the BFKL equation has been given in ref. [16] and we we would like to recall some main properties of this solution.

10.3.1 Eigenfunctions of the BFKL equation.

The eigenfunction of the kernel $K(k_t, k_t')$ is $\phi_f \;=\; (k_t^2)^{f-1}$. Indeed after sufficiently long algebra we can see that

$$\frac{1}{\pi}\int d^2k_t' K(k_t, k_t')\;\; \phi_f(k_t'^2)\;\; =\;\; \chi(f)\;\; \phi_f(k_t^2) \tag{76}$$

where

$$\chi(f)\;\; =\;\; 2\,\Psi(1)\;\; -\;\; \Psi(f)\;\; -\;\; \Psi(1-f) \tag{77}$$

and

$$\Psi(f)\;\; =\;\; \frac{d\;\ln\Gamma(f)}{d\;f}\;,$$

$\Gamma(f)$ is the Euler gamma function.

10.3.2 The general solution of the BFKL equation.

From eq. (76) we can easily find the general solution of the BFKL equation using double Mellin transform:

$$\phi(y, k_t^2)\;\; =\;\; \int\;\frac{d\omega}{2\pi\, i} e^{\omega\, y}\phi(\omega, k_t^2)\;\; =\;\; \int \frac{d\omega df}{(2\pi\, i)^2} e^{\omega\, y}\phi_f(k_t^2)\, C(\omega, f) \tag{78}$$

where the contours of integration over ω and f are situated to the right of all singularities of $\phi(f)$ and $C(\omega, f)$. For $C(\omega, f)$ the equation reads

$$\omega\, C(\omega, f) \;=\; \frac{\alpha_S N}{\pi}\, \chi(f)\, C(\omega, f)\ . \tag{79}$$

Finally, the general solution is

$$\phi(y, k_t^2) \;=\; \frac{1}{2\pi\, i} \int df\, e^{\frac{\alpha_S N}{\pi}\, \chi(f) y\, +\, (f-1)\, r}\, \tilde{\phi}(f) \tag{80}$$

where $\tilde{\phi}(f)$ should be calculated from the initial condition at $y = y_0$ and $r = ln\frac{k_t^2}{q_0^2}$ (q_0^2 is the value of virtuality from which we are able to apply perturbative QCD) .

10.3.3 Anomalous dimension from the BFKL equation.

We can solve eq. (79) in a different way and find $f = \gamma(\omega)$. $\gamma(\omega)$ is the anomalous dimension in LL(log (1/x)A [§] and for $\gamma(\omega)$ we have the following series [19]

$$\gamma(\omega) \;=\; \frac{\alpha_S N}{\pi} \cdot \frac{1}{\omega} \;+\; \frac{2\alpha_S^4 N^4 \zeta(3)}{\pi^4} \cdot \frac{1}{\omega^4} \;+\; O(\frac{\alpha_S^5}{\omega^5}) \tag{81}$$

•

Problem 16: Get eq.(81) from eq.(79), expanding it with respect to $f = \gamma(\omega)$.

•

The first term in eq. (81) is the anomalous dimension of the GLAP equation [11] in leading order of α_S at $\omega \to 0$, which gives the solution for the structure function at $x \to 0$ and corresponds to so called double log approximation of perturbative QCD (DLA).The DLA sums the contributions of the order $(\alpha_S\, log(1/x)\, log(Q^2/q_0^2))^n$ in the perturbative series of eq.(45).

However, we would like to stress that eq. (81) is valid only at fixed α_S while the anomalous dimension in the GLAP equation can be calculated for running α_S. It means that we have to introduce the running α_S in the BFKL equation to achieve a matching with the GLAP equation in the region where $\omega \ll 1$ and $\frac{\alpha_S}{\omega} < 1$.

The second remark is the fact that we can trust the series of eq. (81) only for the value of $\omega \gg \omega_L$, where

$$\omega_L \;=\; \frac{\alpha_S\, N}{\pi} \cdot \chi(\,\frac{1}{2}\,) \;=\; \frac{4N\, ln2\, \alpha_S}{\pi}\ . \tag{82}$$

[§]From eq. (78) one can notice that moment variable N defined such that N = ω + 1.

In vicinity $\omega \rightarrow \omega_L$ we have the following expression for $\gamma(\omega)$:

$$\gamma(\omega) \;=\; \frac{1}{2} \;+\; \sqrt{\frac{\omega \;-\; \omega_L}{\frac{\alpha_S N}{\pi}\, 14\zeta(3)}}\;. \tag{83}$$

•

Problem 17: Get eq.(83) front eq. (79), using the property of $\Psi(f)$.

•

Substituting eq. (83) in eq. (78) we have

$$\phi(y,k_t^2) \;=\; \int \frac{d\omega}{2\pi\, i}\; e^{\omega\, y}\phi(\omega,k_t^2) \;=\; \int \frac{d\omega}{2\pi\, i}\; e^{\omega\, y \,+\, (\,\gamma(\omega)\,-\,1\,)\, r}\tilde{\phi}(\omega) \;= \tag{84}$$

$$\int \frac{d\omega}{2\pi\, i}\; e^{(\,\omega\,-\,\omega_L\,)\, y \,+\, (\,-\frac{1}{2}\,+\,\sqrt{\frac{\omega\,-\,\omega_L}{\frac{\alpha_S N}{\pi}\, 14\zeta(3)}}\;\,)\, r}\;\tilde{\phi}(\omega)\;.$$

Evaluating the above integral using saddle point approximation we obtain

$$\omega_S \;=\; \omega_L \;+\; \frac{1}{\frac{\alpha_S N}{\pi}\, 14\zeta(3)}\cdot\frac{r^2}{4\, y^2} \tag{85}$$

which gives the answer:

$$\phi(y,k_t^2) \;=\; \frac{1}{\sqrt{k_t^2\, q_0^2}}\cdot\tilde{\phi}(\omega_S)\cdot\sqrt{\frac{2\,\pi\,(\,\omega_S-\omega_L\,)}{y}}\cdot e^{\omega_L\, y \,-\, \frac{ln^2\frac{k_t^2}{q_0^2}}{\frac{\alpha_S N}{\pi}\, 28\zeta(3)\, y}}\;. \tag{86}$$

We can trust this solution in the kinematic region where $(\,ln\frac{k_t^2}{q_0^2}\,)^2 \;\leq\; \frac{\alpha_S N}{\pi}\, 28\zeta(3)\, y$. The solution of eq. (86) illustrates one very important property of the BFKL equation, namely k_t^2 can be not only large, but with the same probability it can also be very small. It means that if we started with sufficiently big value of virtuality q_0^2 at large value of $y \;=\; ln(1/x)$ due to evolution in y the value of k_t^2 could be small ($k_t \;\sim\; \Lambda$, where Λ is QCD scale). Therefore, the BFKL equation is basically not perturbative and the worse thing, is that we have not yet learned what kind of assumption about the confinement has been made in the BFKL equation.

Our strategy for the further presentation is to keep $k_t^2 \;>\; q_0^2$ and to study what kind of nonperturbative effect we can expect on including the running α_S in the BFKL equation, as well as changing the value of ω_L in the series of eq. (81).

10.3.4 The bootstrap property of the BFKL equation.

We have discussed the BFKL equation for the total cross section, however this equation can also be proved for the amplitude at transfer momentum $q^2 \neq 0$, and not only for colorless state of two gluons in t-channel. The general form of the BFKL equation in ω - representation looks as follows [16] (see eq. (78):

$$(\omega - \omega^G(k_t^2) - \omega^G((q-k_t)^2))\phi(\omega, q, k_t) = \frac{\alpha_S}{2\pi}\lambda_R \int \frac{d^2k'_t}{\pi} K(q, k_t, k'_t)\phi(\omega, q, k'_t) , \quad (87)$$

where the kernel $K(q, k_t, k'_t)$ describes only gluon emission and

$$K(q, k_t, k'_t) = \frac{k_t^2}{(k_t - k'_t)^2 k_t'^2} + \frac{(q-k_t)^2}{(k_t - k'_t)^2 (q-k'_t)^2} - \frac{q_t^2}{(q_t - k'_t)^2 k_t'^2} , \quad (88)$$

λ_R is colour factor where $\lambda_1 = 2\lambda_8 = N$ for singlet and (N^2-1) representations of colour SU(N) group and $\omega^G(k_t^2) = \alpha^G(k_t^2) - 1$ (see eq. (67)).

The bootstrap equation means that the solution of the BFKL equation for octet colour state of two gluons (for colour SU(3)), should give the reggeizied gluon with the trajectory $\alpha^G(k_t^2)$ (or $\omega^G(k_t^2)$) given by eq. (67). The fact that the gluon becomes a Regge pole have been shown by us in the example of the next to the Born Approximation, and has been used to get the BFKL equation in the singlet state. It means that the solution of the BFKL equation in the octet state should have the form of a Regge pole :

$$\phi(\omega, q, k_t) = \frac{Const}{\omega - \omega^G(q^2)} \quad (89)$$

Assuming eq. (89), one arrives to the following bootstrap equation:

$$\omega^G(q^2) - \omega^G(k_t^2) - \omega^G((q-k_t)^2) = \frac{\alpha_S}{2\pi}\lambda_8 \int \frac{d^2k'_t}{\pi} K(q, k_t, k'_t) , \quad (90)$$

It is easy to check that the trajectory of eq. (67) satisfies this equation. It is interesting to mention that we can use eq. (90) to reconstruct the form of the kernel $K(q, k_t, k'_t)$, if we know the expression for the trajectory (see ref.[20]).

10.4 Corect degrees of freedom at low x.

In the previous subsections we gave the traditional derivation of the BFKL equation, which is rather difficult and demands a good experience in calculation of Feynman diagrams. It

is very important to understand better the physical meaning and the formal grounds of the BFKL equation. I firmly believe that during this year A. Mueller [21] (see also related papers [22]) has achieved the considerable progress in both understanding and formal derivation of the BFKL equation and its generalization. Mueller's main idea is to construct the small x infinite momentum partonic wavefunction of a hadron in QCD while BFKL calculated the amplitude for n - gluon production in so called multireggeon kinematic region. The wavefunction gives us much richer information on the hadron interaction, has very transparent physical meaning and makes the bridge between our parton approach to "hard" processes and new phenomena that we anticipate in the region of high density QCD.

1.

The technical trick that has been used is also very instructive, namely it turns out that the wavefunction looks much simpler in the mixed representation in which each parton is labeled by its fraction of the total hadron momentum x_i and the transverse coordinate r_{ti}. The transverse coordinate is especially useful since in the low x_i region the i^{th} gluon can be considered as being emitted from the system of $i-1$ partons with spatial transverse coordinates of these "sources" being frozen during the emission of $i-th$ gluon. Thus we can consider these of $i-1$ partons as a system of $(i-1)$ $q\bar{q}$ dipoles since each gluon can be viewed as quark - antiquark pair if number of colours N_c is big enough. So the only thing that one needs to write down is the emission of the $i-th$ gluon by such a system of dipoles. This problem has been solved in ref.[21]. For example for emission of gluon $(x_2, r_{tG} = r_2)$ from one dipole which is the quark $(x_q = 1-x_1, r_{tq} = r_0 = 0)$ and antiquark $(x_{\bar{q}} = x_1, r_{t\bar{q}} = r_1)$ is equal to

$$\psi^{(1)}(x_1, x_2; r_1, r_2) \;=\; -\frac{igT^a}{\pi}\psi^{(0)}(x_1; r_1)\{\frac{r_{2\lambda}}{r_2^2} \;-\; \frac{r_{21\lambda}}{r_{21}^2}\}\cdot\epsilon_2^{\lambda}\;. \tag{91}$$

2.

Mueller made one very important step in our understanding of our parton system, namely he found what sum rule plays the role of the momentum sum rules in the GLAP approach for low x_i partons. This sum rules is the normalization of the partonic wavefunction:

$$\int\prod^{n}\frac{dx_i}{x_i}\prod^{n}d^2r_{ti}|\Psi(x_1,...x_n;r_{t1},...r_{tn})|^2 \;=\; 1\;. \tag{92}$$

Using this equation one can easily take into account so called virtual corrections, which in this case are mostly known as gluon reggeization or non -Sudakov form factor. The importance of this step can be compared only with the transition from Gribov - Lipatov

form of usual evolution equation with Sudakov form factor in the kernel to well known Lipatov - Altarelli - Parisi elegant form based on direct use of the momentum sum rules in QCD.

3.

The physical application of this new approach has not been considered but Mueller noted at his Durham talk [23] that his approach will be able to resolve the old problem with the BFLK equation. Indeed, the physical meaning of the growth of the structure function at $x_B \to 0$ is the increase of the number of "wee" partons (N) that can interact with the target ($N \propto x_B^{-\omega_0}$)(see, for example, review [24]). However the multiplicity of gluons calculated as the ratio $\int \frac{E d^3\sigma}{dA^3 p_{jet}}/\sigma_t$ turns out to be small (of the order of $\alpha_s \ln \frac{1}{x_B}$). It means that partons are in a very coherent state in a typical inelastic event. However the behaviour of the parton cascade at large multiplicity should be quite different from Poisson distribution since at large multiplicity all N parton can be freed in the interaction.

.

The main progress was related to the fact that they discovered the correct degrees of freedom for the region of small x in QCD. They showed that if we discuss the deeply inelastic processes not in terms of quark and gluons as we did before but introducing new degrees of freedom, namely the color dipole of the definite size (d), we still can use the simple probabilistic interpretation in the region of low x. It means that the physical meaning of the deep inelastic structure function is not the number of quark or gluons but the number of the color dipoles with the sizes larger than $1/Q$ ($d > \frac{1}{Q}$). It is worthwhile mentioning that at $x \sim 1$ we still can use our old interpretation as probability to find parton but as well as a new one.

•

Problem 18: Read Mueller's paper[21] and try to understand how simple looks the BFKL equation in new degrees of freedom.

•

The main progress in the Mueller approach was related to the fact that he discovered the correct degrees of freedom for the region of small x in QCD. He showed that if we discuss the deeply inelastic processes not in terms of quark and gluons as we did before but introducing new degrees of freedom, namely the colour dipole of the definite size (d), we still can use the simple probabilistic interpretation in the region of low x. It means that the physical meaning of the deep inelastic structure function is not the number of quark or gluons but the number of the colour dipoles with the sizes larger than $1/Q$

($d > \frac{1}{Q}$). It is worthwhile mentioning that at $x \sim 1$ we still can use our old interpretation as probability to find parton but as well as a new one.

This idea shed a light on all technicalities of the BFKL equation which was the manifestation of the artistic skill in the calculation of Feynman diagrams and reduced the high art to normal physics understandable for a normal post-doc. I anticipate a big progress in the development of all kind problems related to high energy QCD based on Mueller approach.

11 New physical phenomena at small x_B:

Let us outline the new phenomena which we anticipate to occur in the region of small x_B in perturbative QCD for the case of deeply inelastic scattering. Three of them are particularly important and determine the physical picture of the parton evolution, or cascade as we shall call it, in the region of small x_B, namely:

1. The increase of the parton density [16] at $x_B \to 0$.

2. The growth of the mean transverse momentum of a parton inside the parton cascade at low x_B [16] [25].

3. The saturation of the parton density [25].

Before discussing each of these phenomena in turn, let us try to understand these new phenomena at small x_B by recalling some facts regarding perturbation theory and deeply inelastic scattering. According to the factorization theorem, the deep-inelastic structure function is a product of a parton density and a short distance coefficient function, which is calculable in perturbation theory. Both factors depend on the factorization scale, which we choose equal to Q^2. Concentrating on the gluon density, in the kinematical region we are considering the former can be represented as

$$xG(x,Q^2) = \Sigma_n C_n(Q_0^2)(\alpha_s L)^n \ + \ O(\alpha_s(\alpha_s L)^n) \ , \tag{93}$$

where L is the large logarithm in our problem. The coefficients $C_n(Q_0^2)$ contain nonperturbative information and depend on the initial scale Q_0^2 of the cascade, see Fig.28,

To see what kind of large logarithm could occur, one can examine the probability of emission P_i of the i-th parton in the cascade. Near $x = 0$ it can be written as

$$P_i = \frac{N_c \alpha_s}{\pi} \cdot \frac{dx_i}{x_i} \cdot \frac{dq_{it}^2}{q_{it}^2}$$

1. In the region of large virtualities of the photon in deep inelastic scattering (but not at very small values of x_B) L is equal to $\ln Q^2$.

2. At Q^2 fixed ($Q^2 \simeq Q_0^2 \gg m^2_{proton}$) but at small value of x_B we have a different large logarithm in eq.(2), namely $L = \ln \frac{1}{x_B}$.

3. When both $\ln Q^2$ and $\ln \frac{1}{x_B}$ are large ($Q^2 \gg Q_0^2$ $x_B \to 0$) the large logarithm has a more complicated form, namely $L = \ln Q^2 \ln \frac{1}{x_B}$. In this case one can apply the so-called double logarithmic approximation (DLA) of pQCD. The objective now is to resum these large logarithms in eq.(9), so that we can estimate the behavior of the parton densities in the corresponding kinematical regimes. This resummation is performed via evolution equations, which differ depending on the type of large logarithm under consideration.

11.1 Increase of the gluon (quark) density at $x_B \to 0$.

We now investigate the new phenomena at small x_B, but begin by discussing the evolution equations that sum particular classes of large logarithms in the parton densities.

Gribov - Lipatov - Altarelli - Parisi (GLAP) evolution equation.

The GLAP equation sums those contributions in the parton cascade which compensate the smallness of the QCD coupling constant α_s by the large logarithm $\ln Q^2$. It reads

$$\frac{d}{d \ln Q^2} \phi(x, Q^2) = \alpha_s(Q^2) \int_x^1 \frac{dz}{z} P(z) \phi(\frac{x}{z}, Q^2) \tag{94}$$

where $P(z)$ is the Altarelli-Parisi evolution kernel, calculable in perturbation theory, and $\phi(x, Q^2)$ is a generic parton density (matrix).

Clearly, from the expression for P_i, we need strong ordering ($Q^2 \gg ... \gg q_{it}^2 \gg ..... \gg \frac{1}{R_p^2} = Q_0^2$) in transverse momenta of emitted partons since only under such a condition does one get a $\ln Q^2$ contribution for each integration over q_{it} in the parton cascade in Fig.28. This strong ordering means that the GLAP evolution equation allows us to calculate the probability to find a parton of transverse size $r_t \approx \frac{1}{Q}$ inside the initial parton (quark or gluon) in the hadron at fixed x_B (see Fig.29). In the case where both Q^2 and $1/x_B$ are very large (the DLA approximation), the AP kernel simplifies to $P(z) = N_c \alpha_s / \pi z$, and the solution to the GLAP equation for the gluon density reads then

$$xG(x, Q^2) \sim xG(\omega_0, Q_0^2) \exp(\sqrt{\frac{4 N_c \alpha_s}{\pi} \ln \frac{Q^2}{Q_0^2} \ln \frac{1}{x}}) \sqrt{\frac{\omega_0^3}{3 \alpha_s \ln \frac{Q^2}{Q_0^2}}},$$

where $\omega_0 = (\frac{N_c\alpha_s}{\pi} \ln \frac{Q^2}{Q_0^2} / \ln \frac{1}{x})^{1/2}$, and Q_0 is the initial scale of the parton cascade.

•

Problem 19: Find the exact solution of the GLAP equation at low x (see eq, (94)), using $P(z)|_{z\to 0} \to \frac{N_c\alpha_S}{\pi z}$.

•

Note that the solution of the GLAP equation decreases as Q^2 increases. This agrees with the intuitive notion that, because of asymptotic freedom, the hadron should be almost empty at small distances.

Balitski- Fadin -Kuraev - Lipatov (BFKL) evolution.

The situation changes crucially if we consider the behavior of the parton density ϕ in another extreme regime: at fixed Q^2 but small x_B. Here we have the large logarithm $L = \ln \frac{1}{x_B}$. The picture of the parton cascade, Fig.30, shows that the number of partons increases drastically in the region of small x_B, since each parton in the basic branching process in Fig.28 is allowed, due to the abundance of available energy, to decay in its own chain of daughter partons. Let us estimate the total multiplicity of gluons N_G associated with this complicated process.

We are able to estimate the number of cells in this chain diagram, which corresponds to the typical number of parton (gluon) emissions in one *sub*process in our parton cascade ($\overline{n_G}$). The characteristic value of $\Delta y_{i,i+1}$, the rapidity difference between two adjacent rungs of the ladder, is equal to $\Delta y_{i,i+1} \propto 1/\alpha_s$, from the expression for gluon emission P_i. Thus

$$\overline{n_G} = \frac{\ln \frac{1}{x_B}}{\Delta y_{i,i+1}} \propto \alpha_s \cdot \ln \frac{1}{x_B} . \tag{95}$$

The total number of N_G partons that could interact with the target can then be calculated as follows (see Fig.30):

$$N_G \propto e^{\overline{n_G}} = e^{c\alpha_s \ln 1/x_B} = (\frac{1}{x_B})^{c\alpha_s} , \tag{96}$$

where the constant c should be calculated using the exact BFKL equation [16]. In first approximation $c\alpha_s = 0.5$.

11.2 A new scale for the deeply inelastic process at $x_B \to 0$.

Thus in the region of small x_B the density of partons increases. A careful study of the behavior of the parton cascade shows that also the mean transverse momentum of the parton increases. The reason is as follows. In the case where we neglect the running coupling constant of QCD our theory is dimensionless so each emission leads to a value of the transverse momenta of the daughter gluons which is of the same order as the transverse momentum of the parent gluon. This could be seen just from the explicit expression of P_i. We introduce the ratio $|\ln q_{i,t}^2/q_{i+1,t}^2|$ which characterizes the emission. It is roughly constant.

After n_G emissions

$$< |\ln(q_{n,t}^2/Q_0^2)| > \propto \sqrt{n}_G \approx \sqrt{\alpha_s \ln \frac{1}{x_B}} , \tag{97}$$

since the parton cascade corresponds to a random walk in the variable $\ln(q_{n,t}^2/Q_0^2)$ [16][26] (see Fig.30). Although we will not explicitly present the BFKL equation here, we will give the solution to this equation with the initial condition $x_B G(x_B = x_0) = \delta(\ln(Q^2/Q_0^2))$. This is instructive because it shows explicitly all the properties mentioned in the above:

$$G(y - y_0, r - r_0) = \sqrt{\frac{Q^2}{Q_0^2}} \cdot \frac{1}{\sqrt{\pi \Delta \omega (y - y_0)}} \cdot \exp\{\omega_0 (y - y_0) - \frac{(r - r_0)^2}{8 \Delta \omega_0 (y - y_0)}\}$$

where

$$\omega_0 = \frac{\alpha_s(Q_0^2) N_c}{\pi} 4 \ln 2, \ \Delta = \frac{14\zeta(3)}{4 \ln 2}, \ y - y_0 = \ln \frac{x_0}{x_B}, \ r - r_0 = \ln \frac{Q^2}{Q_0^2}$$

•

Problem 20: Calculate the mean value of $\ln(Q^2/Q_0^2)$ using the solution of the BFKL equation.

•

11.3 Saturation of the gluon density.

The increase of the parton density leads to a new problem in deeply inelastic scattering, namely the violation of s-channel unitarity. This is the requirement that the total cross section for virtual photon absorption be smaller than the size of a hadron.

$$\sigma(\gamma^* N) \ll \pi R_h^2 \tag{98}$$

At small x_B the gluon density dominates and we can write

$$\sigma(\gamma^* N) \;=\; const\frac{\alpha_{em}}{Q^2}\; xG(x,Q^2) \tag{99}$$

where $const\ \alpha_{em}/Q^2$ approximates the cross section $\sigma(\gamma^* g)$. We have shown previously that the value of the gluon density increases very rapidly as $x \to 0$. Using the DLA result (see eq.(11)), we can rewrite the unitarity constraint in the following way, dropping the *const*:

$$\frac{\alpha_s(Q^2)}{Q^2} \cdot (\frac{1}{x_B})^{c\alpha_s(Q^2)} \leq \pi R_N^2. \tag{100}$$

Here we replaced α_{em} by α_s since the probe can also be a virtual gluon, not just a virtual photon.

¿From this expression alone one can conclude that **unitarity will be violated** [25] at

$$x < x_{\rm cr} \quad \text{where} \quad \log\frac{1}{x_{\rm cr}} \;=\; \frac{1}{c}\cdot\frac{1}{\alpha_s(Q^2)}\ln(\frac{\pi R_N^2 Q^2}{\alpha_s(Q^2)}) \tag{101}$$

Therefore unitarity is violated even for (very) large values of Q^2 when $x < x_{\rm cr}$. Clearly the miraculous confinement force cannot prevent this from happening. Thus we have to look for the origin and solution of this problem within pQCD.

Let us try to understand what happens in the region of small x_B by examining the parton distribution in the transverse plane (see Fig.29) [¶]. Our probe (photon) feels those partons whose size is of the order of $\frac{1}{Q}$. To begin, at $x \sim 1$ we have only several partons that are distributed in the hadronic disc. If we choose Q^2 such that

$$r_p^2 \approx \frac{1}{Q^2} \;\ll\; R_h^2. \tag{102}$$

then the distance between partons in the transverse plane is much larger than their size and we can neglect the interaction between partons. The only process which is essential here is the emission of partons that is taken into account in the usual evolution equation. As x decreases the number of partons increases and at some value of $x = x_{\rm cr}$ partons start to densely populate the whole hadron disc. For $x < x_{\rm cr}$ the partons overlap spatially and begin to interact throughout the disc. For such small x-values the processes of recombination and annihilation of partons should be as essential as their emission. Both these processes are however not incorporated into either the GLAP or BFKL evolution equations.

[¶]Recall that a high energy hadron in the parton model can be represented as a Lorentz contracted disc.

What happens in the kinematical region $x < x_{cr}$ is anybody's guess but there is enough experience with some models [27] to suggest the so-called **saturation of the parton density** [25]. This means that the parton density ϕ, which we discussed before, is constant in this domain.

12 Shadowing correction and nonlinear evolution equation.

12.1 Qualitative Derivation of Nonlinear Gribov-Levin-Ryskin Evolution Equation

In section 11.3 we remarked that at small x (high energies), the density of gluons becomes so large that the unitarity constraint is violated, even at large values of Q^2. We argued that the physical processes of interaction and recombination of partons, which are usually omitted in perturbative calculations, become important in the parton cascade at a large value of the parton density. To take interaction and recombination into account we must identify a new small parameter that lets us estimate the accuracy of our calculations. This small parameter is [25]

$$W \;=\; \frac{\alpha_s}{Q^2}\;\rho(x,Q^2)\;. \tag{103}$$

The first factor is the cross section for absorption of a gluon by a parton in the hadron; the transverse density ρ is defined in eq.(44). Effectively, W is the probability of a parton recombination during the cascade. We can rewrite the unitarity constraint eq.(100) in the form

$$W \;\leq\; 1\;. \tag{104}$$

Thus, W is the natural small parameter in our problem. Amplitudes that take gluon recombination into account can be expressed as a perturbation series in this parameter [25]. We can resum this series, and the result [25] can be understood easily by considering the structure of the QCD cascade in a fast hadron. Two processes occur inside the cascade

$$\text{emission}\;\;(\,1\,\rightarrow\,2\,);\quad \text{probability}\;\propto\;\alpha_s\,\rho\;; \tag{105}$$

$$\text{annihilation}\;\;(\,2\,\rightarrow\,1\,);\quad \text{probability}\;\propto\;\alpha_s^2\,r^2\,\rho^2\;\propto\;\alpha_s^2\,\frac{1}{Q^2}\,\rho^2\;,$$

where r is the size of a parton produced in the annihilation process. For deep inelastic scattering $r^2 \propto 1/Q^2$.

At $x \sim 1$ only the production of new partons (emission) is essential because $\rho \ll 1$, but at $x \to 0$ the value of ρ becomes so large that the annihilation of partons becomes important. This simple parton picture allows us to write an equation for the density of partons that properly accounts for all these processes. The number of partons in a phase space cell $(\Delta y = \Delta \ln(1/x), \Delta \ln Q^2)$ increases through emission and decreases through annihilation. Thus the balance equation reads

$$\frac{\partial^2 \rho}{\partial \ln \frac{1}{x} \partial \ln Q^2} = \frac{\alpha_s N_c}{\pi} \rho - \frac{\alpha_s^2 \tilde{\gamma}}{Q^2} \rho^2 , \tag{106}$$

or in terms of the gluon structure function $xG(x, Q^2)$

$$\frac{\partial^2 xG(x,Q^2)}{\partial \ln \frac{1}{x} \partial \ln Q^2} = \frac{\alpha_s N_c}{\pi} xG(x,Q^2) - \frac{\alpha_s^2 \tilde{\gamma}}{\pi Q^2 R^2} (xG(x,Q^2))^2 . \tag{107}$$

This is the so-called Gribov-Levin-Ryskin (GLR) equation [25]. The parameter $\tilde{\gamma}$ can in fact be calculated order by order in W perturbation theory. Mueller & Qiu [28] found it to be

$$\tilde{\gamma} = \frac{81}{16} \quad \text{for } N_c = 3.$$

12.2 The Scale of the Shadowing Corrections

The second term in Equation 107 describes shadowing corrections (SC). Its size crucially depends on the value of R^2. The physical meaning of R^2 is clear: R is the correlation length between two gluons in a typical hadronic situation (at $x \sim 1$). In our derivation of the GLR equation we assumed that there are no correlations between gluons except those imposed by their confinement in a disc of radius R.

If $R = R_h$ the value of the SC is negligibly small.

If $R \ll R_h$, the SC could be large (see Refs. [29], [30] and [31]). Recently Braun et al [32] performed the first theoretical estimates of the value of R within the framework of QCD sum rules. They found

$$R = 0.3 - 0.35\, fm \sim \frac{1}{3} R_h .$$

an encouraging result for experimental study of SC at present energies. For the gluon structure function the solution of the GLR equation is shown in Fig.32 and the value

of $xG(x,Q^2)$ from which saturation starts depends on the value of R^2 . For $R = R_p$ saturation starts from

$$xG(x,Q^2) > 150 \;\; at \;\; Q^2 = 10GeV^{-2}$$

while for $R = \frac{1}{3}R_p$

$$xG(x,Q^2) > 15 \;\; at \;\; Q^2 = 10GeV^{-2} \; .$$

It should be stressed that the GLR equation predicts the value of the maximal packing factor (PF) which is

$$PF \;\; = < |r^2_{constituent}| > \cdot \rho \tag{108}$$

PF does not depend on the value of the radius R and for parton with $< |r^2_{constituent}| > = \frac{1}{Q^2}$ the GLR equation gives:

$$(PF)_{max} \;=\; 0.21 \;\; for \;\; N_c \;=\; 3$$

12.3 New Scale of Transverse Momentum (the Critical Line)

12.3.1 The main property of a solution of the GLR equation

First, let us rewrite the GLR equation (see eq.(107)) in terms of new variables: $F = xG(x,Q^2)$; $y \;=\; 8N_c/b \cdot \ln(1/x)$ and $\xi \;=\; \ln\ln(Q^2/\Lambda^2)$, as

$$\frac{\partial^2 F}{\partial y \partial \xi} \;=\; \frac{F}{2} \cdot \{\, 1 \;-\; \gamma' exp[\, -\xi \;-\; e^{\xi}\,]\, F\} \; , \tag{109}$$

where $\gamma' \;=\; 2\pi\tilde{\gamma}/bR^2\Lambda^2$. The terms e^{ξ} ($-\xi$) in the exponential correspond $1/Q^2$ (α_s). Note that the term proportional to γ' corresponds to the recombination probability W, defined below Equation (26). By inspecting eq.(109) we can guess the main property of the solution. At the start of the evolution, when the value of the structure function is small, we can neglect the nonlinear term. The derivative with respect to y is here positive, so the structure function increases monotonically with y, or $\ln(1/x)$. This growth continues up to the value

$$F_{max} \;=\; \frac{1}{\gamma'} \cdot exp[\xi \;+\; e^{\xi}\,],$$

where the derivative vanishes. If $F > F_{max}$ the derivative from the GLR equation becomes negative and F_{max} is thus the limiting value of the gluon density and the solution of the GLR equation as $x \to 0$.

Therefore, at each value of Q^2 there is a critical value of $x \equiv x_{cr}$ when $F = F_{max}$ or, conversely, at each value of x there is a critical value of $Q^2 = q_0^2(x)$ when $F = F_{max}$. This value $Q^2 = q_0^2(x)$ introduces a new transverse momentum scale in the parton cascade. The behavior of the gluon density changes crucially at $Q^2 = O(q_0^2(x))$. Indeed,

$$F = F^{GLAP}(x, \ln Q^2) \quad \text{for } Q^2 > q_0^2(x),$$

where F^{GLAP} means that F is a solution of the linear GLAP equation and a smooth function of $\ln Q^2$. Alternatively

$$F \propto \frac{Q^2}{q_0^2(x)} \quad \text{for } Q^2 < q_0^2(x) F_{max} \, .$$

We postpone the discussion of the physical meaning of this new scale and instead determine first the x dependence of $q_0^2(x)$.

12.3.2 Trajectories

A semiclassical analysis offers new insights into solutions of the GLR equation. It is easiest to find the solution to the linear equation by passing to a moment (ω) representation and introducing the anomalous dimension γ. In moment representation the solution is as follows:

$$F(x, Q^2) = \int \frac{d\omega}{2\pi i} M_0(\omega, Q^2) e^{\omega y + \gamma(\omega)\xi} \, , \tag{110}$$

where $M_0(\omega, Q^2)$ is the initial distribution at $Q^2 = Q_0^2$ and the anomalous dimension $\gamma(\omega) = 1/2\omega$. At large y (small x) we can evaluate the integral in the saddle point approximation. The position of the saddle point is determined by:

$$y = -\frac{d \ln M_0(\omega)}{d\omega} - \frac{d\gamma(\omega)}{d\omega} \cdot \xi \, . \tag{111}$$

This equation describes a family of curves $y = y(\xi)$ that can be considered as semiclassical trajectories of parton evolution because ω is a constant of a motion in the linear evolution equation. The semiclassical values of F along the trajectory give an approximate estimate of the structure function at fixed Q^2 and x. Although this method yields no new understanding for the linear equation, it can be generalized to the nonlinear case.

12.3.3 Semiclassical Solution to the GLR Equation

In semiclassical approximation we parametrize the solution to the GLR equation by writing

$$F \;=\; e^S, \quad \text{assuming } \; S_y\, S_\xi \;\gg\; S_{y\xi} \;,$$

where $S_y \;=\; \partial S/\partial y$, $S_\xi \;=\; \partial S/\partial \xi$ and $S_{y\xi} \;=\; \partial^2 S/\partial y \partial \xi$. The solution to the linear equation is $S = \sqrt{2y\xi}$, for which one can check that the above inequality holds to good accuracy.

Thus in the semiclassical case the GLR equation can be reduced to the form:

$$S_y\, S_\xi \;=\; \frac{1}{2}(1 \;-\; \gamma'\; exp\{\, S \;-\; e^\xi \;-\; \xi\,\}) \;. \tag{112}$$

Eq.(112) can be solved using the method of characteristics, or trajectories ([25] [33] [34]). By introducing an intrinsic time coordinate t along the trajectory and denoting the derivatives with respect to this time variable by $\dot{y}$ etc we can rewrite the GLR equation as the following system of ordinary equations:

$$\begin{aligned}
\dot{y} \;&=\; S_\xi \\
\dot{\xi} \;&=\; S_y \\
\dot{S} \;&=\; 2\, S_y\, S_\xi \\
\dot{S_y} \;&=\; -\gamma'\; S_y\; exp\{\, S \;-\; e^\xi \;-\; \xi\,\} \\
\dot{S_\xi} \;&=\; -\gamma'\; [\, S_\xi \;-\; 1 \;-\; e^\xi\,]\; exp\{\, S \;-\; e^\xi \;-\; \xi\,\} \;.
\end{aligned} \tag{113}$$

In the linear case ($\gamma' = 0$) this system of equations has a simple solution:

$$S_y \;=\; \omega \;=\; Const \;; \quad S_\xi \;=\; \frac{1}{2\omega} \;=\; Const \;,$$

which coincides with eq.(111). We introduce ω here such that it corresponds to ω in eq. (111). From eq.(113) we find

$$y - y(t=0) = \frac{1}{2\omega} t \;\;,\;\; \xi - \xi(t=0) = \omega t \;\;,\;\; S = \frac{1}{2} t$$

Thus we obtain

$$S = \sqrt{2(y - y(t=0))(\xi - \xi(t=0))} \;\;,\;\; y - y(t=0) = \frac{1}{2\omega^2}(\xi - \xi(t=0))$$

The second of these equations corresponds to Equation 33 with $\gamma = 1/\omega$, the correct anomalous dimension in the GLAP equation for $x \to 0$. Along each trajectory of the

linear equation, the rescattering probability $W = \gamma' exp\{S - e^{\xi} - \xi\}$ increases at the beginning when $\dot{S} \approx 1$, reaches a maximum value when $S_\xi = (1 + e^{\xi})$ and then decreases at larger ξ. However, the trajectories of the GLR equation become quite different from the linear ones. Indeed, in the region where W becomes of order one, the derivatives S_y and S_ξ are not small and trajectories are not straight lines. A number of papers ([25] [33] [34]) have shown that critical line separates the region of almost-linear trajectories (small values of $W \leq 0(\alpha_s)$) and strongly nonlinear solutions (see Fig.33).

It is easy to check explicitly that for large ξ,

$$y_{cr} = \frac{e^{2\xi}}{4}; \; S = e^{\xi} - \ln\gamma'; \; S_y = e^{-\xi}; \; S_\xi \approx \frac{e^{\xi}}{2} \tag{114}$$

is the solution of eq.(113) and of the GLR equation as well. To the right of the critical line ($x > x_{cr}$) the equation $y_{cr} = \frac{e^{2\xi}}{4}$ may be recast as

$$\ln\frac{1}{x_{cr}} = \frac{b}{32N_c}\ln^2(Q^2/\Lambda^2). \tag{115}$$

The nonlinear corrections are so small that we can neglect them and use the trajectory of the standard GLAP equation. However, when x becomes smaller than x_{cr}, $W \to 1$ and we have to use the nonlinear trajectory. Remarkably, this trajectory cannot cross the critical trajectory (see Fig.33). Using this property, one can suggest the following way to solve the GLR equation. To the right of the critical line it suffices to find the solution of the linear (GLAP) equation with the new boundary condition $F = e^S$ with $S = e^{\xi} - ln\gamma'$ on the critical line (see eq.(114)). To the left of the critical line we have a separate system of trajectories. The solutions to the left do not depend on the solutions to the right of the critical line. Here we enter the very interesting kinematic region of hdQCD. Even the GLR equation is not the right tool to solve problems in this region because in addition to the recombination of two partons, simultaneous interactions of three, four and more partons are also important in this region.

12.4 The Physical Meaning of the New Scale for the Typical Transverse Momentum in the Parton Cascade

The equation for the critical line (eq.(115)) introduces a new scale for the value of the typical transverse momentum in the parton cascade, namely

$$q_t^2 = q_0^2(x)\,|_{x\to 0} \to \Lambda^2\, e^{\sqrt{\frac{32N_c}{b}\ln\frac{1}{x}}}. \tag{116}$$

This new scale plays the role of an infrared cutoff in inclusive production. This new infrared cutoff has a dynamical origin: parton-parton recombination in the parton cascade. It is not related to confinement.

The quantity $q_0(x)$ is also the Landau-Pomeranchuk momentum [36] in the parton medium. Indeed, in the saturation region $q_t < q_0(x)$ the mean free path λ does not depend on x. In this region $\lambda = 1/\sigma T$ where σ is the cross-section of parton-parton interaction ($\sigma \propto \alpha_s 1/q_t^2$) and $T = xG(x,q_t)$ is the number of partons with transverse momentum q_t at fixed x. If $q_t < q_0(x)$ $T \propto q_t^2 \phi_0$ and $\sigma T = Const(q_t)$. Thus λ is equal to the formation length of a parton with $x = x_0$, which can be derived from the relation $q_0(x_0) = q_t$. If $q_t > q_0(x)$ then $\sigma T \propto xG(x,q_t)/q_t^2 \ll 1/mx$ so λ is big. Therefore, $q_0(x)$ is precisely the LP momentum, and the factor C that interpolates between coherent and incoherent emission of gluon with transverse momentum q_t and fraction of energy x_j can be rewritten as follows:

$$C \;=\; \frac{1}{1 \;+\; \frac{x_0(q_t)}{x} \,.\, \frac{q_0(x_j)}{q_t}} \;. \tag{117}$$

12.5 Correlations

We assumed that the only correlations between gluons in the cascade arise from the fact that the gluons are distributed in a disc of radius R. The probability to find two partons with the same value of $\ln(1/x)$ and $\ln Q^2$ is

$$P_2 \;\propto\; \rho^2 \;. \tag{118}$$

However this assumption is only correct if the number of colors is large ($N_c \to \infty$) [35]. If N_c is not large, Bartels and Levin et al claim [35] claim that

$$\frac{P_2}{\rho^2} \;\to\; \exp\,(\sqrt{\frac{4N_c\alpha_s}{\pi}\;\ln\frac{1}{x}\,\ln\frac{Q^2}{Q_0^2}\;\frac{1}{(\,N_c^2\,-\,1)^2}}) \;. \tag{119}$$

Bartels & Ryskin [37] found that this correlation reduces the correlation radius R by a factor of 1.3 - 1.4 in the HERA kinematic region.

It is also very instructive to write down the evolution equation that takes into account the correlation of eq.(119). This is a system of two equations, instead of the single equation of eq. (107), namely

$$\frac{\partial^2\rho}{\partial\ln\frac{1}{x}\,\partial\ln Q^2} \;=\; \frac{\alpha_s N_c}{\pi}\,\rho \;-\; \frac{\alpha_s^2\,\tilde{\gamma}}{Q^2}\,P_2 \;, \tag{120}$$

$$\frac{\partial^2 P_2}{\partial\ln\frac{1}{x}\,\partial\ln Q^2} \;=\; \frac{4\alpha_s N_c}{\pi}(1+\frac{1}{(N_c^2-1)})\,P_2 \;-\; \frac{2\alpha_s^2\,\tilde{\gamma}}{Q^2}\,P_2\rho \;. \tag{121}$$

Here we assume that the probability to find three partons in the same cell of the parton phase space is $P_3 = P_2 \cdot \rho$. Without this assumption the last term in Equation (121) reads as $2\alpha_s^2\gamma/Q^2 \cdot P_3$. The general equation for P_n is (see Ref.[31] for details)

$$\frac{\partial^2 P_n}{\partial \ln \frac{1}{x} \partial \ln Q^2} = \omega\gamma_n P_n - \frac{n\alpha_s^2\gamma}{Q^2} P_{n+1} \tag{122}$$

This equation indicates the need for the solution of two theoretical problems.

(i) We should find a general equation for γ_n, which has the formal meaning of the anomalous dimension of a high twist $(2n)$ operator (Refs.[31],[38], [35]).

(ii) We need a closed form of the equation which incorporates all P_n for the deep-inelastic structure function, and its solution.

The first problem was solved by A.G. Shuvaev and us in Ref.[38]. The complicated problem of gluon-gluon interaction was reduced to that of interaction of colorless "gluon ladders" (Pomerons). It was shown in Ref.[35] that this idea works for the case of the anomalous dimension of the twist four operator, in other words, for the case of P_2. The fact that we can consider the rescattering of n Pomerons to find γ_n (or P_n) signifies that we are dealing with a quantum problem: the calculation of the ground state energy for an n-particle bosonic system where the interaction is attractive and given by a four-Pomeron contact term, with a coupling proportional to $\lambda = 4\alpha_s/(N_c^2 - 1)$. This observation simplifies the problem and enabled us to reduce it to solving the nonlinear Schrödinger equation for n Pomerons in the t-channel. It should be stressed that this effective theory is a two-dimensional one, the two dimensions being spanned by $\ln(1/x)$ and $\ln Q^2$: the Schrödinger equation can be written for n particles on a line. It is well-known that this problem can be solved exactly (e.g. by Bethe Ansatz) and the answer was found to be

$$\gamma_n = \frac{N_c\alpha_s n^2}{\omega\pi}[1 + \frac{1}{3}\frac{1}{(N_c^2-1)^2}(n^2-1)] \tag{123}$$

Although Pomerons are bosonic, maximally two Pomerons occupy a single-particle level in this groundstate configuration, thus behaving like fermions. This is due to the two-dimensional nature of this problem. The second problem has also been (partly) solved by us (unpublished but see Ref.[31] for results). We introduce the generating function

$$P(x, Q^2, \eta) = \sum_{n=1}^{\infty} P_n e^{n\eta} \tag{124}$$

with $P_1 = \rho$. Using eq.(122) we obtain

$$\begin{aligned} \frac{\partial^2 P}{\partial \ln \frac{1}{x} \partial \ln Q^2} &= \frac{N_c\alpha_s}{\pi}(P_{\eta\eta} + \frac{1}{3}\frac{1}{(N_c^2-1)^2}(P_{\eta\eta\eta\eta} - P_{\eta\eta}) \\ &\quad -\alpha_s^2\gamma e^{-\ln(Q^2)} e^{-\eta}(P_\eta - P), \end{aligned} \tag{125}$$

where $P_\eta = \partial P/\partial\eta$, $P_{\eta\eta} = \partial^2 P/\partial\eta^2$ etc. The deep-inelastic structure function is the solution of this equation at $\eta = -\ln(Q^2)$, viz.

$$x\,G(x,Q^2) = \pi R^2 P(x,Q^2,\eta = -\ln(Q^2). \tag{126}$$

Eq.(125) is a new evolution equation which allows one to take into account both initial and dynamical correlations between gluons in the parton cascade. The key problem in solving it is nonperturbative in nature, namely to determine an initial condition at $x = x^0$. The dependence of $P(x^0,Q^2,\eta)$ on η describes the correlations between gluons in the hadron near $x \sim 1$. The simplest case is to neglect this initial correlation and use the eikonal approach for $P(x^0,Q^2,\eta)$, namely

$$P(x^0,Q^2,\eta) = \sum_{n=1}^{\infty} e^{n\eta}\frac{(-1)^{n+1}}{n!}P_1(x^0,Q^2)^n = 1 - \exp(-e^\eta P_1(x^0,Q^2)) \tag{127}$$

The solution of this equation has not yet been found (see Ref.[31] for more details).

13 A look at the first small x HERA data.

13.1 25 nb^{-1} of Experimental Data

Let us list conclusions from the first experimental results at small x from the H1 and ZEUS collaborations at HERA ([39]):

1. The increase of the value of the deep inelastic structure function F_2 at $x \to 10^{-4}$ shows that the gluon density is large:

$$xG(x,Q^2) \;\to\; 40-50 \text{ at } x_B = 10^{-4} \text{ and } Q^2 = 20\,GeV^2\ .$$

The value for $xG(x,Q^2) \sim 50$ was determined from the $MRSD-'$ [40] parameterization that roughly describes the new data.

2. The ZEUS collaboration measured the diffraction dissociation (DD) [‖] cross section and found

$$\frac{\sigma^{DD}_{\gamma^* p}}{\sigma_{\gamma^* p}} \;=\; \frac{5.2\ nb}{80\ nb} \;= 6\times 10^{-2} \text{ at } x = 10^{-4} \text{ and } Q^2 > 10\,GeV^2\ .$$

[‖]DD is the process in which a number of hadrons are produced in association with a recoil proton, whose energy fraction is close to one.

where $\sigma_{\gamma^* p}$ is the total cross-section for virtual-photon absorption. We will say more about the diffractive component shortly.

3. The structure function F_2 can be described by the GLAP evolution equation assuming that at the initial virtuality $Q_0^2 \sim 5GeV^2$ the gluon structure function increases rapidly at $x \to 0$ as $xG(x, Q_0^2) \propto x^{-\lambda}$ and $\lambda \geq 0.3$. Note that at sufficiently large Q_0^2 λ approaches ω_0, which occurs in the solution of the BFKL equation (see section 11.2).

4. Both collaborations measured the total photoproduction cross section σ_t for very small virtualities of the incoming photon and also for real photons. This cross section exhibits a common property of soft processes, namely $\sigma_t \to s^{\Delta}$ where $\Delta \sim 0.08$.

13.2 The Value of the Shadowing Corrections from HERA Data

Let us first try to understand the large number of gluons (between 40 and 50 at $x = 10^{-4}$)). An interesting way to do this is to compare the proton at $x = 10^{-4}$ and $Q^2 = 15GeV^2$ with an iron nucleus, which has a similar number of *nucleon* constituents. If we calculate the packing fraction by assuming the size of the constituents to be $R_h = 0.86\ fm$ for the nucleons and $r_G = 1/Q$ for the gluons, we find that the two packing factors are very similar if one assumes the size of the gluon disc to be $R_h/3$ (see section 4.2). Thus, in this sense, we see that a proton $x = 10^{-4}$ and $Q^2 = 15GeV^2$ is very similar to an iron nucleus.

We now estimate the size of shadowing correction ΔF_2 for the deep inelastic structure function. Let us write it as

$$F_2(x, Q^2) \ = \ F_2^{GLAP}(x, Q^2) \ - \ \Delta F_2(x, Q^2) \ , \tag{128}$$

where F_2^{GLAP} is the solution of the usual (GLAP) evolution equation. A straightforward estimate gives

$$\frac{\Delta F_2}{F_2} \ \propto \ \alpha_s < r_G^2 > \rho \ \to \ 0.1 \ \text{for} \ Q^2 \ = \ 15\, GeV^2 \ \text{and} \ x \ = \ 10^{-4} \ . \tag{129}$$

However, the ZEUS data on diffraction dissociation let us better estimate the value of SC. Indeed, Levin & Wuesthoff [41] showed that

$$|\Delta F_2| \ = \ F_2^{DD}, \tag{130}$$

where F_2^{DD} relates to $\sigma_{\gamma^* p}^{DD}$ in the same way that F_2 relates to $\sigma_{\gamma^* p}$. In other words $|\Delta\sigma_{\gamma^* p}/\sigma_{\gamma^* p}| \ = \ \sigma_{\gamma * p}^{DD}/\sigma_{\gamma^* p}$. ¿From the ZEUS data we can then conclude that $|\Delta F_2|/F_2 \ >$

$6 \cdot 10^{-2}$. Note that in this case we can begin not only to discuss whether there are SC, but even whether we could predict this SC value in our theory.

The details of the evolution equation for F_2^{DD} were discussed in Ref. [41], in which Levin & Wuesthoff suggested measuring the sum $F_2 + F_2^{DD}$ in which all contributions of SC cancel. One can use the GLAP equation for this sum, even at small x.

13.3 Saturation of the Parton Density or Different Physics for "Soft" and "Hard" Processes?

The HERA data allow us to raise the question that is the title of this subsection. Indeed, we can distinguish two regions in Q^2 that have quite different energy behavior of the photoproduction cross section. The experimental facts that pertain to these regions are as follows:

1. $Q^2 \ll 1\,GeV^2$. (a) The total cross section is essentially constant here (or increases slightly with energy); (b) $\sigma^{DD}/\sigma_t \approx 10\%$. Thus in this kinematic region the photoproduction process seems to be a typical soft process like a hadron-hadron collision.

2. $Q^2 > 5\,GeV^2$. (a) The total cross section increases rapidly with energy (x) $\sigma_{\gamma^* p} \propto x^{-\lambda}$; (b) $\sigma^{DD}_{\gamma^* p}/\sigma_{\gamma^* p} \sim 10\%$. This is the typical deeply inelastic scattering process. Both experimental facts arise from the contribution of a so-called hard Pomeron, which is a solution to the BFKL equation [16] and leads to $\sigma_{\gamma^* p} \propto x^{-\omega_0}$ with $\omega_0 > 0.4$ while the smallness of the ratio $\sigma^{DD}_{\gamma^* p}/\sigma_{\gamma^* p}$ has a natural explanation in the small values of SC.

What happens for intermediate value of photon virtualities $1GeV^2 < Q^2 < 5GeV^2$? There are two different scenarios for this kinematic region:

1. Landshoff picture At $Q^2 < 1GeV^2$ all experimental data for photoproduction as well as for other soft processes can be described by the exchange of the soft Pomeron, which is a standard Regge pole, with intercept $\alpha_P = 1 + \epsilon$ ($\epsilon \sim 0.08 \ll \omega_0$) (see Ref.[3]). The small value of the ratio σ^{DD}/σ_t can then be interpreted as an indication that the SC are small and can be treated perturbatively. In particular Donnachie and Landshoff considered only two Pomeron exchanges. In this scenario the region of deeply inelastic scattering has different underlying physics described instead by a hard Pomeron. The distinction between the hard and soft regions seems quite arbitrary at present. However, this approach is very simple and provides an elegant description of all available experimental data on soft processes.

2. Saturation of the parton density The second scenario is intimately related to the hypothesis that the parton density saturates. In this scenario the hard Pomeron is

responsible for the behavior of the total cross-section in both kinematic regions, but the small value of the ratio σ^{DD}/σ_t is interpreted differently for large and small virtualities: For large virtualities it supports a small value of SC, but at small ones we interpret it as an indication that the SC become very large and lead to a black-disc constituent quark. The greatest advantages of this scenario are the unified description of both the diffractive and inclusive processes, and that its solid theoretical background, namely properties of the hard Pomeron and the shadowing correction in perturbative QCD. It is worthwhile to mention that strong SC correction gives rise sumalteneously the saturation of the parton density, smooth behavior of the total cross section at high energy, a natural explanation of the transition from steep energy behavior of the "hard" Pomeron to smooth energy dependance of the "soft" total cross section and small value of the diffraction dissociation cross section in both kinematic regions (see ref. [43] for more information). However the data have not yet been described within this hypothesis.

These two scenarios result in different behavior in the region of intermediate virtualities of photon. In the second scenario we expect some transition region with smooth behavior of σ_t vs Q^2. A first attempt to extract this behavior from available experimental data shows that such a transition region does not contradict such scenario [42], but it is still too early to draw a definite conclusion.

14 How to measure the high density event.

Let me list here the main ideas how to measure the new physics that we anticipate at high density system of partons:

1. The probability of double parton interaction should be large (of the order of the maximum value of the packing factor) about 20%.

The double parton interaction can be seen not only as cross section for production of two pair of hard jets with the same value of rapidity,but also as a cross section of the inclusive production of hadrons in the window of rapidity $y + \Delta y, y - \Delta y$ where y is the rapidity of a hard jet with transverse momentum p_t and $\Delta y = \ln \frac{p_t}{p_0}$, where p_0 is the transverse momentum of produced hadron. It could be also seen as a long range correlation in rapidity between produced hard jet and produced hadron which is not specially hard.

2. In the high density event we should see the Landau - Pomeranchuk suppression of the emission of gluons with transverse momentum smaller that the typical momentum $q_0(x_B)$ which can be found from the equation:

$$\frac{xG(q_0^2(x), x)}{q_0^2(x)\pi R^2} \; = \; (PF)_{max} \; . \tag{131}$$

Such a suppression can be seen as the deviation from the factorization theorem for jets with $p_t \leq q_0(x)$.

3. . Decorrelation effect for jets with transverse momentum p_t of the order of q_0. The value of transverse momentum for such a jet is compensated not by one jet in the opposite direction but by a number of jets with average transverse momentum about q_0.

4. Polarization of produced hadrons allows us to measure the typical transverse momentum in the process since in the region of pQCD polarization should be equal to zero.

5. It is seen directly from eq.(9) that the saturation reaches in the system with small size at larger transverse momentum (smaller value of the gluon structure function). So this is why we have to create experimentally such compact system. We have three ideas how to confine the gluons in the disc of the small size:

A. to find a carrier of partons with small size. Even hadron could be such a carrier if the hypothesis of constituent quarks with small radius will be confirmed experimentally. However better to use the virtual photon or Pomeron. The last is not well theoretically defined object and what is Pomeron is one of the questions that the future experiment should answer. However even available experimental information confirm the idea that Pomeron's size is much smaller that hadron one and of the order of $R_P \approx \sqrt{\alpha'_P} \sim 0.5 GeV^{-1} \sim 0.1 Fm$. Thus hard diffraction with Pomeron can give a good possibility to localize the parton system in small disc and to see high density phenomena in the most clear way.

B. to find the experiment (microscope) that can resolve the small part of the hadron and investigate it in detail. This idea is realized in so called Mueller - Navalet process [44] or "hot spot" hunting [45] (see Fig.34).

This process allows us to measure the small $\propto \frac{1}{p_{t2}}$ part of the hadron and using the two jets with sufficiently large transverse momentum as a trigger e can study the system with large parton density in many details.

C. Bjorken [46] pointed out that the large rapidity gap (LRG) processes can give us new way to look inside the high density parton system. Indeed, due to intimate relation between inelastic processes and elastic one coming from new reggeon-like approach the process with the LRG such as two high transverse momentum jet production with rapidities y_1 and y_2 but without any hadron with rapidities $y_1 > y_h > y_2$ can be described as the exchange of "hard" Pomeron (see Fig.35). The properties of the " hard" Pomeron exchange is well known theoretically (see ref. [16]) and can be checked experimentally.

6. One of the way to measure the high parton density is to select the event with large multiplicity of produced hadrons. More discussion on this subject you can find in the report of Fermilab Working Group on QCD [47]

TOMORROW:

EFFECTIVE THEORY at HIGH ENERGY from NONPERTURBATIVE QCD

15 Summary.

Let us summarize where we stand in the theoretical development at high energy physics and what of the fundamental problems listed in section 9.3 have been solved.

As we have discussed in section 9.5 we struggle with two major problems in pQCD: (a) Our perturbative series have a natural small parameter α_S, but its smallness is often compensated by large logs, which are different in different processes. In the case of the processes at high energies (small x) the real parameter of the perturbation series is $\alpha_S \ln(1/x)$ which is not small. (b) The perturbation series is asymptotic because the coefficient C_n in eq.(45) behaves as $n!$ at large n.

The first problem is mainly technical and has been solved by the BFKL equation. However this equation carries with two problems, namely, the next order corrections have yet not been found and the solution of the BFKL equation is influenced by confinement region. Moreover, such confinement corrections have not been localized in something like the matrix element of some operator.

The second problem is much more complicated one and it can be solved only if we understand better the nonperturbative origin (renormalons, instantons,etc) of behaviour of coefficients C_n. We are only in the beginning of the systematic study of the nonperturbative effects in high energy problem (see ref. [48]).

The origin of the shadowing corrections is also nonperturbative one, but it is new kind of nonperturbative phenomena which closely related to the high density of the partonic system. At the moment we can control them theoretically only in the transition region between pQCD and hdQCD in Fig.19.

Coming back to the list of our hopes in section 9.5 we can conclude that we have understood better the kinematic region in which we can trust pQCD.

16 Nearest Future = Theory in the transition region.

I firmly believe that in the nearest future :

1.

a theory for the transition region between pQCD and hdQCD (see Fig.19) based on the BFKL Pomeron and Pomeron interactions will be completed.

2.

we will understand better the manifestation of the BFKL Pomeron and SC (shadowing corrections) and coming experiments from HERA and Tevatron will help us to understand better in which kinematic region we can restrict ourselves by new Reggeon Calculus based on the BFKL Pomeron.

3.

we will find the values of all nonperturbative parameters that we need (like R in the GLR equation) with help of the nonperturbative QCD methods such as lattice calculation or QCD sum rules.

The Mueller approach as well as the deep understanding of the correct degrees of freedom allows us to start to built the effective theory for high energy interaction. It is interesting to emphasize that this effective theory will be a theory of interaction of the dimensional objects (colour dipoles). Therefore, at high energy we have such a system of partons (particle) in which we can study the theory of interaction of the dimension degrees of freedom. It seems very attractive, because we can check our theoretical imagination with experimental data, while the string gang who is doing basically the same trying to understand how can we build the relativistic theory for dimension degrees of freedom still have to rely only on theory without any experimental support.

17 Toward the effective theory.

I hope that I have convinced you that the main direction of our movement is toward the effective theory based on nonperturbative QCD approach, because the principle problems of high density partonic system cannot be solved without understanding of npQCD. We hope that in the future we will find:

1. a selfconsistent effective theory for a high density system in QCD;

2.the analytic solution of hdQCD,using the smallness of the coupling QCD constant in this kinematic region;

3. a new collective phenomena in hdQCD.

At the present we can see two harbingers of this shining future:

17.1 Effective Lagrangian for high energy QCD.

The first attempt to develop nonperturbative approach to low x_B problems was to write down the effective Lagrangian for the region of small x_B. Intrinsically we assume that such a Lagrangian should be simpler that the QCD one and allows one to apply some direct numerical procedure (lattice calculation for example) to calculate the scattering amplitude with this Lagrangian. It should be stressed the attempts to calculate the amplitude with full QCD Lagrangian have failed by now. At the moment we have two effective theories on the market: one was proposed by Lipatov [49] which looks not much simpler that full QCD but it certainly incorporates all results of perturbative calculations, and the second was suggested by Verlinde and Verlinde [50], which is much simpler and is suited for lattice -like calculation but it has not been checked how well this effective theory describes the perturbative results. Moreover there is some indication [51] that this theory cannot describe the virtual correction in the BFKL Pomeron.

17.2 Thermodynamics of high density QCD.

I firmly believe that we need to write down the correct kinetic equation for high density QCD. Such an approach has certainly at least one big advantage: the smooth matching with the GLR equation. Unfortunately we have not yet understood how to write such an equation in our nonequilibrium situation. However we have understood better the physical meaning of the new typical momentum in our parton cascade ($\langle |p_t| \rangle$ in section 11.2). It turns out that this momentum is the Landau - Pomeranchuk momentum for our parton medium [24]. Thus the gluon emission with transverse momentum less that $\langle |p_t| \rangle$ is small due to destructive interference between emission before and after collision of the parton with other partons in the medium. The experience with the calculation of the anomalous dimension of high twist gluonic operators also give us understanding why for bosonic degrees of freedom such as a gluon there could be saturation of gluon density. Indeed, our cascade is rather a one dimensional one and for such a system the direction of motion plays the role of spin for fermions.

18 Conclusions.

We can perhaps summarize our discussion with the following statements.

1. The new kinematic region of *high density QCD* is wide open for theoretical and experimental investigation.

2. Perturbative QCD methods have been developed to explore the transition region between the region routinely analyzed by perturbative calculations for hard processes and the hdQCD region.

3. Between the kinematic region of soft processes (key words: unitarity, analyticity, Reggeons, Reggeon Calculus, hadronization models, etc) and the kinematical region of hard processes (key words: quarks, gluons, parton distributions, asymptotic freedom, pQCD, evolution equations, etc) is the region of **semi-hard processes**, where the cross sections can be as large as the geometrical size of the hadron but with a typical transverse momentum large enough that methods of pQCD can be applied.

4. New probes have been developed for this high-density QCD region. Although we still lack some theoretical understanding and cannot provide reliable estimates for these probes, we firmly believe that they provide a deeper insight into QCD and could lead to new experimental discoveries.

Phase Transition.

We can represent the predictions of the previous section as a phase transition between different forms of hadronic (partonic) matter. Our prediction can then be summarized as the possibility of a phase transition from a *quark - gluon ideal gas* to a *gluon liquid* (see Fig. 36).

Indeed, in the *pQCD* region (see Fig.19) we can regard a partonic system as an ideal gas of quarks and gluons because we can neglect their interactions (only emission is essential here).

When the density of partons increases we approach the region where we must consider the interactions between partons in a simple approximation and in a situation where this interaction is not too big. This then is a Van der Waals gas of quarks and gluons. Here we have a theory based on a nonlinear evolution equation that is the analogue of the Van der Waals equation for a parton system.

For even larger values of the density, the smallness of the coupling constant results a small correlation between partons. We call this system of partons a *gluon liquid*. We

recall that the density is high primarily because of emission of gluons and quarks inside this system, which still can be treated in a perturbative way.

The border between the gluon liquid and the Van der Waals gas is the critical line we discussed in Section 12.3. The trajectory of the GLAP evolution equation that touches the critical line separates the Van der Waals gas from the ideal gas. The asymptotic of these borders are also calculable.

In conclusion we want also to recommend you the list of the reviews on the subject [52] which, we hope, you will be able to understand after these lectures.

Acknowledgments:

I would like to thank the CNPq for financial support and the organizing committee of the Third Gleb Watagin school for invitation to read these lectures. I am very grateful to all my friends especially F. Caruso, A. Gotsman, U.Maor and A. Santoro with whom I discussed the ideas of such lectures and who supported me in this rather difficult job.

Figure Caption:

Fig.1: The exchange of the resonance with spin j.

Fig.2: The exchange of the Reggeon.

Fig.3: The Reggeon trajectories.

Fig.4: Resonance - Reggeon Duality.

Fig.5: The Pomeron structure in the Veneziano model.

Fig.6: The structure of the parton cascade.

Fig.7: The random walk of parton in transverse plane.

Fig.8: The single diffraction dissociation process in the Pomeron approach

Fig.9: The triple Pomeron diagram.

Fig.10: An example of enchanced Pomeron diagrams.

Fig.11 The AGK cutting rules for two Pomeron exchange.

Fig.12: Hadron -dueteron interaction.

Fig.13: The process with multiplicity $2 < n_N > (a)$ and $< n_N > (b)$.

Fig.14: The ν Pomeron exchange diagram with μ cut Pomeron.

Fig.15: Pomeron diagrams for the total,elastic and diffraction dissociation cross sections.

Fig.16: Pomeron diagrams for inclusive cross section (a) and rapidity correlations (b).

Fig.17: One and two parton shower processes.

Fig.18: Single diffraction dissociation in Reggeon approach.

Fig.19: The map of QCD.ρ is the parton (gluon) density and r is the distances resolved in an experiment.

Fig.20: The "Pomeron" Calculus in QCD.

Fig.21: The Born Approximation (BA) of pQCD.

Fig.22: The next to BA of pQCD for quark-quark scattering: emission of one extra gluon.

Fig.23: The next to BA of pQCD for quark-quark scattering: α_S^2 correction to elastic amplitude.

Fig.24: The next to BA of pQCD for quark -quark scattering: gauge invariance trick.

Fig.25: The next to BA of pQCD for quark -quark scattering: the resulting answer for one extra gluon emission.

Fig.26: The relation between colour coefficients.

Fig.27: The BFKL equation.

Fig.28: The basic branching process in DIS.

Fig.29: The parton distribution in the transverse plane.

Fig.30: Structure of the parton cascades at low x and the coherence in "ladder" diagrams.

Fig.31: The random walk picture in $\ln k_t^2$.

Fig.32: The behaviour of $xG(x, Q^2)$ versus Q^2 at fixed x.

Fig.33: Trajectory of the nonlinear GLR equation.

Fig.34: The Mueller - Navalet process.

Fig.35: Large Rapidity Gap process.

Fig.36: The phase diagram for hadron - hadron collisions for zero rapidity in cm frame. W is the absorption probability defined in eq. (103).

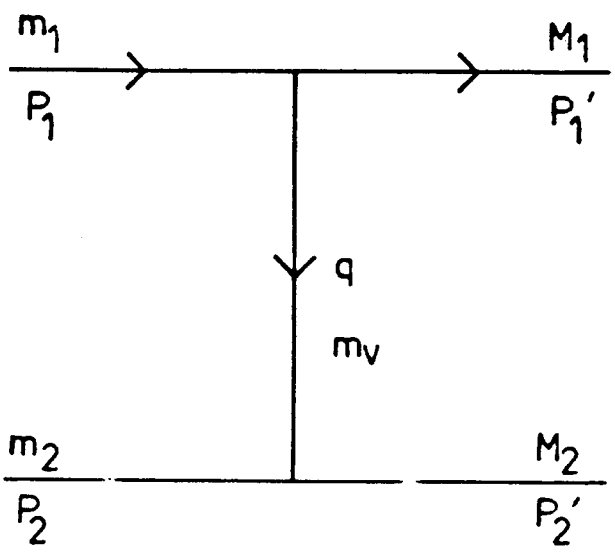

FIG. 1

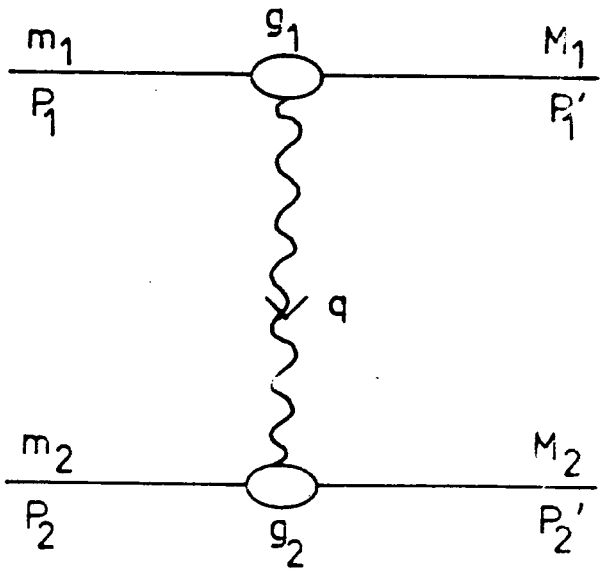

FIG. 2

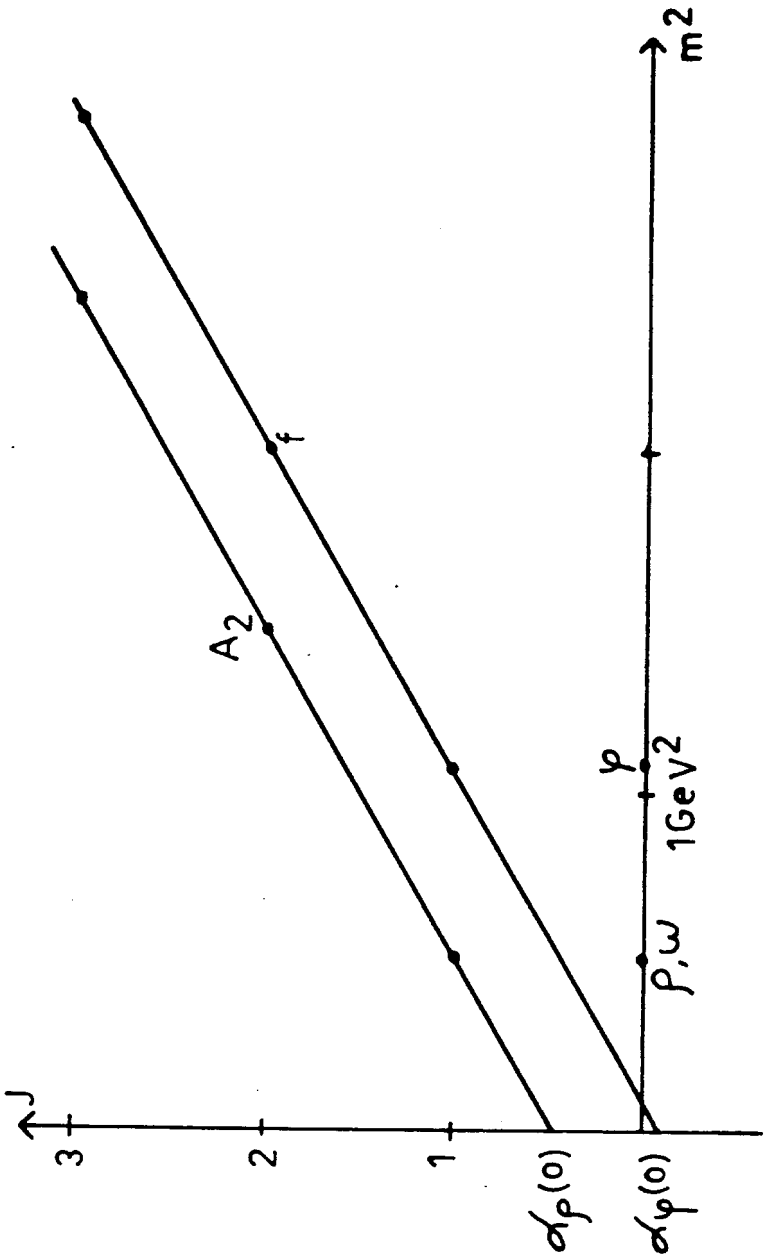

FIG. 3

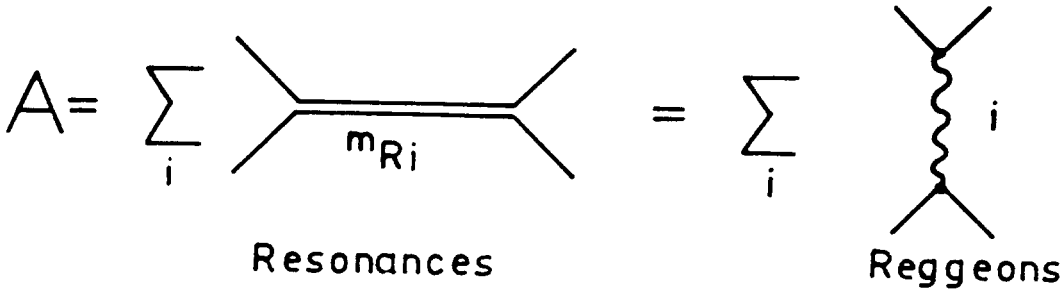

FIG. 4

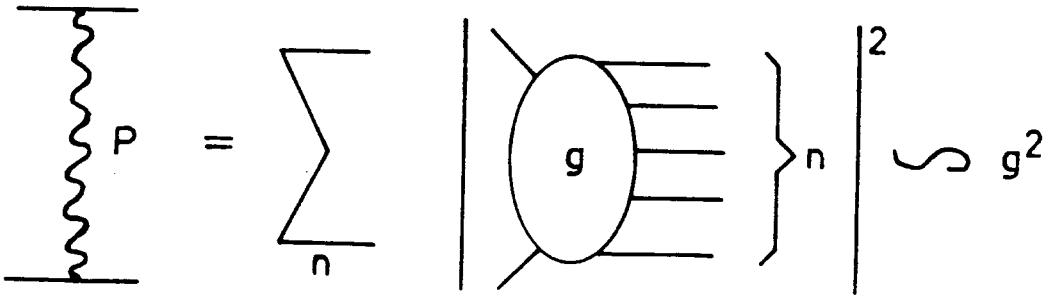

FIG. 5

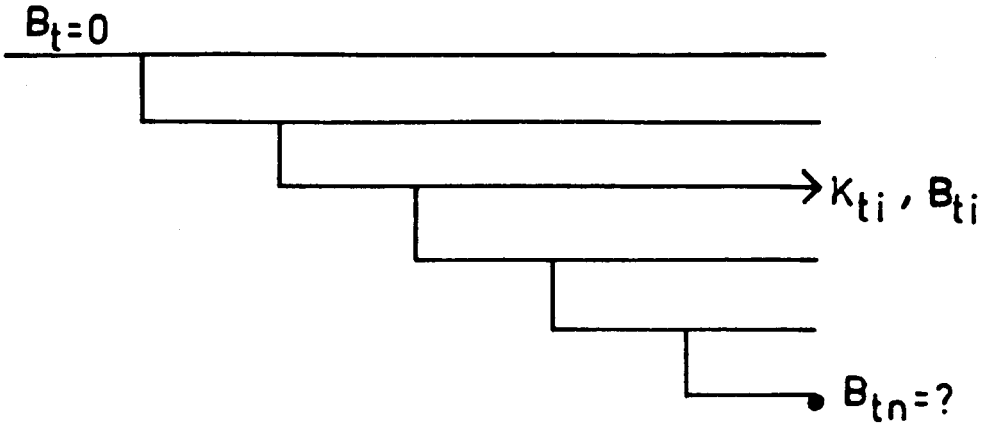

FIG. 6

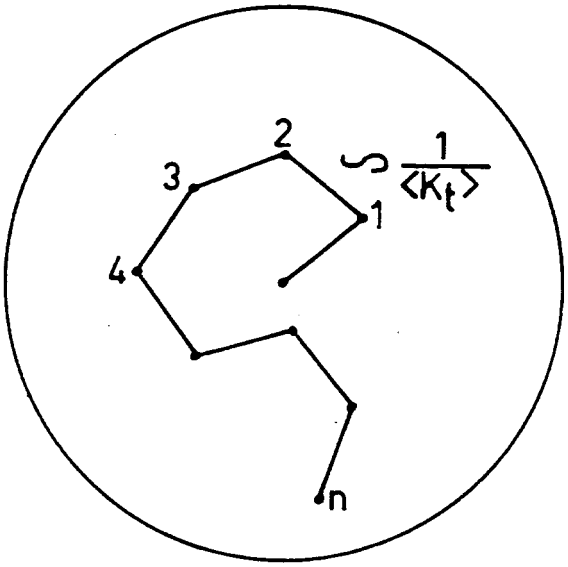

FIG. 7

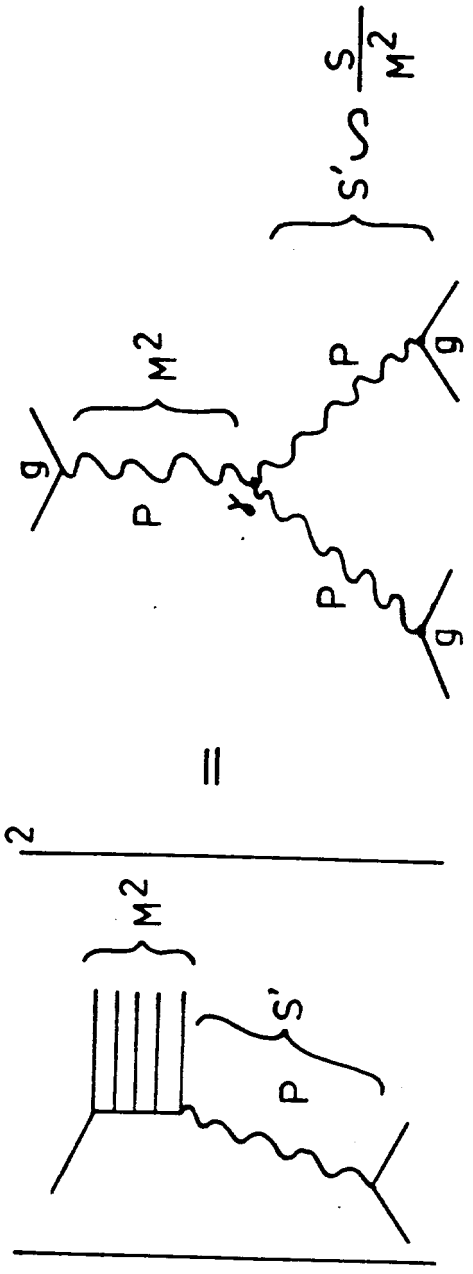

FIG. 8

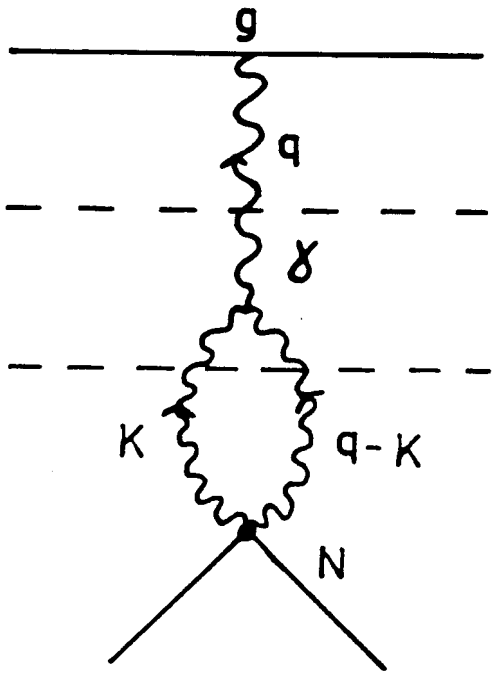

FIG. 9

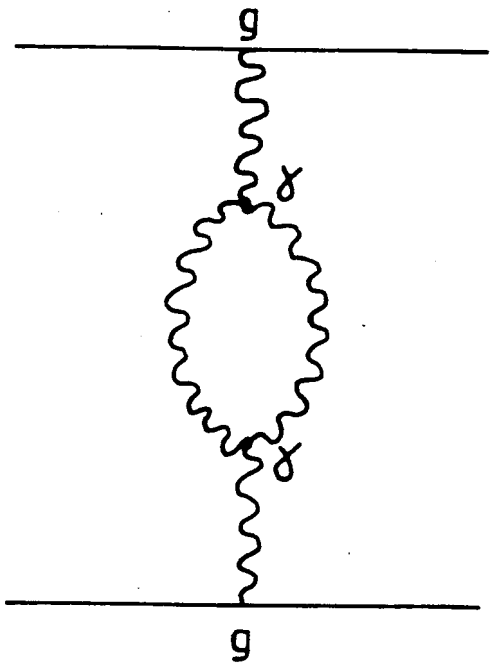

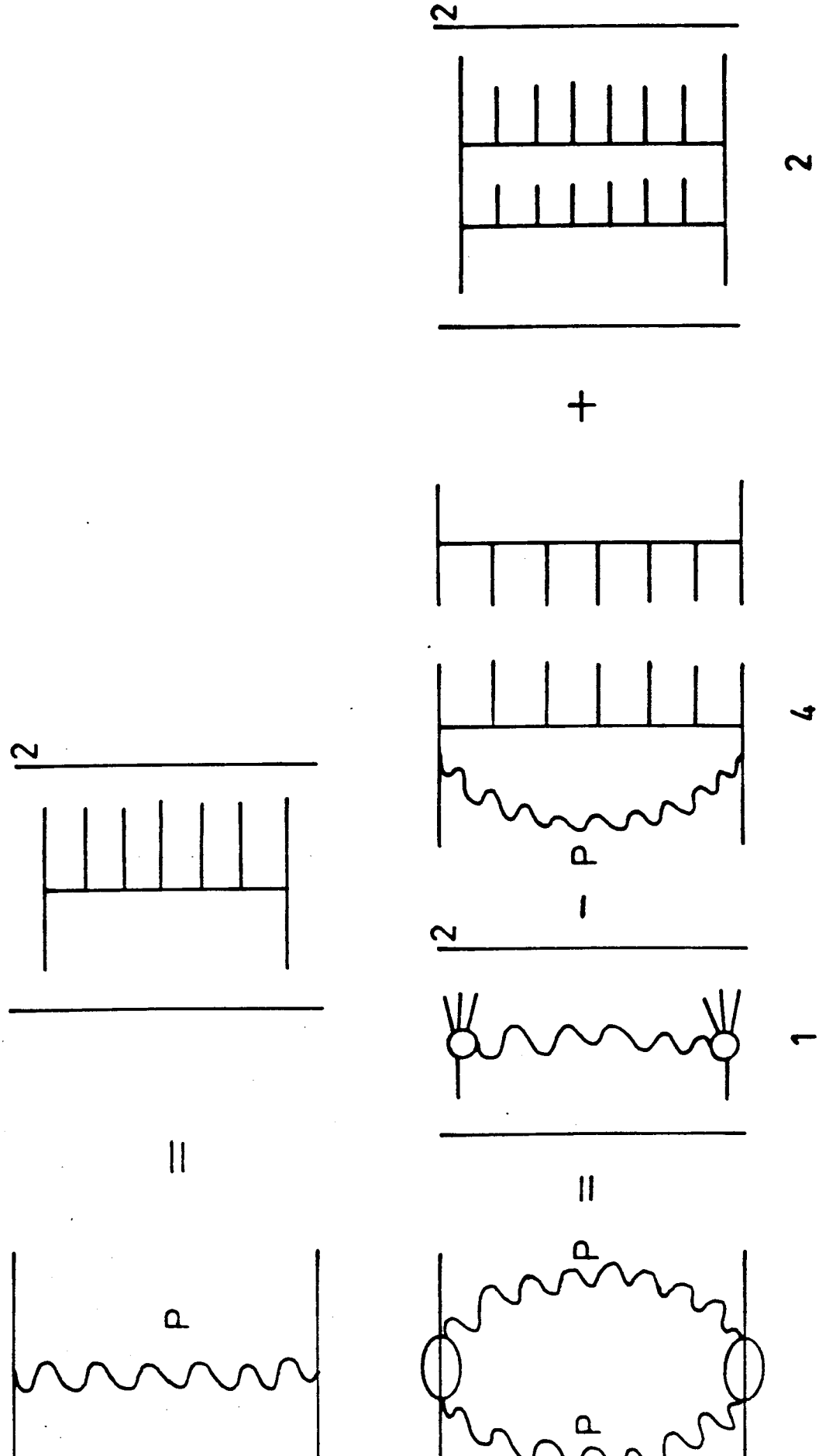

FIG. 11

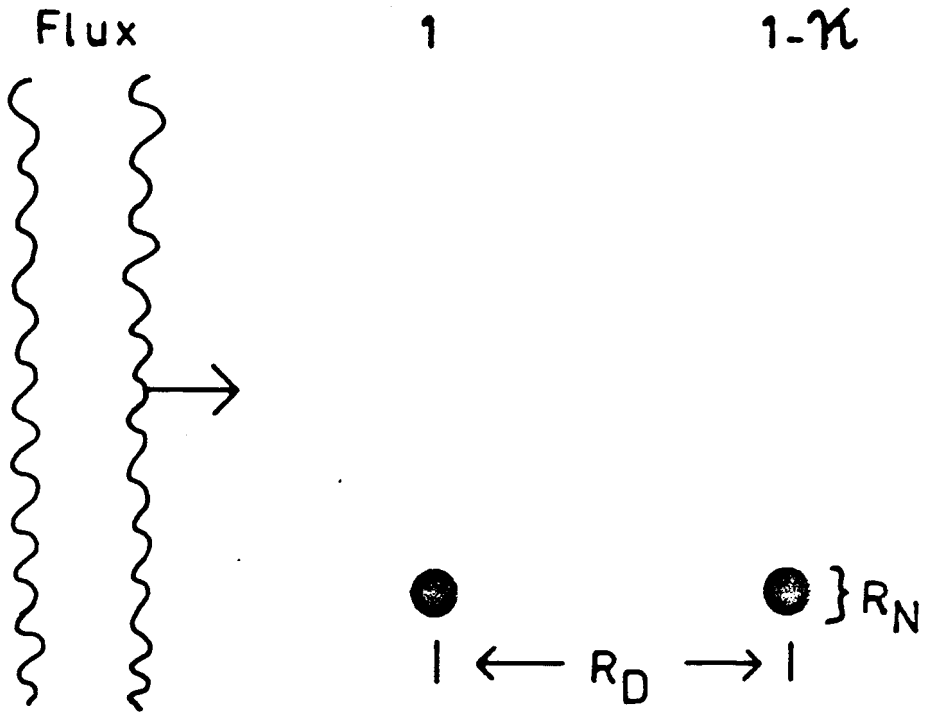

FIG. 12

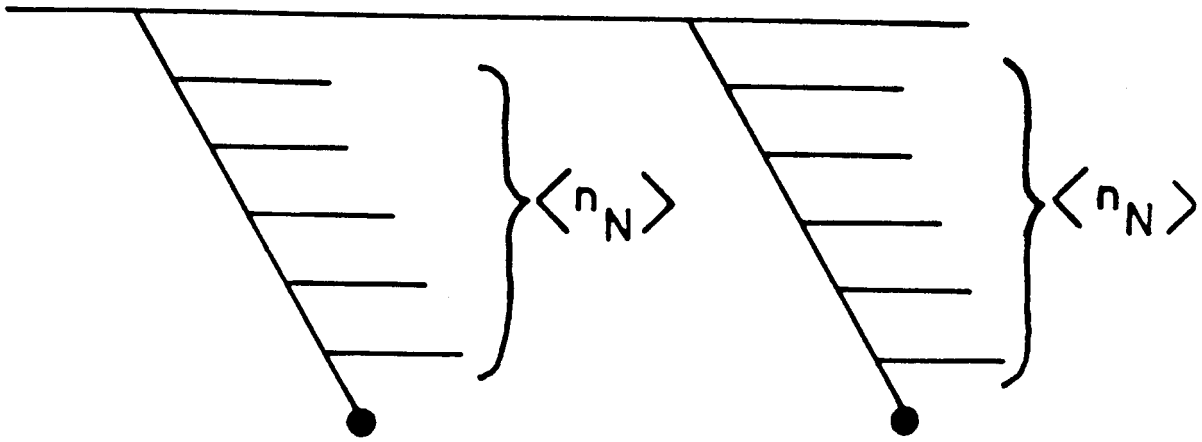

(a)

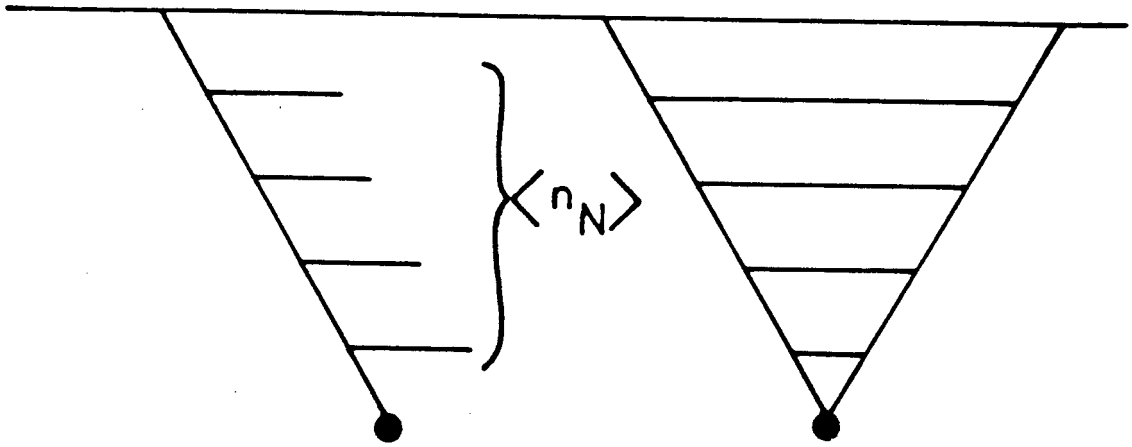

(b)

FIG. 13

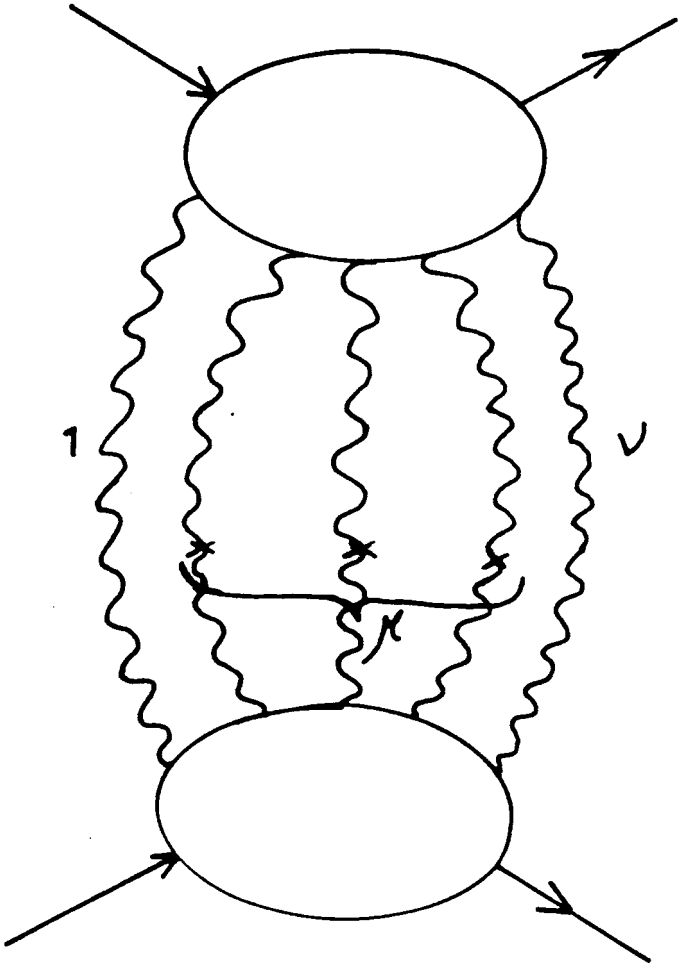

FIG. 14

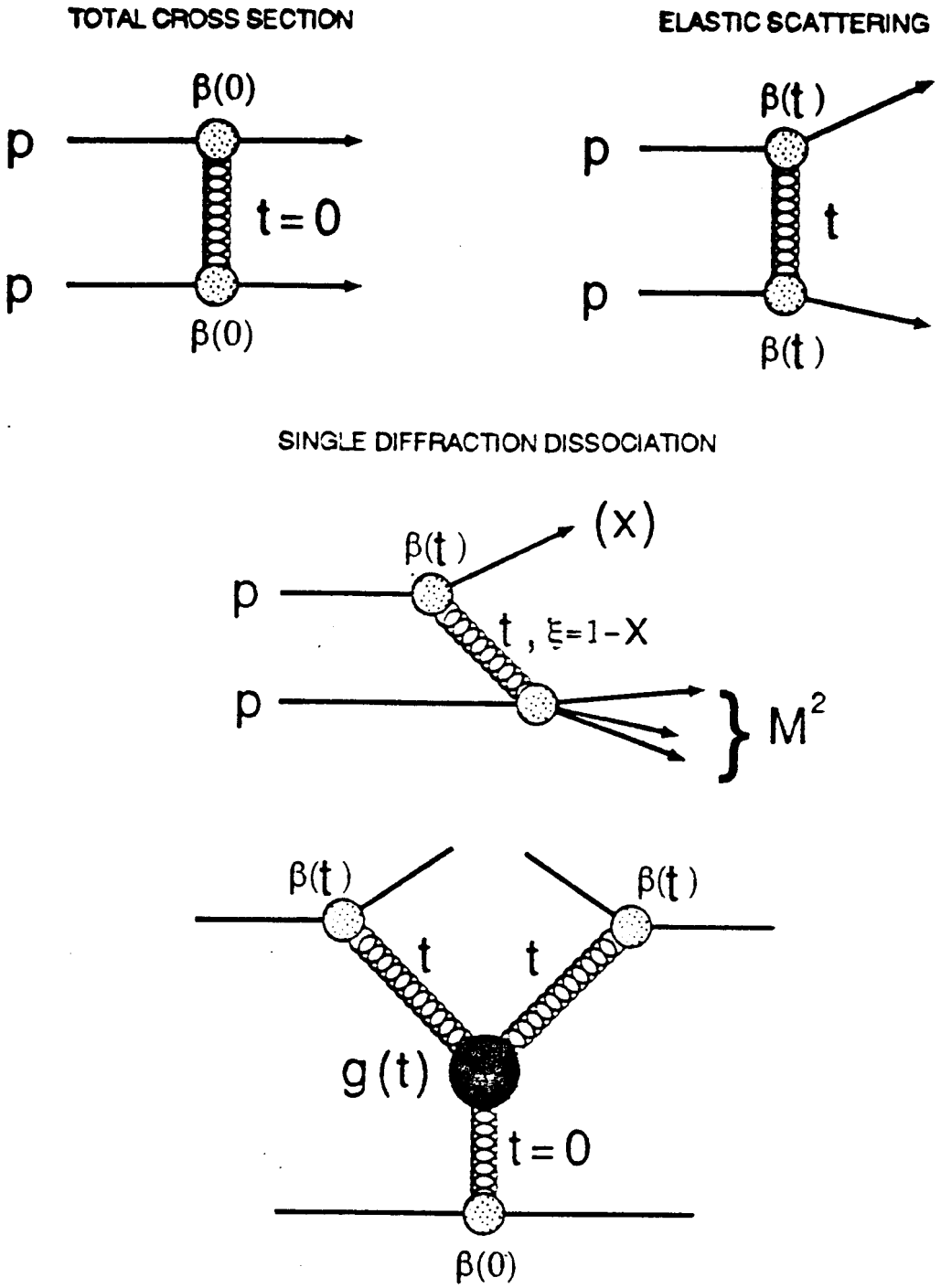
TOTAL CROSS SECTION
β(0)
p
t=0
p
β(0)
ELASTIC SCATTERING
β(t)
p
t
p
β(t)
SINGLE DIFFRACTION DISSOCIATION
(x)
β(t)
p
t , ξ=1-X
p
M²
β(t)
β(t)
t
t
g(t)
t=0
β(0)

Fig. 15

DOUBLE DIFFRACTION DISSOCIATION

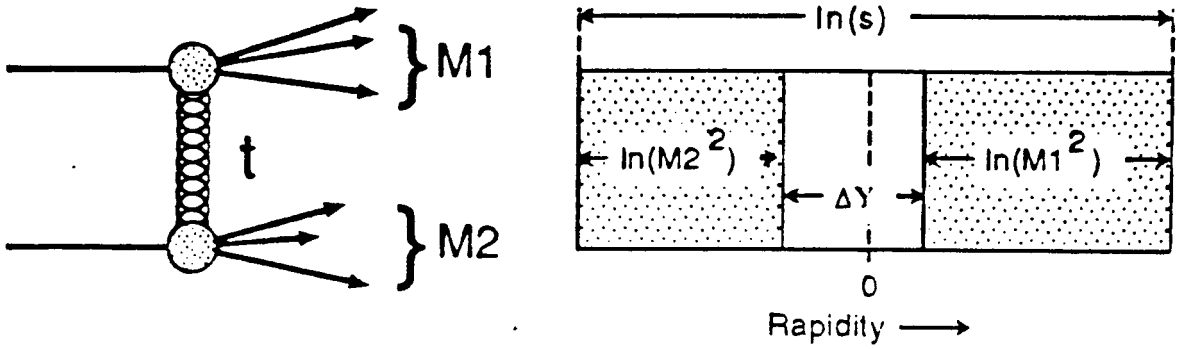

DOUBLE POMERON EXCHANGE

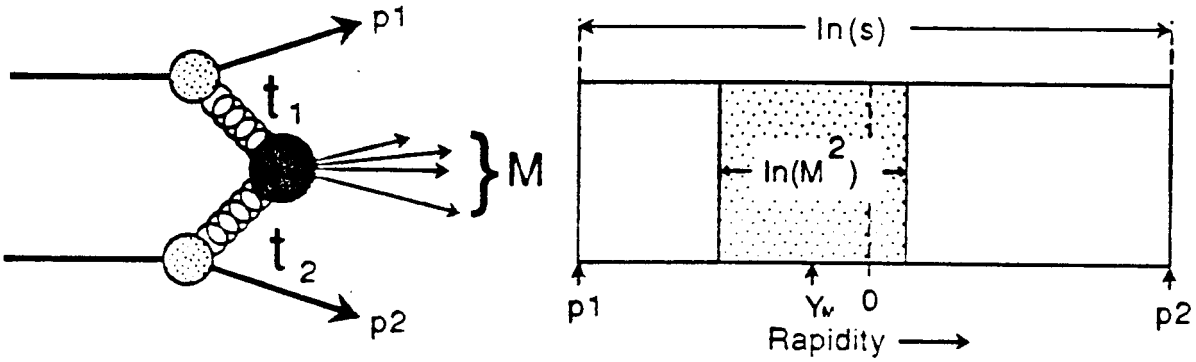

Fig. 15

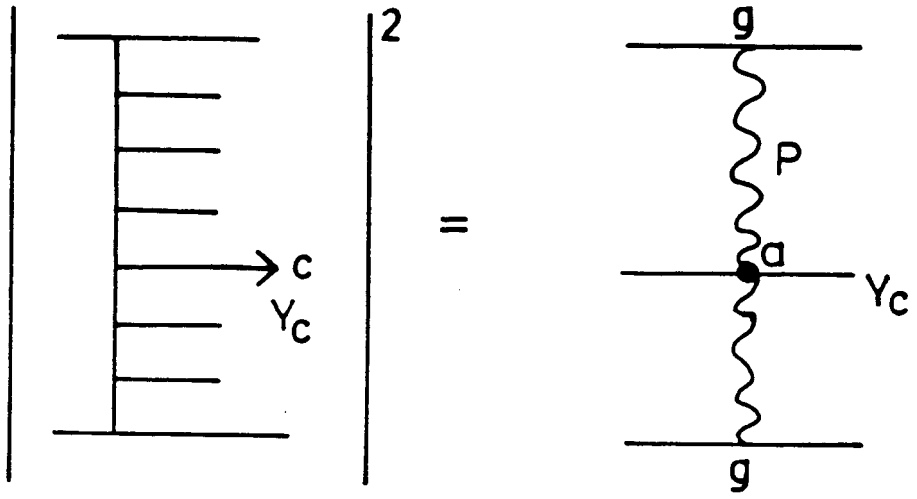

(a)

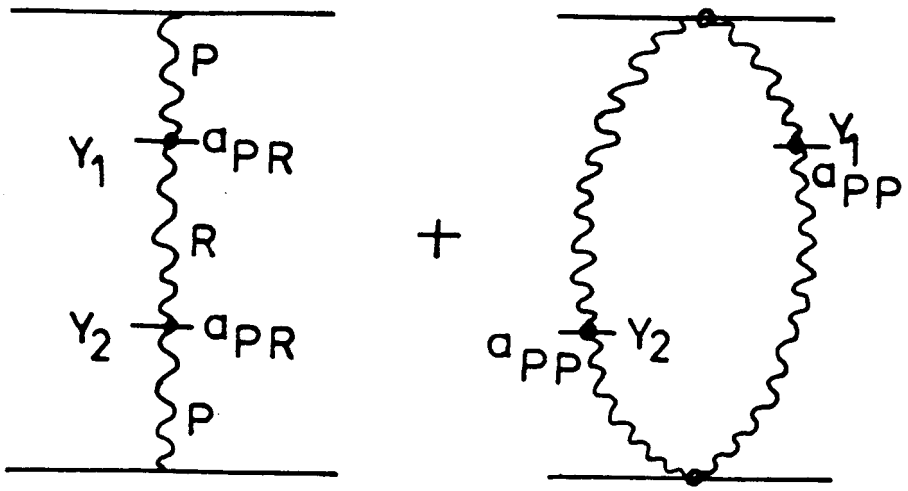

(b)

FIG. 16

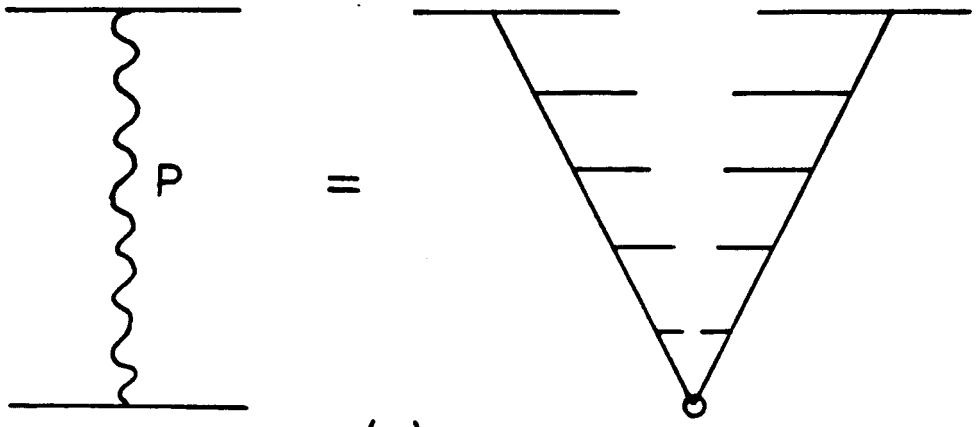

(a)

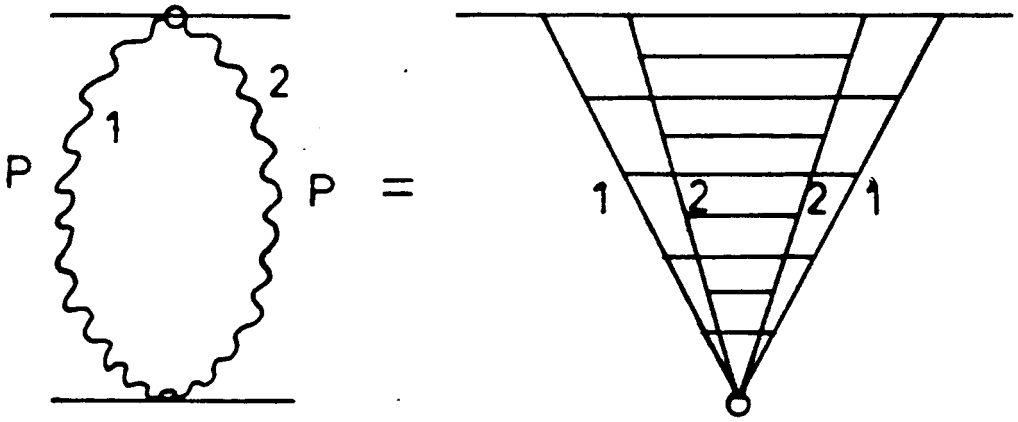

(b)

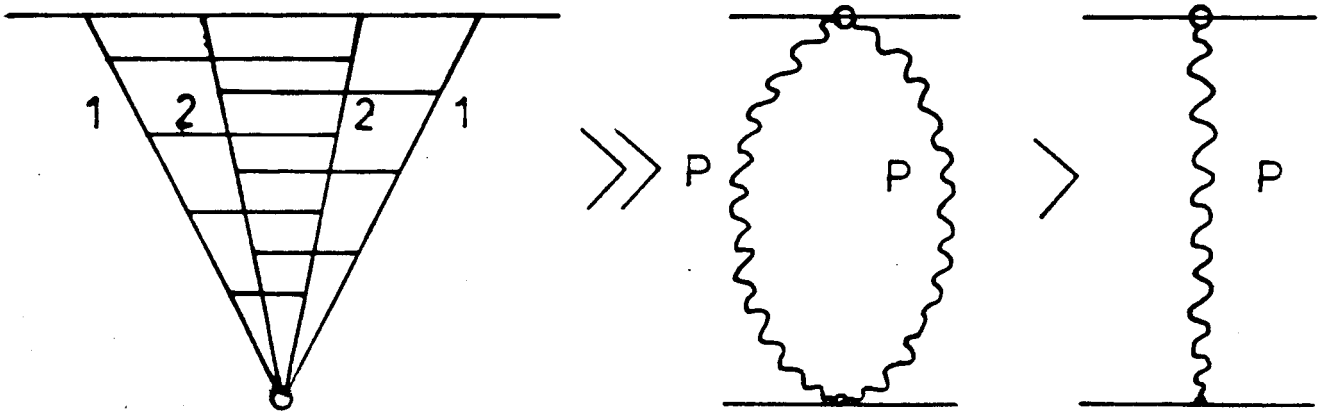

FIG. 17

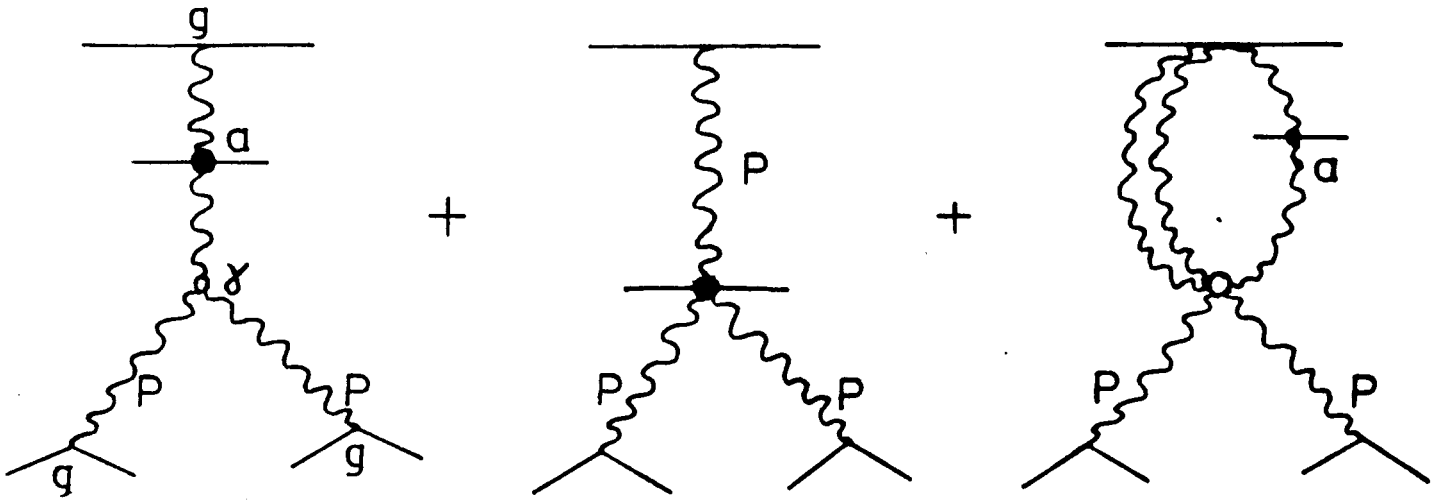

FIG. 18

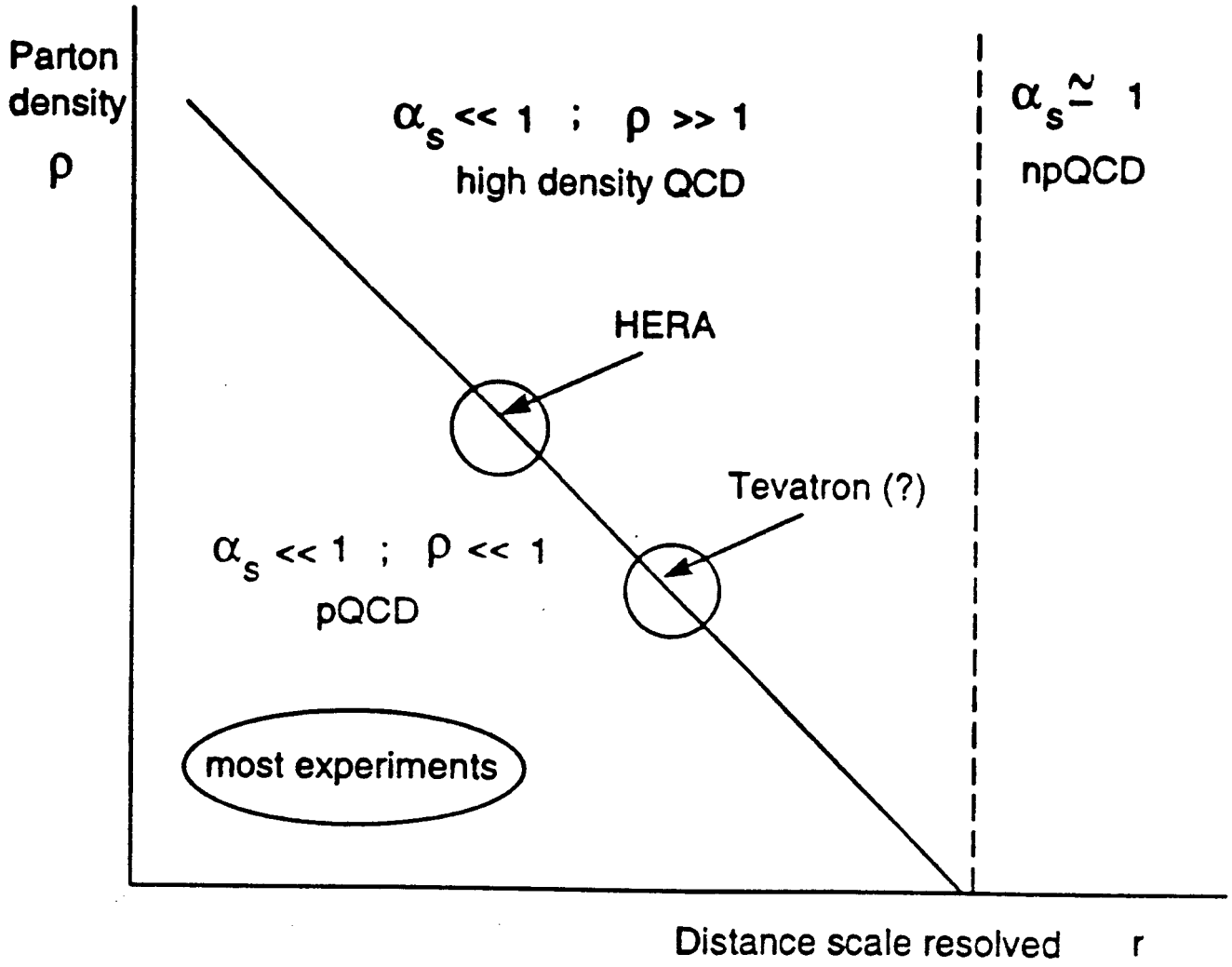
Parton density ρ
$\alpha_s \ll 1$; $\rho \gg 1$
high density QCD
$\alpha_s \simeq 1$
npQCD
HERA
Tevatron (?)
$\alpha_s \ll 1$; $\rho \ll 1$
pQCD
most experiments
Distance scale resolved r

Fig. 19

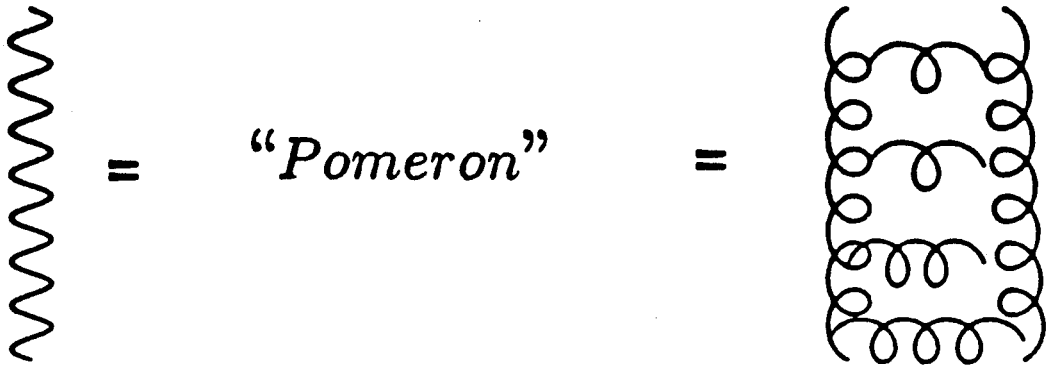

"Pomeron" Interactions :

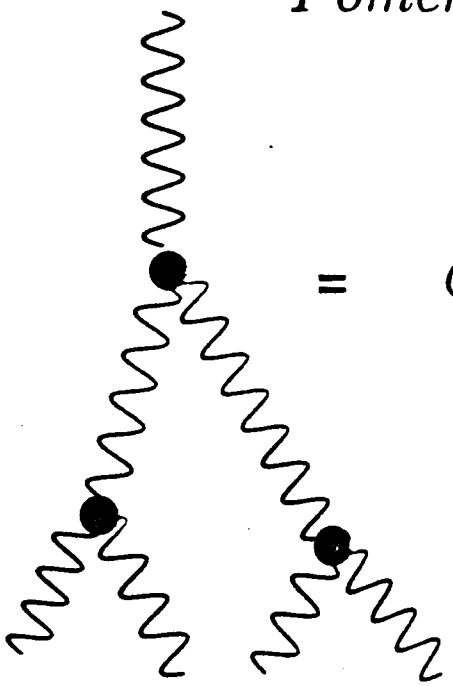

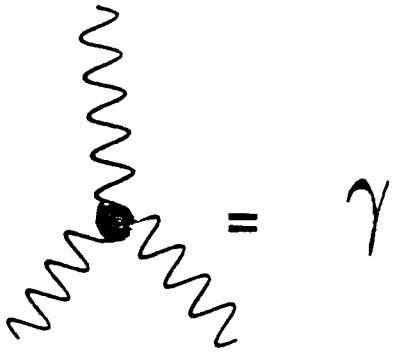

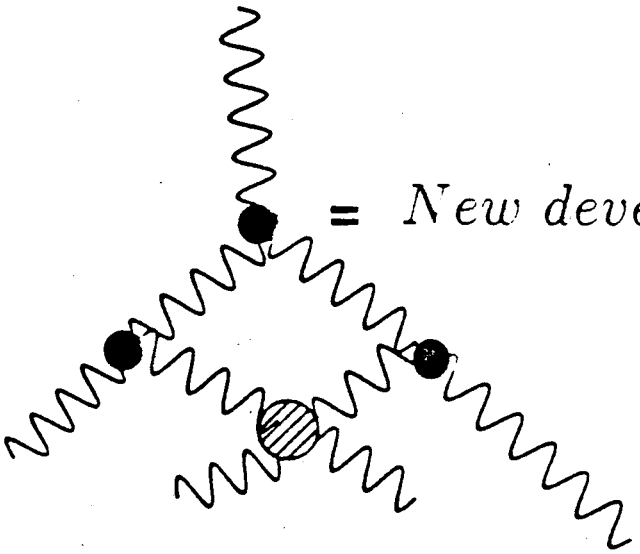

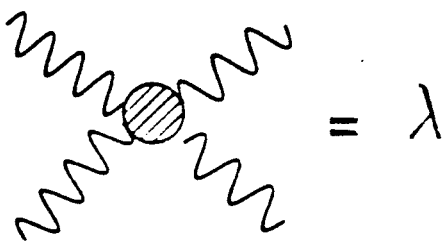

Fig. 20

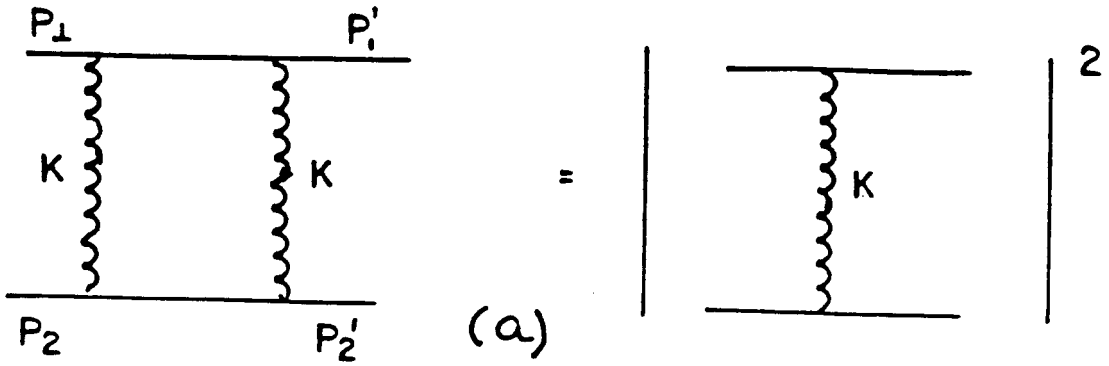

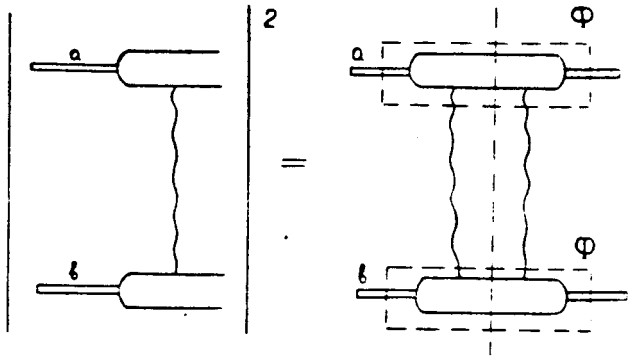

(B)

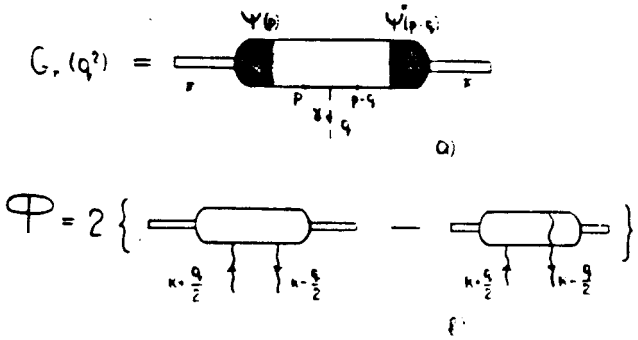

(C)

Fig. 21

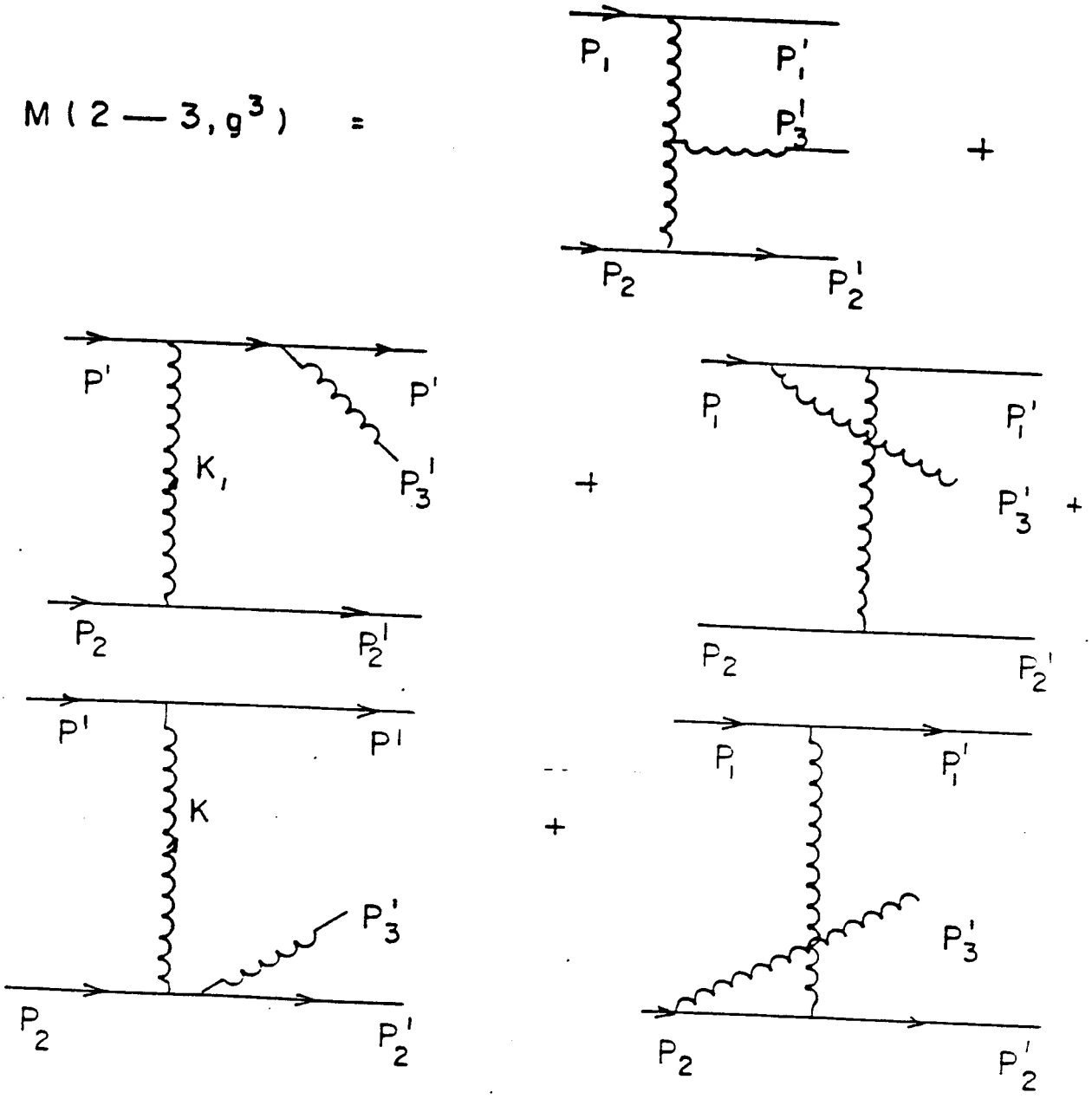
M (2 — 3, g³) =
P1
P1'
P3'
P2
P2'
+
P'
P'
K1
P3'
P2
P2'
+
P1
P1'
P3'
P2
P2'
+
P'
P'
K
P3'
P2
P2'
+
P1
P1'
P3'
P2
P2'

Fig. 22

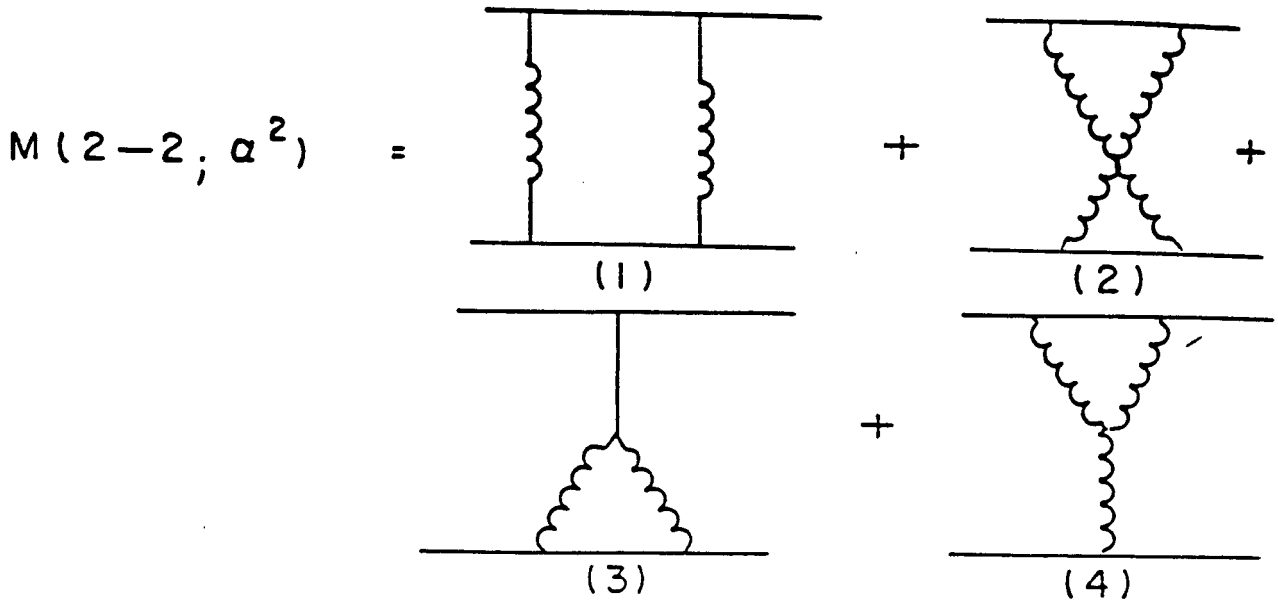

Fig. 23

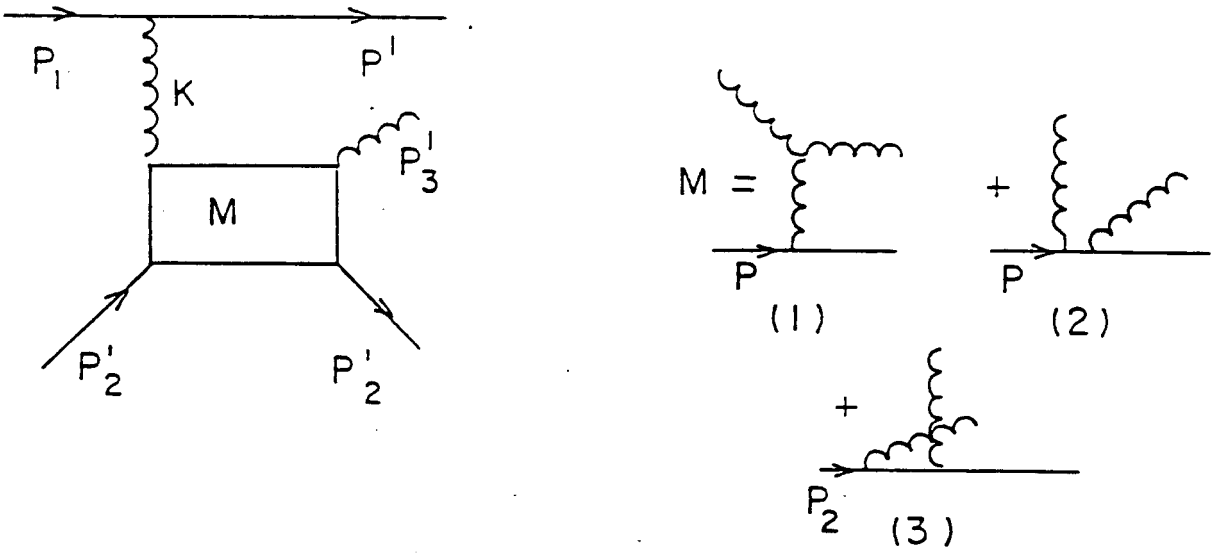

Fig. 24

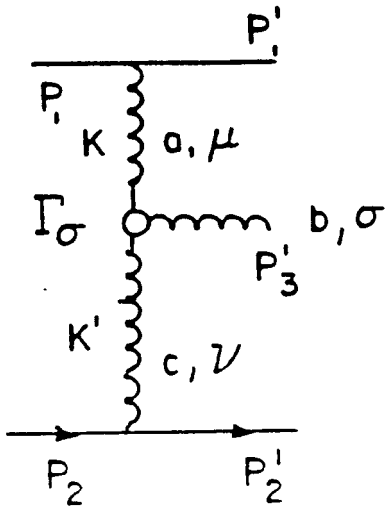

Fig. 25

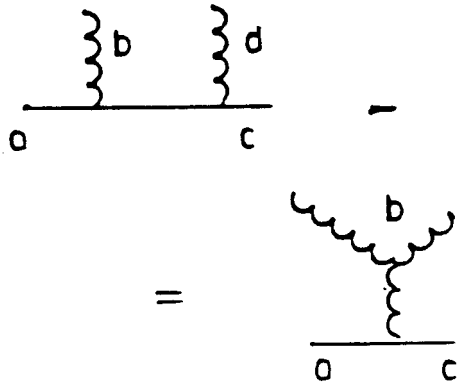

Fig. 26

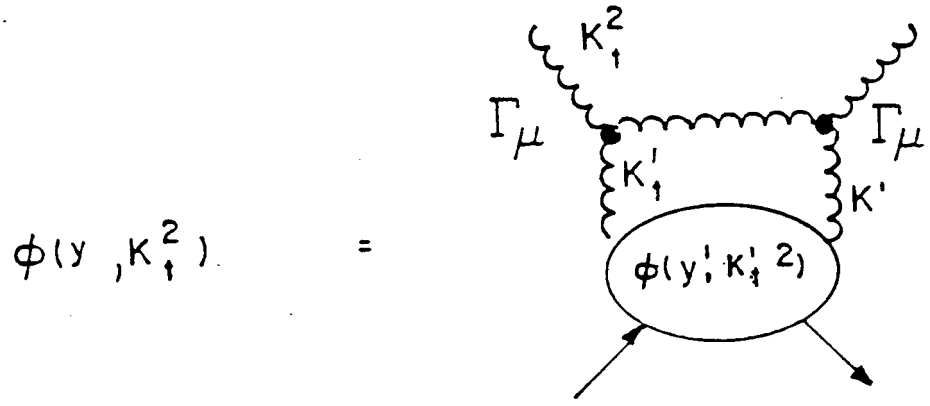

Fig. 27

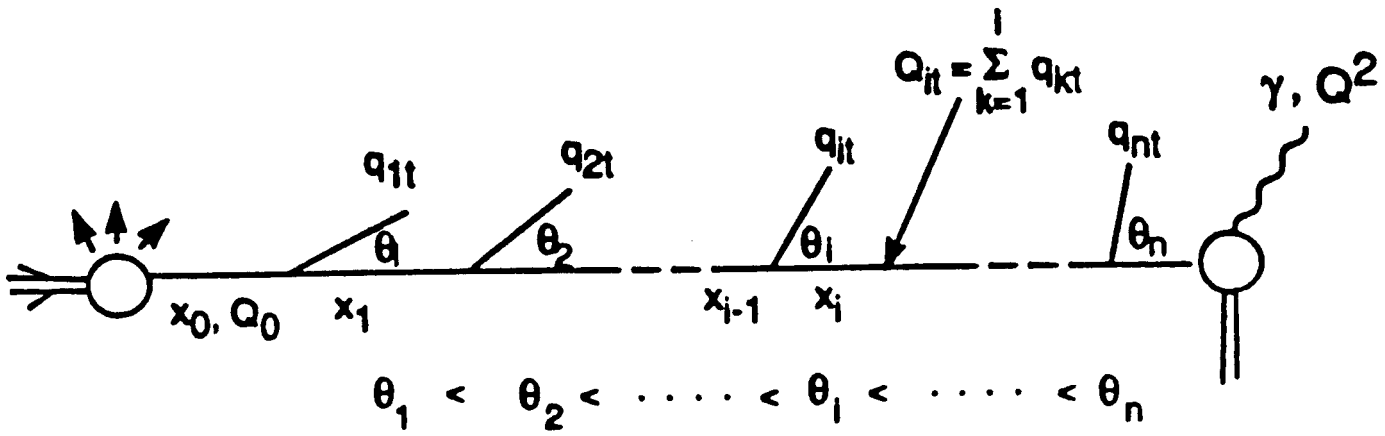
$Q_{it} = \sum_{k=1}^{i} q_{kt}$
γ, Q^2
q_{1t}
q_{2t}
q_{it}
q_{nt}
θ_1
θ_2
θ_i
θ_n
x_0, Q_0
x_1
x_{i-1}
x_i
$\theta_1 < \theta_2 < \cdots < \theta_i < \cdots < \theta_n$

Fig. 28

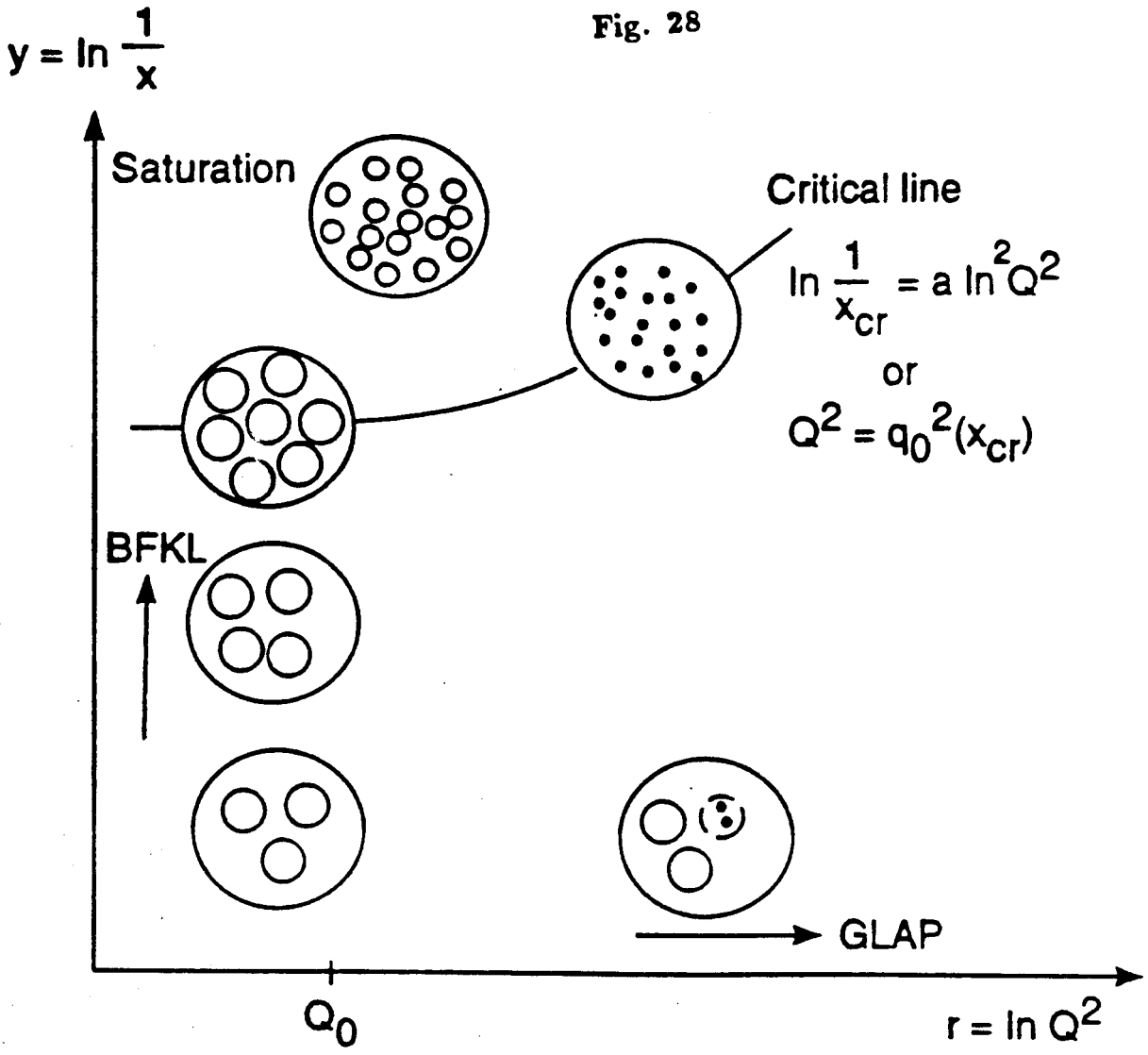
$y = \ln \frac{1}{x}$
Saturation
Critical line
$\ln \frac{1}{x_{cr}} = a \ln^2 Q^2$
or
$Q^2 = q_0^2(x_{cr})$
BFKL
GLAP
Q_0
$r = \ln Q^2$

Fig. 29

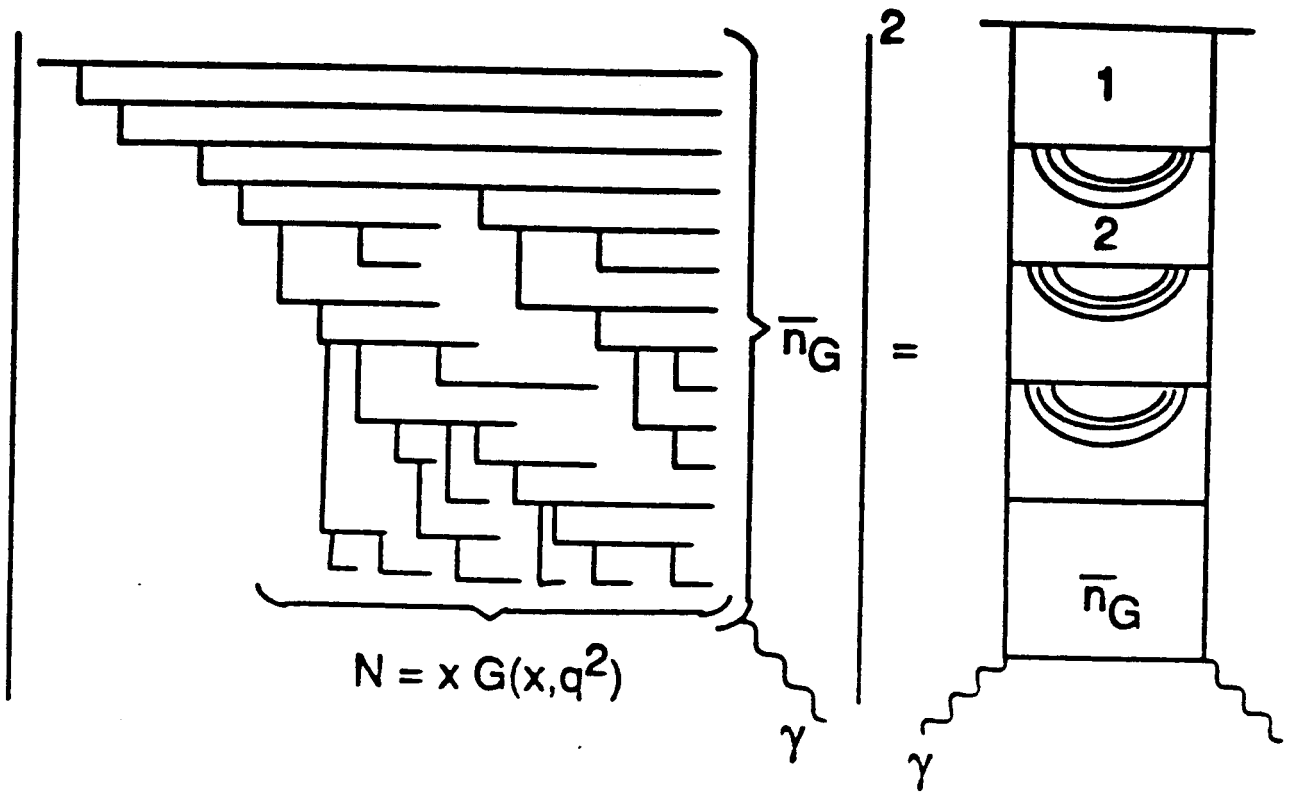

Fig. 30

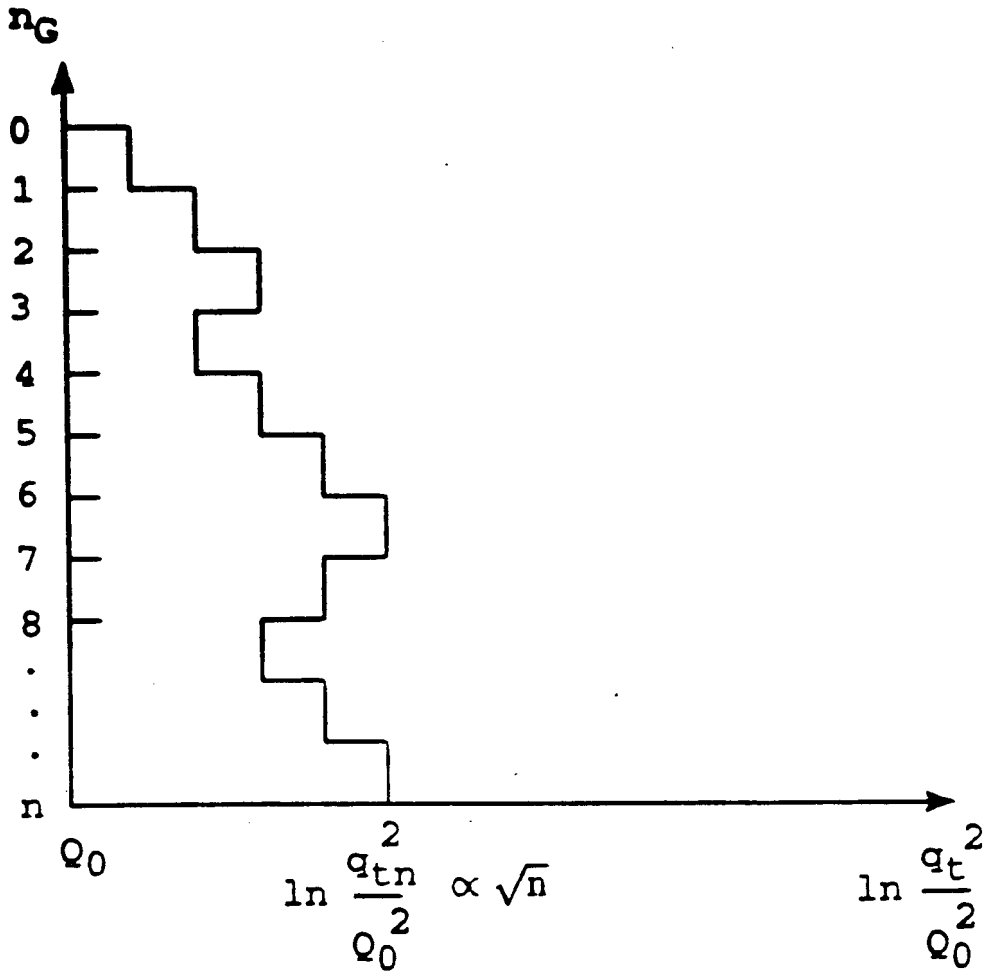
n_G
0
1
2
3
4
5
6
7
8
n
Q_0
$\ln \frac{q_{tn}^2}{Q_0^2} \propto \sqrt{n}$
$\ln \frac{q_t^2}{Q_0^2}$

Fig. 31

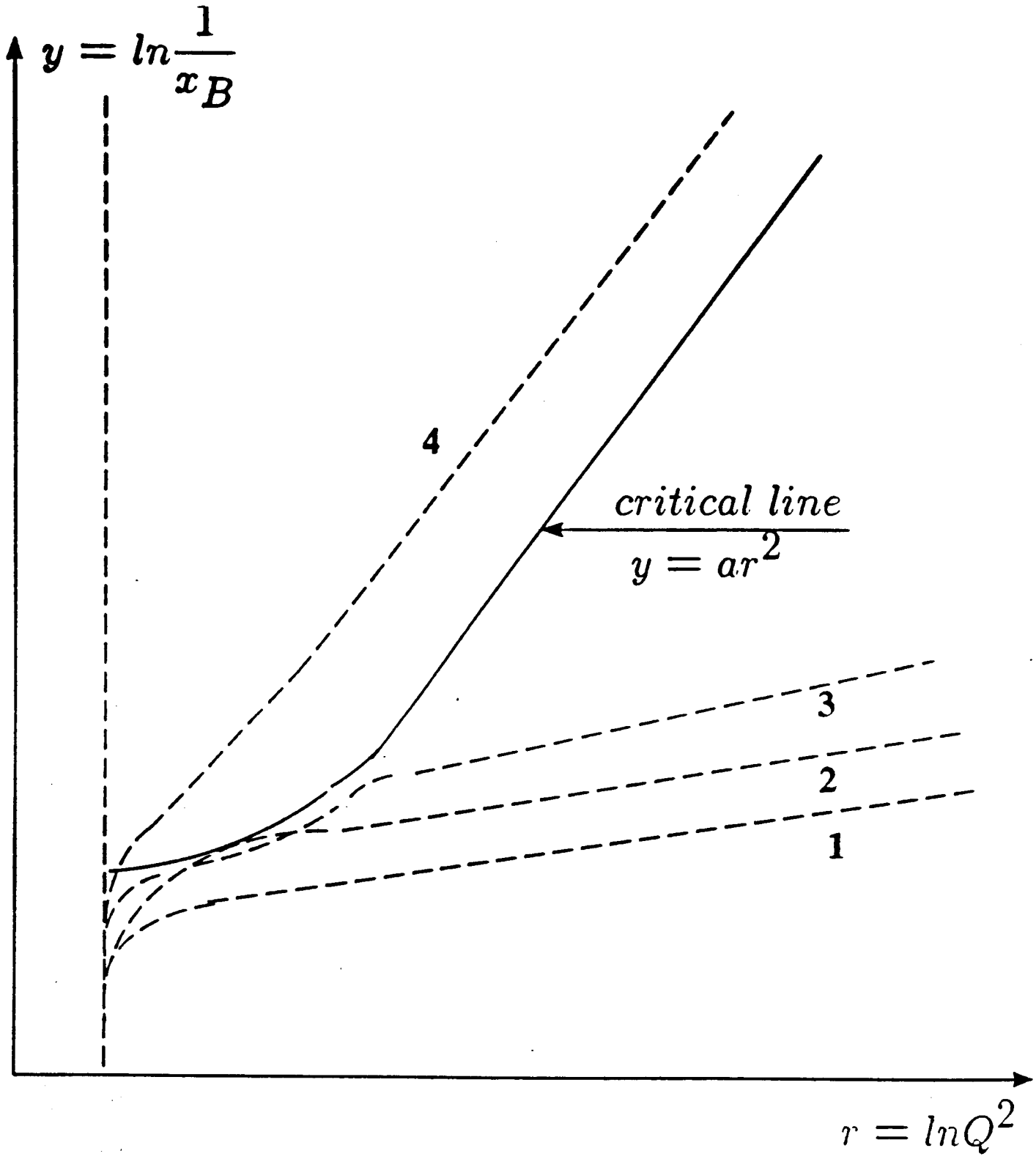

Fig. 33

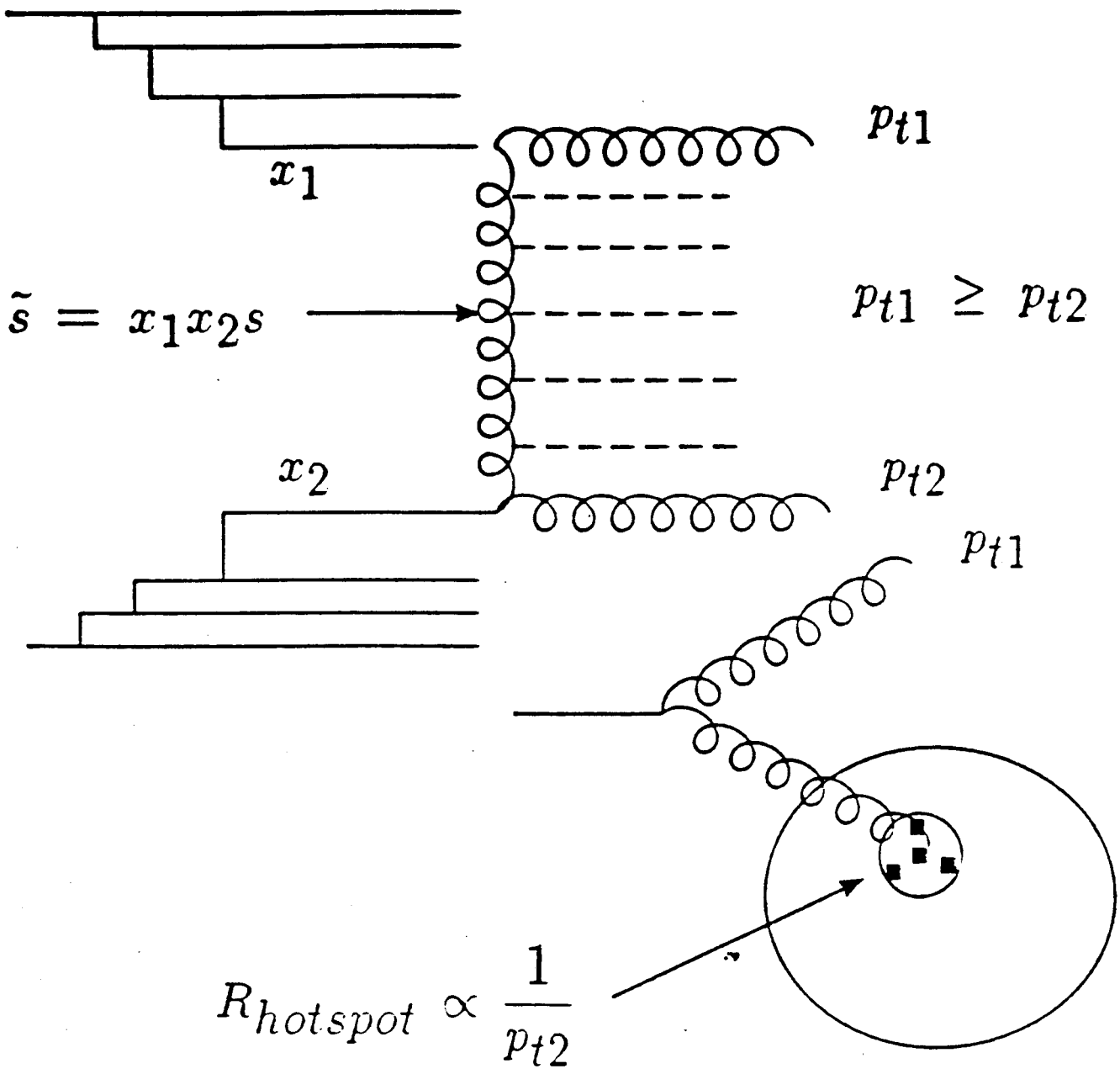
p_{t1}
x_1
$\tilde{s} = x_1 x_2 s$
$p_{t1} \geq p_{t2}$
x_2
p_{t2}
p_{t1}
$R_{hotspot} \propto \frac{1}{p_{t2}}$

Fig. 34

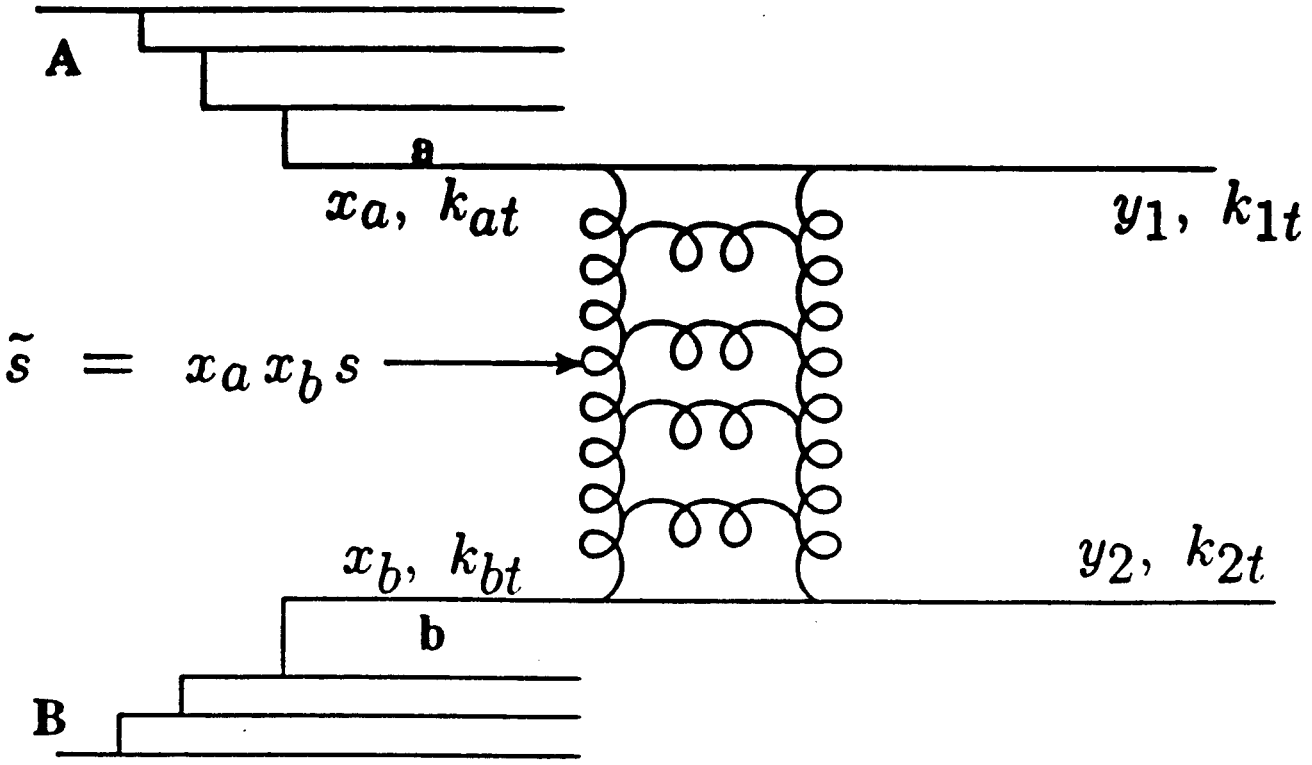

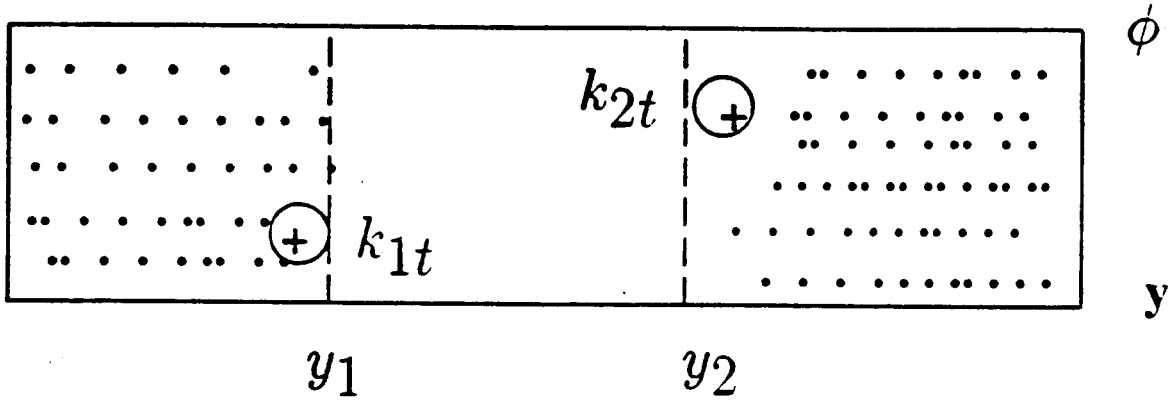

Fig. 35

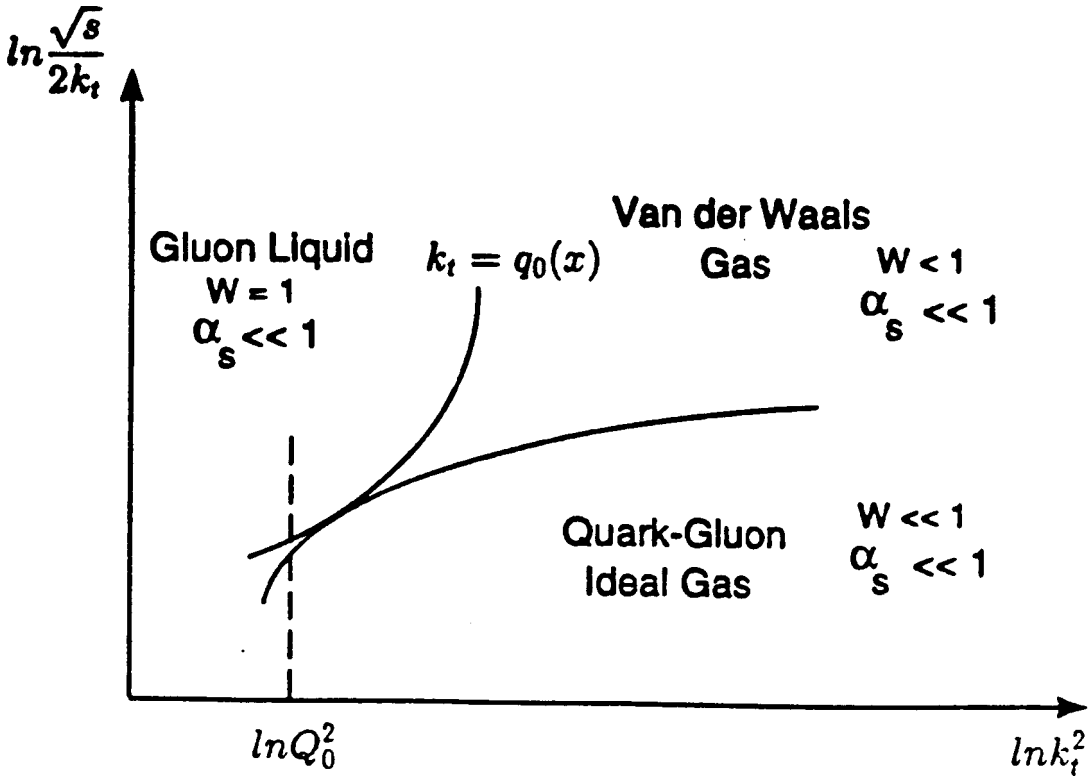
$ln\frac{\sqrt{s}}{2k_t}$
Gluon Liquid
W = 1
$\alpha_s << 1$
$k_t = q_0(x)$
Van der Waals
Gas
W < 1
$\alpha_s << 1$
Quark-Gluon
Ideal Gas
W << 1
$\alpha_s << 1$
lnQ_0^2
lnk_t^2

Fig. 36

References

[1] G. Veneziano: *Nuovo Cim.* **57A** (1968) 190; *Phys. Rep* **C9** (1974) 199.

[2] T.Regge: *Nuovo cim.* **14**(1959) 951.

[3] A.Donnachie and P.V. Landshoff: *Nucl. Phys.* **B244** (1984) 322; *Nucl. Phys.* **B267** (1986) 690; P.V.Landshoff: In *Proc. of the LP - HEP'91 Conference*. Volume 2 p.363, Singapore: World Scientific (1992)

[4] R. Feynman: *Phys. rev. lett.* **23** (1969) 1415; "Photon - hadron Interaction" N.Y.Benjamin, 1972.

[5] V.N. Gribov: *Sov. J. Nucl. Phys.* **9** (1969) 640; Proc. VIII LNPI Winter School, 1973, vol. II,p.5.

[6] J.D. Bjorken: *Phys. Rev.* **179** (1969) 1547; J.D. Bjorken and E. Pschos: *Phys.Rev* **185** (1969) 1975.

[7] V.N. Gribov: *ZhETF* **57** (1967) 654.

[8] V.A.Abramovski,V.N. Gribov and O.V. Kancheli: *Sov. J. Nucl. Phys.* **18** (1973) 308.

[9] A.H. Mueller: *Phys. Rev.* **D23** (1970) 2963.

[10] B.M. Mc Coy and T.T. Wu: *Phys. Rev.* **D12** (1975) 546,577, S.G.Matinian and A.G.Sedrakian: *JETP letter* **23** (1976) 588,**24** (1976) 240, *Sov. J. Nucl. Phys.* **24** (1976) 844.

[11] V.N. Gribov and L.N. Lipatov: *Sov. J. Nucl. Phys.* **15** (1972) 438; L.N. Lipatov: *Yad. Fiz.* **20** (1974) 181; G. Altarelli and G. Parisi:*Nucl. Phys.* **B 126** (1977) 298; Yu.L.Dokshitzer: *Sov.Phys. JETP* **46** (1977) 641.

[12] Yu. L. Dokshitzer, V.A. Khoze, A.H. Mueller and S.I. Troyan: *Basics of Perturbative QCD*. Gif-sur-Yvette Cedex: Editions Frontieres (1992)

[13] J.C.Collins, D.E. Soper and G. Sterman: *Nucl. Phys.* **B308** (1988) 833; J.C.Collins, D.E. Soper and G. Sterman: In *Perturbative Quantum Chromodynamics* , ed. A.H Mueller. Singapore: World Scientific (1989) and references therein.

[14] A.S. Kronfeld and P.B. Mackenzie: *Ann. Rev. Nucl. Part. Sci.* **43** (1993) 793.

[15] M. A.Shifman: *Proceedings of the Workshop "QCD - 20 Years Later"*, ed. P.M. Zerwas, H.A. Kastrup. Volume 2 p.775 (1992).

[16] E.A. Kuraev, L.N. Lipatov and V.S. Fadin: *Sov. Phys. JETP* **45** (1977) 199 ; Ya.Ya. Balitskii and L.V. Lipatov:*Sov. J. Nucl. Phys.* **28** (1978) 822; L.N. Lipatov: *Sov. Phys. JETP* **63** (1986) 904.

[17] F.E.Low: *Phys. Rev.* **D12** (1975) 163; S. Nussinov: *Phys. Rev. Lett.* **34** (1975) 1286.

[18] V.V. Sudakov: *Zh. ETF* **30**(1956) 187.

[19] T. Jaroszewicz: *Phys. Lett.* **B116** (1982) 291.

[20] M. Braun: Reggeizied Gluons with a Running Coupling Constant, US - FT /11 - 94, Oct. 1994.

[21] A.H. Mueller: *Nucl. Phys.* **B415** (1994) 373.

[22] A.H. Mueller and B. Patel: *Nucl. Phys.* **B425** (1994) 471; N.N. Nikolaev and B.G. Zakharov: *Phys. Lett.* **B333** (1994) 250,**B 328** (1994) 486, **327** (1994) 149, 157, *(Sov. Phys. JETP* **78** (1994) 806, *(JETP Lett.* **59** (1994) 6; Mao Li and Chung - I Tan: BROWN - HET -943, July 1994, hep - ph/ 9407299.

[23] A.H. Mueller : *Journal of Physics* **G19** (1993) 1463.

[24] E. Laenen and E. Levin : *Ann. Rev. Nucl. Part. Sci.* **44** (*in print*).

[25] L. V. Gribov, E. M. Levin and M. G. Ryskin: *Phys.Rep.* **100** (1983) 1.

[26] E.M.Levin and M.G. Ryskin: *Sov. J. Nucl. Phys.* **41** (1985) 300.

[27] A.H. Mueller: *Nucl. Phys.* **B335** (1990) 115; *Nucl. Phys.* **B317** (1989) 573; *Nucl. Phys.* **B307** (1988)) 34.

[28] A.H.Mueller and J. Qiu: *Nucl. Phys.* **B268** (1986) 427.

[29] A.D.Martin: *J. Phys.* **G19**931603 and references therein.

[30] A.J.Askew,J. Kwiecinski, A.D.Martin and P.J. Sutton: *Phys. Rev.* **D 47** 3775 (1993); J.Kwiecinski: *J. Phys.* **G19**931443 and references therein.

[31] E. Levin: *J. Phys.* **G19**931453 and references therein

[32] V.Braun, J. Gornicki, L. Mankievicz and A. Shafer: *Phys. Lett.* **B302** (1993) 291.

[33] J.Bartels, J. Blumlein and G. Schuler: *Z. Phys.* **C50** (1991) 91.

[34] J.C.Collins and J. Kwiecinski: *Nucl. Phys.* **B335** (1990) 89.

[35] J.Bartels: DESY preprint DESY-93-028; *Phys. Lett.* **B298** (1993) 204; E.M. Levin,M.G. Ryskin and A.G. Shuvaev: *Nucl.Phys.* **B 387** (1992) 589.

[36] L.Landau and I. Pomeranchuk: *Doklady Akad. Nauk USSR* **92**(1953) 535; **92**(1953)735; A. B. Migdal: *Phys.Rev.* **103**(1956) 1811; *Sov. Phys.* JETP **5** (1957) 527.

[37] J.Bartels and M.G. Ryskin: DESY preprint DESY-93-081, *Z.f.Phys. C in print.*

[38] E.Laenen,E. Levin and A.G. Shuvaev: *Nucl.Phys.* **B419** (1994) 39.

[39] A.DeRoeck (H1 Collaboration): *J. Phys.* **G19**931549; S.R.Magill (ZEUS Collaboration): *J. Phys.* **G19**931535; M.Besanson M (H1 Collaboration): To appear in *Proceedings of Blois Workshop on Elastic and Diffractive Scattering*, Brown University, Providence, June 1993; M.Krzyzanowski (ZEUS Collaboration): To appear in *Proceedings of Blois Workshop on Elastic and Diffractive Scattering*, Brown University, Providence, June 1993.

[40] A.D.Martin,R.G. Roberts and W.J. Stirling: *Phys. Lett.* **B306** (1993) 145.

[41] E. Levin and M. Wuesthoff: *Phys. Rev.* **D50** (1994) 4306.

[42] H. Abramowicz,E.M. Levin, A. Levy and U Maor: *Phys. Lett.* **B269** (1991) 465.

[43] E.M.Levin and M.G. Ryskin: *Phys. Rep.* **189** (1990)267.

[44] A.H. Mueller and H. Navelet: *Nucl. Phys.* **B 282**(1987) 727.

[45] A.H Mueller: *Nucl. Phys. B (Proc. Suppl.)* **18C**(1991)125; J.Bartels,A. De Roeck and M. Loewe: *Z. Phys.* **C54** (1992) 635; J. Kwiecinski, A.D.Martin and P.J. Sutton: *Phys. Lett.* **B287** (1992) 254; *Phys. Rev.* **D46** (1992) 921; W -K Tang: *Phys. Lett.* **B278** (1991) 363; J.Bartels: *J. Phys.* **G19**931611; E. Laenen and E. Levin: *J. Phys.* **G19**931582.

[46] Yu. L.Dokshitzer, V.A. Khoze and T. Sjostrand: *Phys. Lett.* **B274** (1992) 116; J.D.Bjorken: *Phys. Rev.* **D45** (1992) 4077; *Phys. Rev.* **D47** (1992) 101; *Nucl.Phys. B (Proc. Suppl.* **23C**(1992)250; *Acta Phys. Pol.* **B 23**(1992) 637.

[47] M.Albrow et al: *Future Experimental Studies of QCD at Fermilab: report of the QCD section:option for a Fermilab Strategic Plan"* FERMILAB - FN 622, Aug. 1994.

[48] E. Levin:"Renormalons at low x", TAUP 2221 - 94,CBPF -NF 001/95. December 1994,hep-ph/9412345.

[49] L.N.Lipatov: *Phys. Lett.* **B309** (1993) 394; *Nucl. Phys.* **B365** (1991) 614.

[50] H. Verlinde and E. Verlinde: Princeton preprint PUPT-1319.

[51] Miao Li and C-I Tan:"High energy Scattering in 2 + 1 QCD", BROWN - HET-932.

[52] L.N. Lipatov: Pomeron in Quantum Chromodynamics, in *Perturbative Quantum Chromodynamics*, A.H. Mueller ed. World Scientific, 1989; E.M. Levin and M.G. Ryskin: *Phys. Rep.* **189** (1990) 267; E. Levin: *Orsay Lectures*, Orsay preprint LPTHE - 91 / 02 (1992); B. Bodelek, K.Charchula, M. Krawczyk and J. Kwiecinski: *Rev. Mod. Phys.* **64** (1992) 927 and references therein; A.J. Askew, J. Kwiecinski, A.D. Martin, P.J. Sutton: *Phys. Rev.* **D 47** (1993) 3775; A.D. Martin: *J. Phys.* **G19**931603 and references therein; J. Kwiecinski: *J. Phys.* **G19**931443 and references therein; E. Levin: *J. Phys.* **G19**931453 and references therein; E. Laenen and E. Levin: Parton Densities at High Energies, FERMILAB - PUB - 94 - 089 - T, April 1994, to appear in *Annual Review of Nuclear and Particle Physics* v. **44**, 1994.